ABSTRACT

Title of Document: EFFECT OF ENCAPSULATION ON ELECTROLYTE LEAKAGE IN ALUMINUM ELECTROLYTIC CAPCITORS UNDER CONSTANT THERMAL AND ELECTRICAL LOADING

Ehsan Parsa, Master of Science, 2014

Directed By: Professor Abhijit Dasgupta
Co-Advisor Dr. Michael Azarian
Department of Mechanical Engineering

This study focuses on the influence of encapsulation (with silicone elastomer potting compound) on electrolyte leakage in aluminum electrolytic capacitors. Experiments were conducted on potted capacitors at constant elevated temperature and rated DC voltage, and results were compared to those from a control batch of unpotted capacitors. The weight, ESR and capacitance were periodically monitored. Encapsulation was found to decelerate electrolyte loss rate and ESR degradation. There was an increasingly discernible deceleration of capacitance degradation but the magnitude did not reach statistically significant thresholds within the test period.

A simplified axisymmetric finite element model was constructed for theoretical understanding of the electrolyte loss process. The experimental measurements were used to guide the selection of the material properties in the model. The model addresses several possible sources of non-uniformities in the mass flux density in the

test specimen: (i) radial nonuniformity of mass transport properties of the rubber seal; and (ii) delamination between the potting compound and the capacitor leads. This model was then used: (i) to conduct parametric investigation of the effect of mass transport properties of the potting compound; and (ii) in conjunction with the experimental results to estimate the electrolyte mass loss from the capacitor through the rubber seal.

EFFECT OF ENCAPSULATION ON ELECTROLYTE LEAKAGE IN ALUMINUM ELECTROLYTIC CAPCITORS UNDER CONSTANT THERMAL AND ELECTRICAL LOADING

By

Ehsan Parsa

Thesis submitted to the Faculty of the Graduate School of the
University of Maryland, College Park in partial fulfillment of
the requirements for the degree of
Master of Science
2014

Advisory Committee: Professor Abhijit Dasgupta, Chair/Advisor
Dr. Michael Azarian, Co-Advisor
Professor Bongtae Han

Dedication

All this work is dedicated to my amazing parents and to thank them for all they have done for me. This is also dedicated to my brother who has been a great role model in my life. If it wasn't for my amazing family I would have not been able to complete my Masters of Science degree.

Acknowledgements

I owe my deepest gratitude to all those who helped me grow to who I am today.

First of all I would like to thank my advisor, Professor Abhijit Dasgupta, because if it wasn't for his amazing patience, guidance, help and support, I would have not been able to complete this work. I will always admire his compassion, knowledge, and wisdom. It was an honor for me to have Professor Dasgupta as my advisor.

I would like to thank my co-advisor, Dr. Michael Azarian, for all of his patience and intelligent advise during my thesis work. I would have not been able to complete this work if it wasn't for Dr. Azarian.

I like to thank my final committee member, Professor Bongtae Han, for his contribution to my work.

Finally, I am thankful to all my colleagues and friends Ehsan, Hao, Koustav, Subhasis, Yong, Josh, Matt, Babak, David, Jingshi, Jaemi, Ranjith, Anshul, Anto, Elvis, Swapnesh, Bhanu, Majid, Mark, and Cholmin. Many people have helped me along the way with their valuable contributions and I thank every single one of them for all they have done.

Table of Contents

List of Tables

List of Figures

Chapter 1: Introduction

This chapter will cover motivation, background, capacitor structure, work conducted in this field, and the objective of this study.

1.1 Background and Motivation

Reliability is one of the major concerns when a new product or component is designed and/or developed. Therefore, engineers have to evaluate the effect of environmental stresses, handling stresses and operational stresses on long-term degradation of performance. One of the approaches for increasing the reliability of electronics that are exposed to dynamic mechanical loads, mishandling or abuse, and moisture, is to encapsulate the electronic assembly in an elastomeric potting compound. Silicone elastomer is a good potting compound because of its compliance and low moisture diffusivity. However, the inclusion of the silicone elastomer can have various impacts on the electronics components. A common example in which the driver electronics is potted in the silicone elastomer is the driver electronics for commercially available LED light bulb products. Many researchers have indicated that the conventional commercial LED components in SSL systems have been found to have very long life expectancies which in many cases survive much longer than the driver electronics [1] [2]. Therefore, the driver electronics is the main focus of the reliability in the LED light bulb product. One major component in the LED driver electronics is an aluminum electrolytic capacitor. Historical experience indicates that electrolytic capacitors are often the weakest component in the driver electronics with the lowest rated life expectancy compared to the other components in the system [3]

[4] [5]. One major failure mode of the electrolytic capacitor is considered to be electrolyte leakage especially at high temperatures which is believed to be a possible reason for degradation in the electrical performance and ultimately resulting in electrical failure [6] [7]. The focus of this thesis is on the possible effects of the encapsulation on the electrolyte leakage from the aluminum electrolytic capacitor.

1.2 - Aluminum Electrolytic Capacitor Construction

To explain the importance of electrolyte leakage, the basics of electrolytic capacitors are discussed here. The electrical purpose of a capacitor is to use two conductive parallel plates (electrodes) which are separated by a dielectric layer (insulator) which allows positive charge to build up on one plate (anode) and negative charge to build on the alter plate (cathode). This will produce an electrical field and store potential voltage difference energy between the two plates which can be used as a temporary battery.

In particular the aluminum electrolytic capacitor is constructed with an element which contains the anode, cathode, impregnated paper separator. The anode and cathode layers are thin (0.02 to 0.1mm) and are high purity aluminum foil. To increase the surface area between the anode and cathode plates, the aluminum foil undergoes a special etching process. The anode and cathode foils are then separated by paper which is soaked in electrolyte. This allows the electrolyte to penetrate the etch tunnels as shown in Figure 1.

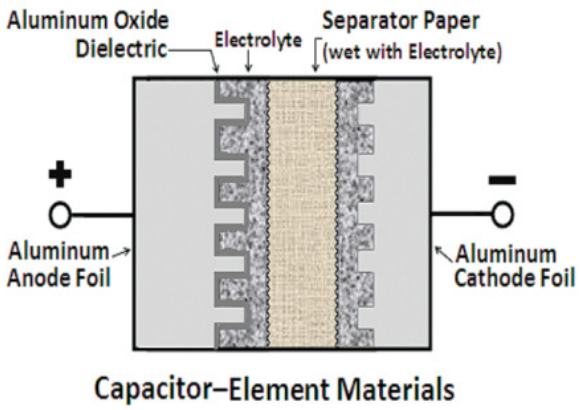

Figure 1: Construction of anode, cathode, and impregnated paper separator (element) [8]

Water is one of the essential compounds in the electrolyte to maintain the aluminum oxide dielectric layer. When leakage current occurs, water molecules break down into hydrogen and oxygen atoms. As a result, oxygen ions bond with the anode foil to recreate the oxide layer on the aluminum foil or so called recovers the leakage region, whereas, the hydrogen is forced to either react with the hydrogen depolarizers or escape to prevent from pressure buildup. Due to this effect it is critical to construct the capacitor in such a way that the electrolyte liquid is conserved and the hydrogen is allowed to escape. Therefore, the electrolytic capacitors are often contained in an aluminum can with a rubber seal with only the terminal leads sticking out as shown in Figure 2.

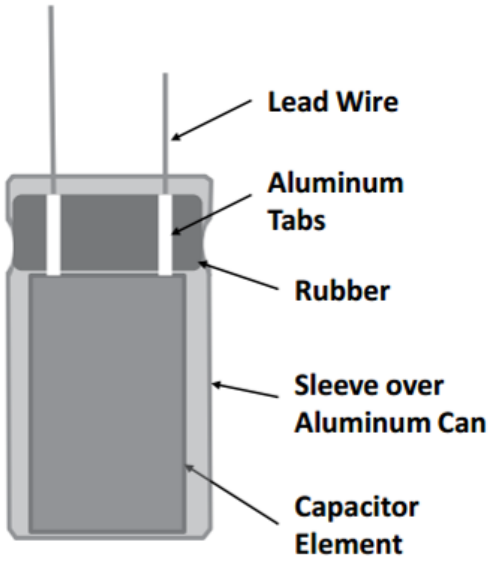

Figure 2: Physical structure of the electrolytic capacitor [8]

In the capacitor neither the hydrogen nor the electrolyte vapor will escape through the aluminum can, therefore, the only leakage pathway will be the rubber seal. This makes the rubber seal a very critical component in the electrolytic capacitor. This indicates that the rubber seal must allow excessive hydrogen atoms to escape to prevent pressure buildup inside the capacitor while it prevents the electrolyte vapor from leaking [8]. As a result, the selection of the rubber sealant material is a tradeoff of electrolyte leakage or pressure buildup inside the capacitor. Researchers and industry experts have suggested that one of the major failure modes of the electrolytic capacitor is due to electrolyte leakage, especially at high temperatures. Therefore, the focus of this research is on electrolyte leakage failure mode of a specific aluminum electrolytic capacitor, and on the role of encapsulant material on the leakage rate.

1.3 Literature Review

Electrolytic capacitors have been used in electronics for many years due to their large capacitance per volume and cost effectiveness. Because of the unreliable nature of electrolytic capacitors, the majority of research on this technology has been directed towards developing a method to estimate the time to failure. This is due to the fact that the electrolytic capacitor has often been the least reliable part of the circuit. The main wear-out failure mode of electrolytic capacitors is considered to be the drying out of the electrolyte inside the element. This process is strongly temperature dependent. Therefore, most of the failure models consider the operating temperature in their life estimates.

1.3.1 Empirical Models of Life Expectancy

Much of the research available in the literature on electrolytic capacitors has tried to develop models to estimate life expectancy. These models are mainly driven by the operational temperature of the capacitor. One of the oldest and most famous models used in many papers and in the industry to estimate life expectancy is motivated by the simple Arrhenius model and is presented in Equation (1) below.

$$L_{exp} = L_o * 2^{\left(\frac{T_o - T_{op}}{10}\right)} \quad \textbf{(1)}$$

L_{exp} = Life expectancy of the capacitor
L_o = Life expected at rated temperature
T_o = Rated Temperature (C)
T_{op} = Operating Temperature (C)

Equation (1) is usually used in industry as a quick rule of thumb and basically states that for every 10°C increase in operating temperature, the life of the electrolytic capacitor reduces by half. This concept and approximation is drawn from the idea that for every 10°C increase chemical reaction speed doubles [9]. This model was later slightly modified by Dehbi & Wondrak [10] to account for the voltage applied as well, as shown below in Equation (2):

$$L_{exp} = L_o * \left(\frac{V_o}{V}\right)^n * 2^{\left(\frac{T_o - T_{op}}{10}\right)} \quad \textbf{(2)}$$

V_o = Maximum rated voltage (V)
V = Operating voltage (V)
n = Capacitor type parameter (0 for axial, 1 for radial)

Gualous & Gallay took a step back and looked at the more generalized Arrhenius model with the activation energy specific for each type of capacitor [11] as shown in Equation (3).

$$L_{exp} = B * e^{\left(\frac{E_A}{k\,T_o}\right)} \quad \textbf{(3)}$$

B = Factor of Arrhenius
E_A = Activation energy (eV)
k = Boltzmann constant
T_o = Temperature (K)

Jánó & Pitică conducted an experiment and compared the models presented so far. As a result they proposed a slightly more complex model which combined Dehbi & Wondrak's and Gualous & Gallay's

models [12]. Equation (4) presents their proposed equation which in their experiment indicated the best estimation among the other Arrhenius models.

$$L_{exp} = B * e^{\left(\frac{E_A}{k\,T_o}\right)} * \left(\frac{V_o}{V}\right)^n \quad \textbf{(4)}$$

Another famous Arrhenius model used to determine the ESR drift was illustrated in [6, 13, 14]. Equation (5) illustrates the inverse linear model, which is considered to provide a reasonably good prediction of ESR as a function of time.

$$\frac{1}{ESR(t)} = \frac{1}{ESR_o} * \left(1 - k * t * e^{\left(-\frac{4700}{T_{op}}\right)}\right) \quad \textbf{(5)}$$

t = Aging time
T_{op} = Operating Temperature (K)
ESR_o = Initial equivalent series resistance
k = Constant which depends on the design and construction of the capacitor

Many researchers use the life expectancy models presented in this subsection. Another aspect of research on electrolytic capacitors is real-time diagnostics and prognostic health management, which is discussed in the next section.

1.3.2 Diagnostic and Prognostic Health Management

Electrolytic capacitors are well known for piece to piece variability. Therefore, many studies attempt to develop real-time diagnostic and prognostic methods. This approach considers the current state of the capacitor's electrical performance and estimates the remaining useful life of the capacitor. There are many proposed methods and algorithms which determine the health and time to failure of the capacitor based on its ESR [3, 4, 6, 7, 15-17, 19, 26-29]. However, most of the work conducted so far has focused primarily on the electrical degradation aspect. There are very few studies in the literature that have focused on the physics of failure of the capacitor.

One of the well-known and well-cited researchers who considered physical electrolyte leakage in his models was M. Gasperi. He used an empirical formula to relate volume of electrolyte to the ESR as shown in Equation (6). [6, 15, 16]

$$\frac{ESR}{ESR_o} = \left(\frac{V_{ol-i}}{V_{ol}}\right)^2 \quad \textbf{(6)}$$

ESR = Equivalent Series Resistance at 20^oC (Ω)
ESR_o = Initial ESR (Ω)
V_{ol} =Volume of Electrolyte ($length^3$)
$V_{ol\text{-}i}$ = Initial volume of electrolyte ($length^3$)

Gasperi then related the volume change to the electrolyte vapor pressure. Since vapor pressure is temperature dependent, the core temperature of the capacitor critically affects the vapor pressure inside

the capacitor. Therefore, he then used physics based models to estimate the core temperature. The equation he used to relate the volume change to the vapor pressure of electrolyte is presented in Equation (7).

$$\frac{dV_{ol}}{dt} = k * P \tag{7}$$

t = Aging time
k = Leak rate constant (length/mmHg/time)
P = Pressure (mmHg)

Another slightly more complex physics based model which related the electrical behavior to the physical volume loss of electrolyte was presented by Kulkarni & Biswas [7, 17, 18]. Equation (8) and Equation (9) present the capacitance and ESR degradation models, respectively, as a function of electrolyte volume loss.

$$C(t) = \left[\frac{2\,\epsilon_R\,\epsilon_o}{d_C}\right]\left[\frac{V_{ol-i} - V_{dol}(t)}{j_{eo}\;t\;w_e}\right] \tag{8}$$

$$ESR(t) = \left[\frac{\rho_E\;d_C\;P_E}{2}\right]\left[\frac{j_{eo}\;t\;\;w_e}{V_{ol-i} - V_{dol}(t)}\right] \tag{9}$$

t = Aging time
V_{dol} = dispersion volume at time t
ρ_E = electrolyte resistivity
d_C = cathode oxide layer thickness
ϵ_R = Relative dielectric constant
ϵ_o = Permittivity of free space
w_e = Volume of ethylene glycol molecules
j_{eo} = evaporation rate ($time^{-1}length^{-2}$)
P_E = correlation factor related to electrolyte spacer porosity and average electrolyte pathway

1.4 Gaps in the Literature and Objectives of this Study

Most researchers studying the electrolytic capacitor have focused on the changes in the electrical parameters of the capacitor, specifically the ESR, due to environmental and operational conditions. Little work has been conducted on the physical root cause mechanism for the degradation of the electrical parameters [6]. There is relatively little quantitative, physics-based study of electrolyte loss and its effect on the electrical performance [7]. In particular, almost no work has been conducted on the effect of encapsulating electrolytic capacitors, as in LED driver electronics.

The objective of this thesis study is to extend the knowledge of electrolytic capacitors by studying the effects of encapsulation on the physical electrolyte mass loss from electrolytic capacitors, under steady thermal and electrical stresses. This study presents an experiment conducted on potted vs. unpotted capacitors at high temperature with constant DC voltage and FEA modeling of the electrolyte leakage from these capacitors. The FEA model is guided by the experimental weight loss results. Conclusions are presented based on the results extracted from this study considering the limitations of the work.

Chapter 2: Experiment

This chapter presents the experimental setup, including design and fabrication of test specimens, temperature and electrical profile, test matrix, instrumentation, discussion of monitored parameters, test results, and statistical analysis of the results.

2.1 Experiment Preparation

The objective of this experiment is to determine the effect of encapsulation on electrolyte leakage in aluminum electrolytic capacitors. The aluminum electrolytic capacitor selected in this study is commonly used in LED lighting product driver electronics, where it is subjected to temperature, DC voltage and AC ripple current. Due to limitations of the test equipment the ripple current could not be replicated in this experiment. Therefore, only a constant VDC was applied to the capacitors. In order to accelerate the electrolyte leakage mechanism, the capacitors were subjected to elevated temperature well beyond their specifications. Due to the absence of ripple current, the capacitors were subjected to constant uniform temperature which did not duplicate the progressive increase of temperature which is expected under the action AC of ripple currents when there is ESR increase due to decreasing electrolyte content. In order to estimate the appropriate temperature level to accelerate the nominal electrolyte leakage process, an overstress test is first conducted on a different batch of identical capacitors, as explained in detail in Appendix I: Overstress Test. The specimen design and fabrication process are described in detail in the next subsection.

2.1.1 Specimen Design

As mentioned previously, the goal of this experiment is to observe and compare the electrical performance drift and electrolyte leakage rates between the two populations of interest, viz. potted vs. unpotted capacitors. In order to measure the electrical properties, leads of the potted capacitors are required to extend out beyond the potting compound. Furthermore, as mentioned in the introduction section, the only leakage pathways for electrolyte vapor from the capacitor is through the rubber seal and through the interfaces of the rubber seal with the aluminum can and lead. Therefore, the only region of interest for encapsulation is the rubber seal. As discussed earlier, any presence of ripple currents creates a time-dependent heat generation source inside the capacitors due to ESR drift caused by electrolyte leakage, which then necessitates a coupled thermal analysis due to changes in the thermal resistance. However, in this study no such ripple current is present and the thermal problem is therefore steady and uniform. Based on the discussed criteria, the best design which serves the purpose of this test is the design shown in Figure 3. The detailed process of the potted specimen preparation is available in

Appendix II: Specimen Preparation.

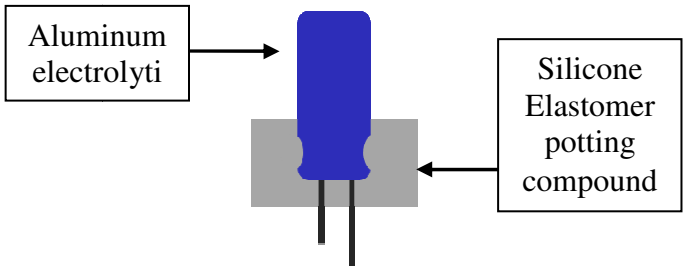

Figure 3: Schematic cross section representation of desired geometry for a potted capacitor

The second (reference) set of population tested is the control population of unpotted capacitors which are not encapsulated in the silicone elastomer. The mass loss due to electrolyte vaporization and leakage from the capacitor was estimated by periodically weighing the weight of the entire system and subtracting the weight of all the components other than the electrolyte. This is critical since the polymeric components are also known to change weight with sustained thermal exposure. The final 'dry' weight is also determined, as described below, to assess the initial weight of just the electrolyte. These weight adjustments are discussed below and the details are provided later in Section ***2.2.1*** *Weight Calculation*.

Electrolytic capacitors are known for their variability and measuring the weight of anode, cathode, paper separator, aluminum can, leads, rubber and potting compound for potted specimen required destruction of the specimen. Destruction of specimen would result in terminating the experiment, therefore, 5 capacitors from a different batch were selected for destructive characterization, for two purposes: (i) to determine the average weight of all the excessive components (ii) to

determine the weight of electrolyte only which is used later in SectionResults from the experiment reveal several interesting characteristics. One immediate finding from the experiment is that the encapsulated capacitors did not burst open due to pressure buildup. However, all capacitors (potted and unpotted) did slightly bulge during the test. This suggested that the hydrogen atoms, which were initially formed as result of chemical reaction, either reacted with the hydrogen depolarizers or escaped through the rubber sealant and silicone elastomer.

2.3.1 Weight for the FEA modeling. However, its understood that this process of using representative samples and using a process of subtraction to identify small changes in weight lead to an increase in uncertainty sue to 'noise' levels in the experimental results. This is one of the limitations of the test method used in this study.

Given an average estimate of weight of the unspotted capacitor sub-elements, the only other non-constant weight is that of the rubber sealant. Due to the fact that polymers lose weight as they age at elevated temperature, a population of samples of just the 'dry' sealant (butyl rubber) was also included in the test matrix so that their weight loss history could also be monitored. The average weight loss history of these rubber seal samples was correct the weight loss measurements of both potted and unpotted specimen populations.

Furthermore, in the potted population, weight change of silicone elastomer due to thermal aging was required to be considered as well. Unlike for the rubber sealant, for which the measured average weight history was assumed to be representative for all capacitors, the initial weight of silicone elastomer was measured exactly for each potted sample. These were done by first measuring the weight of the capacitor which was going to be potted and then measuring the weight of the sample after the potting compound cured. However the subsequent history of fractional weight loss of the silicone potting compound could only be estimated in an average sense, similar to the process used for the butyl rubber sealant. As a result another population of sample was added to the test matrix which was the silicone elastomer to track the weight loss measurement due to mass loss of the polymer. Therefore, the resulting test included 4 set of samples: (i) unpotted capacitors (ii) potted capacitors (iii) rubber sealant (iv) silicone elastomer. All of these samples were placed in the same chamber so that they are all exposed to the same environmental stress history.

2.1.2 Experiment Specimens and Loading

The sample size of capacitors for this experiment consisted of 20 capacitors: 10 are unpotted and 10 are encapsulated in a silicone elastomer potting compound. The geometric configuration of the encapsulation structure, shown in Figure 4**,** is designed to block the

electrolyte leakage path. The goal is to examine whether the encapsulation plays any role in altering the electrolyte leakage rate and hence in extending the capacitor life.

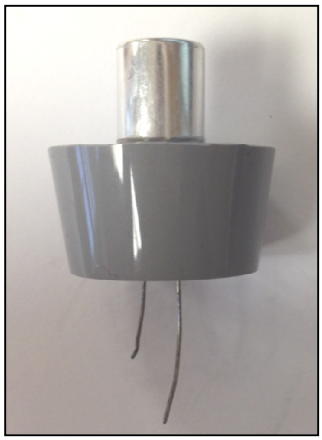

Figure 4: Encapsulated capacitor (potted capacitor)

As discussed earlier, in addition to the two sets of ten capacitors (10 unpotted capacitors and 10 potted capacitors) there were also two other sets of materials place in the same environmental chamber (10 pieces of silicone elastomer, and 10 pieces of rubber sealant). Each sample is uniquely identified for accuracy in the measurement calculations. All of the samples were divided into two groups and were placed on two racks as shown in Figure 5.

Figure 5: Specimen placement inside the chamber

These capacitors were subjected to 155^{o}C constant temperature to accelerate the nominal mechanisms for electrolyte leakage (temperature profile was selected based on overstress test, discussed in **Appendix I: Overstress Test**). These capacitors were charged with 35VDC, which is the rated voltage for these electrolytic capacitors.

As shown, the specimen locations are randomized inside the chamber to ensure that any thermal gradients in the chamber do not cause any systematic biases in the stress levels experienced by the two different specimen sub-populations (potted vs unspotted). This ensures that any unintended variability in the specimen temperatures do not cause any systematic biases in the stresses imposed on different specimen populations. Samples were placed approximately 50 mm away from

the walls to ensure that they were near the center of the chamber, and away from any boundary layers near the walls with relatively stagnant air of lower flow velocities. Air close to the walls is less likely to cycle as much as the air in the center. The top plate shown in Figure 5 contained holes which allowed hot air from the top of the chamber to cycle more uniformly inside the chamber.

2.1.3 Electrical Stress Setup

All of the 20 capacitors were electrically connected in parallel with one another, in order to apply 35VDC to each capacitor with the power supply. The schematic of the physical circuitry is presented in Figure 6. The details of the circuit have been explained in **Appendix III: Circuit Design**. As shown in the physical schematic Figure 6, terminal blocks are used to connect the capacitor leads via screws which clamp the leads to the metallic connection of the terminal. This prevents soldering and desoldering leads to wires which could potentially add additional uncontrollable thermal stress to the capacitors.

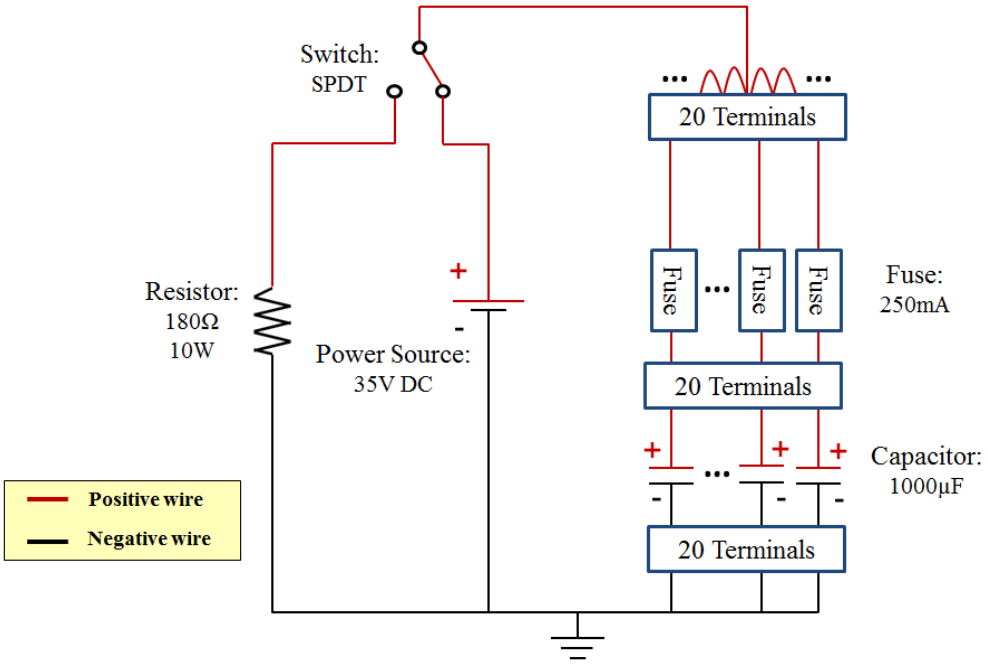

Figure 6: Schematic of the experiment setup

2.1.4 Monitoring Parameters and Measurement Process

Electrolyte leakage from the capacitor is believed to be responsible fora decrease in capacitance and increase in the ESR. Therefore, parameters of interest were capacitance and ESR of the tested capacitors. It was critical to also simultaneously measure the physical weight of the capacitor to record the physical mass loss of the electrolyte liquid inside the capacitor. Therefore, all specimens' weights were measured in grams with up to four decimal places.

During the experiment, all of the measurements were conducted at room temperature since there were no facilities to weigh the specimens in-situ while they were in the thermal chamber. Thus, the experiment was periodically paused, capacitors were discharged through a 180Ω

discharge resistor, cooled for approximately 30min to room temperature and then weighed for changes. In order to reduce bias effect in the measurements, unpotted and potted populations were measured in a mixed sequence. The measurement order followed the following sequence:

U1 (unpotted specimen #1), P1 (potted specimen #1), U2, P2… U10, P10, R1 (rubber #1) … R10, S1 (silicone #1) … S10

First parameter measured was the weight, to minimize the reabsorption of moisture from the ambient lab environment. Once all samples were weighed, the capacitance was measured for all 20 capacitors followed by the ESR measurements, using the same sequence explained above. Capacitance was measured using Agilent 4263B LCR meter with 1V at 120Hz in room temperature as specified in the specification sheet. ESR was measured using the same LCR meter with 1V at 100kHz at room temperature.

2.2 Experiment Post Processing

The thermal and electrical stressing was conducted for approximately 800 hours. Initially parameters were measured frequently to capture any sudden change due to the thermal loading. After the rate of change of the parameters of interest stabilized, the measurement readings were recorded less frequently. The parameters measured as a function of time are the following: (i) weight measurement of potted capacitor, unspotted capacitor, rubber seal, and silicone elastomer; (ii) capacitance of potted and unpotted capacitors; (iii) ESR of potted and unspotted capacitors.

2.2.1 Weight Calculation

Measuring the weight of the electrolyte is challenging but essential for this study. Figure 7 depicts illustration of samples in chamber which were weighed either initially (e.g. silicone encapsulation of the capacitor) or periodically during the stress exposure experiment. The process of electrolyte weight loss measurements is as follows:

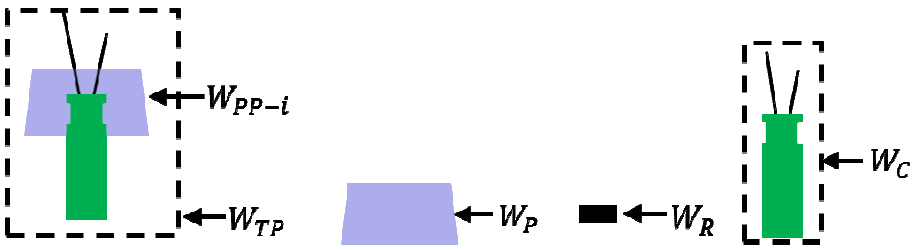

Figure 7: Samples tested in the chamber

$W_{PP\text{-}i}$ = Initial weight of silicone elastomer on the encapsulating the capacitor
W_{TP} = Total weight potted specimen
W_P = Total weight silicone specimen
W_R = Total weight rubber seal
W_C = Total weight unpotted capacitor

In addition, 5 capacitors were destructively disassembled and used to characterize the average 'dry' weights of their sub-elements: aluminum can, leads, anode, cathode, and paper separator. The total weight of these sub-elements is termed the 'dry' weight of the capacitor assembly (W_K). The difference between the average 'dry' weight and average 'wet' weight is identified as the average weight of the electrolyte (W_{EA}). The average weight of the electrolyte is used for the modeling tasks discussed later in Section **3.4** Material Property Estimation. The average 'dry' weight W_K is also used to estimate the approximate initial electrolyte weight of each tested capacitor, as explained below in Equations (10)-(14). In Equations (10)-(14) presented below, subscript *i* stands for initial.

$$W_{PP-i} = W_{TP-i} - W_{CP-i} \quad \textbf{(10)}$$

$$W_{EU} = W_C - {W_{R-i}}^{Avg}\left(\frac{W_R}{W_{R-i}}\right)^{Avg} - {W_K}^{Avg} \quad \textbf{(11)}$$

$$W_{EP} = W_{TP} - {W_{R-i}}^{Avg}\left(\frac{W_R}{W_{R-i}}\right)^{Avg} - W_{PP-i}\left(\frac{W_P}{W_{P-i}}\right)^{Avg} - {W_K}^{Avg} \quad \textbf{(12)}$$

$$W_{Frac\,EU} = \frac{W_{EU}}{W_{EU-i}} \quad \textbf{(13)}$$

$$W_{Frac\,EP} = \frac{W_{E\,P}}{W_{E\,P-i}} \quad \textbf{(14)}$$

Variable definitions are shown in Figure 7 above
$W_{CP\text{-}i}$ = Initial weight of capacitor (potted sample)
W_K = Weight of anode and cathode foil, aluminum case, paper separator and the leads
W_{EU} = Calculated weight of electrolyte in the unpotted sample
W_{EP} = Calculated weight of electrolyte in the potted sample
$W_{Frac\ EU}$ = Fractional residual weight of electrolyte in the unpotted sample
$W_{Frac\ EP}$ = Fractional residual weight of electrolyte in the potted sample

As seen from Equations (10)-(14) above, the estimate of the initial weight of the electrolyte does have some uncertainty because it depends on the average 'dry' weight and not on the actual 'dry' weight of each capacitor. However, this error is applicable to all capacitors, and hence is a random error without any systematic bias. Furthermore, the fact that the weight of silicone elastomer encapsulating the capacitor was explicitly measured for each potted sample during the specimen preparation prevented any systematic biases between the potted vs unspotted populations. Although, the mass loss of silicone

elastomer is averaged, the actual mass of the silicone elastomer has a relatively small effect on the fractional weight loss of the electrolyte. In summary, the measurement approximations are somewhat mitigated by the fact that we are only using the fractional residual weight in this study, to characterize any differences between the potted vs. unpotted populations.

2.2.2 ESR

As seen from many experiments in the literature, ESR of capacitors is expected to increase as a result of electrolyte leakage. ESR is the equivalent series resistance of a capacitor, which occurs due to imperfect resistive elements of the capacitor. Although this resistance is small, it can have significant effects in the presence of ripple currents. The ESR results in increasing the core temperature of the capacitors which in turn can lead to accelerated degradation of the capacitor. This small resistance is due to copper leads, anode and cathode foil, electrolyte, and the paper separator. Therefore, it is critical to minimize the length of copper leads involved in the measurement. Therefore, in the experimental tasks, the LCR meter was connected as close as possible to the rubber seal for all unpotted capacitors, and as close as possible to the silicone elastomer for all the potted cases. This indicated that the length of the lead in the measurement process was constant for each specimen through the test. One critical error in the potted capacitor group's ESR absolute value

was the 6.5mm additional length of lead due to the geometry of the silicone elastomer. In order to compare the unpotted capacitors against potted capacitors the fractional ESR values will be compared. This normalizes each component with its initial ESR value which allows for better comparison between the two groups.

2.2.3 Capacitance

Capacitance in this experiment is a very critical parameter. This is due to the fact that the physical electrolyte vaporization and leakage results in electrical performance degradation. As seen from the overstress test (Appendix I: Overstress Test) capacitance was the determining factor for the temperature selection. Similar to the weight loss calculation, the main interest of this study is to see the effect of encapsulation on electrolyte leakage, therefore, the changes in fractional capacitance value (compared to the initial value) is of significant interest.

2.3 Experiment Results

Results from the experiment reveal several interesting characteristics. One immediate finding from the experiment is that the encapsulated capacitors did not burst open due to pressure buildup. However, all capacitors (potted and unpotted) did slightly bulge during the test. This suggested that the hydrogen atoms, which were initially formed as result of chemical reaction, either reacted with the hydrogen depolarizers or escaped through the rubber sealant and silicone elastomer.

2.3.1 Weight Measurement

As mentioned in Section ***2.2.1*** *Weight Calculation*, the mass loss of the 20 capacitors along with the two polymers, rubber seal and silicone elastomer, is recorded throughout the duration of this experiment. The results of the weight calculations explained in that section are presented in this section. In the five figures presented below the absolute weight of all samples are plotted. Figure 11 and Figure 12 show that the amount of silicone elastomer potting compound follows a bimodal distribution with 5 samples having a mean weight of 22.0257 gms and the remaining 5 samples having a mean weight of 10.2089 gms. This bimodal distribution was initially selected to identify the effect of the absolute amount of elastomer. However, the results were subsequently examined in terms of fractional residual weight, thus eliminating any difference between these two sub-populations of potted specimens.

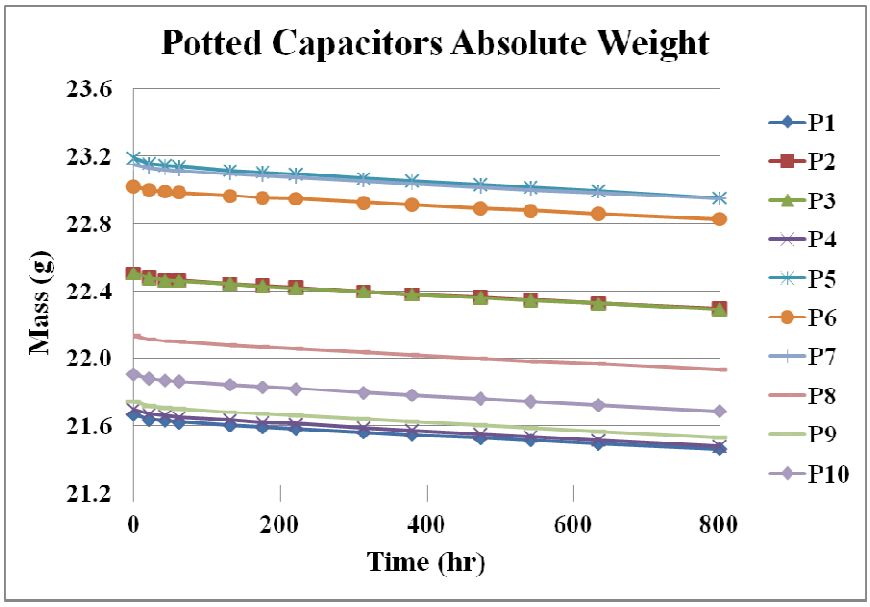

Figure 8: Absolute weight history of the potted capacitor samples (W_{TP}). The initial weight $W_{PP\text{-}i}$ is obtained from these measurements

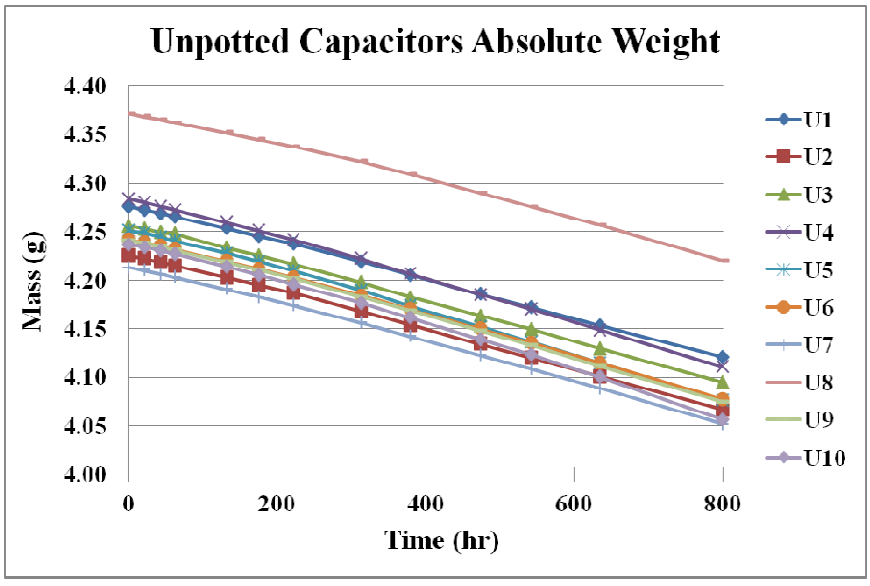

Figure 9: Absolute weight history of the unpotted capacitor samples (W_C)

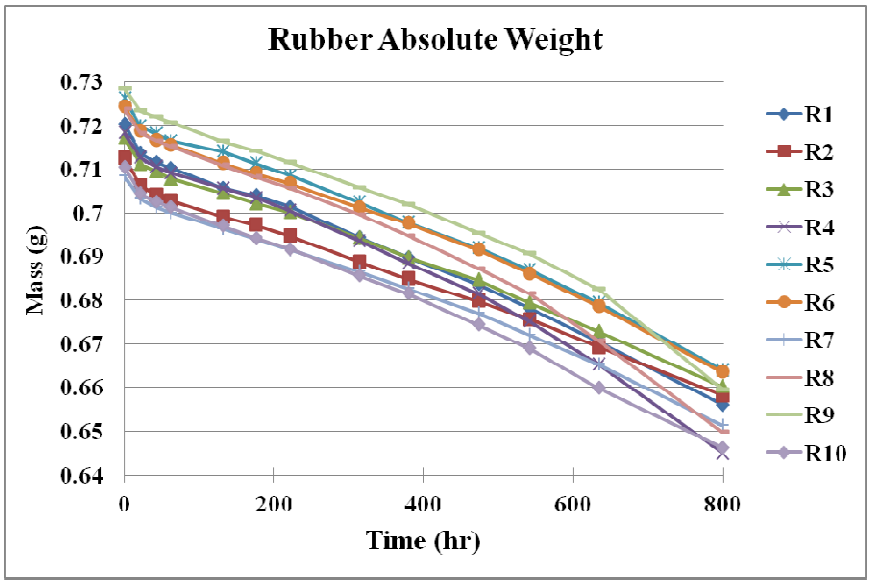

Figure 10: Absolute weight history of the rubber sealant samples (W_R). These values were used to estimate the average weight history of rubber sealant $(W_R)^{avg}$

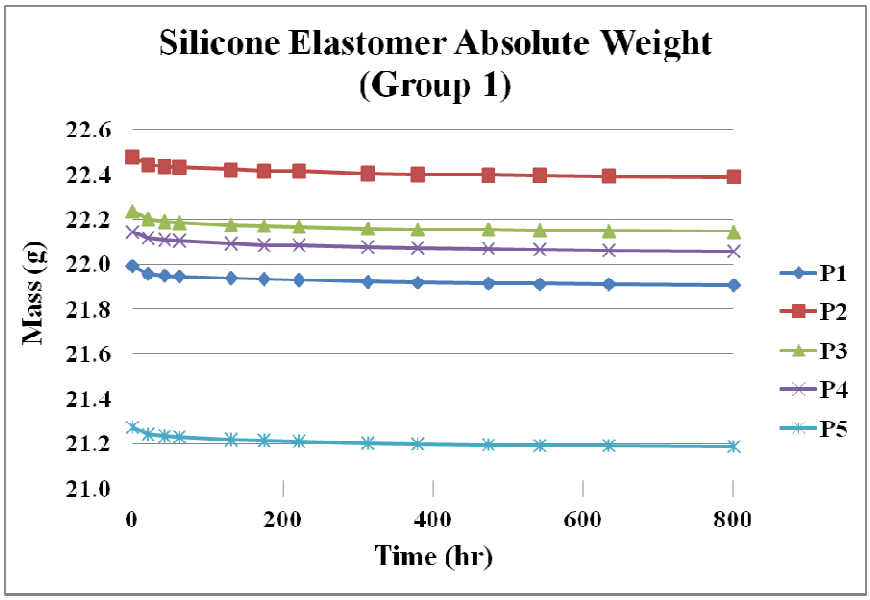

Figure 11: Absolute weight history of the silicone elastomer samples (W_P). This is group 1 with mean absolute initial weight 22.0257 gms.

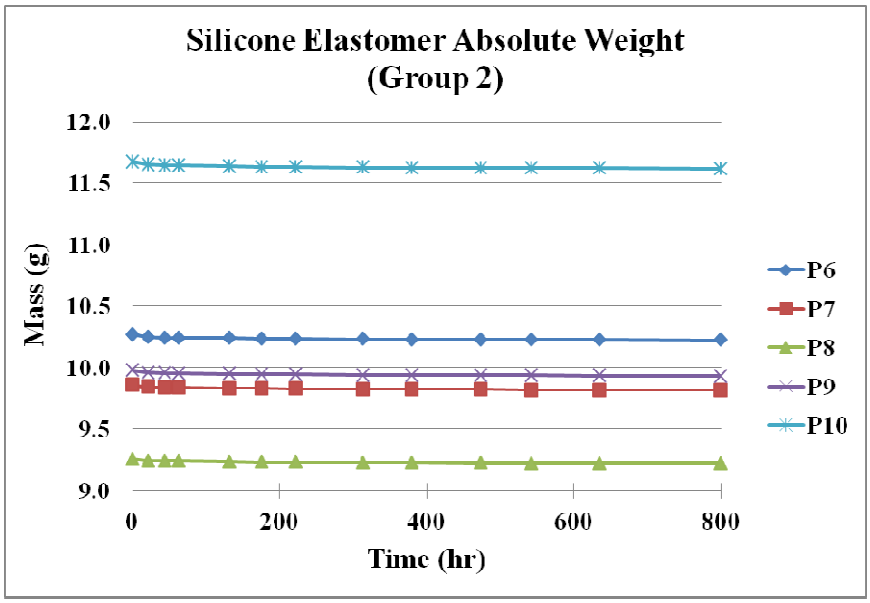

Figure 12: Absolute weight history of the silicone elastomer samples (W_P). This is group 2 with mean absolute initial weight 10.2089 gms.

As mentioned in Section ***2.2.1*** *Weight Calculation*, fractional residual weight ($W_{current}/W_{initial}$) of the two polymers were calculated and plotted. This mass-loss data of the polymers is used to correct the mass loss measurements for accurate determination of electrolyte mass loss in the calculations. Next three figures depict the fractional residual weight of (Figure 13) rubber, (Figure 14) silicone, and (Figure 15) their respective averages. The fractional weight loss of the two sub-groups of silicone elastomer potting compounds is found not to correlate to their absolute weight. Therefore, the data from both groups are combined together for the purpose of assessing the average residual fractional weight. One observation made from the average fractional residual weight is that the rubber seal loses much more mass then the silicone elastomer (on a normalized scale). Rubber specimens on average lose

about 8% of their mass at 800 hours, whereas, the average silicone elastomer mass loss is barely 1% at 800 hours.

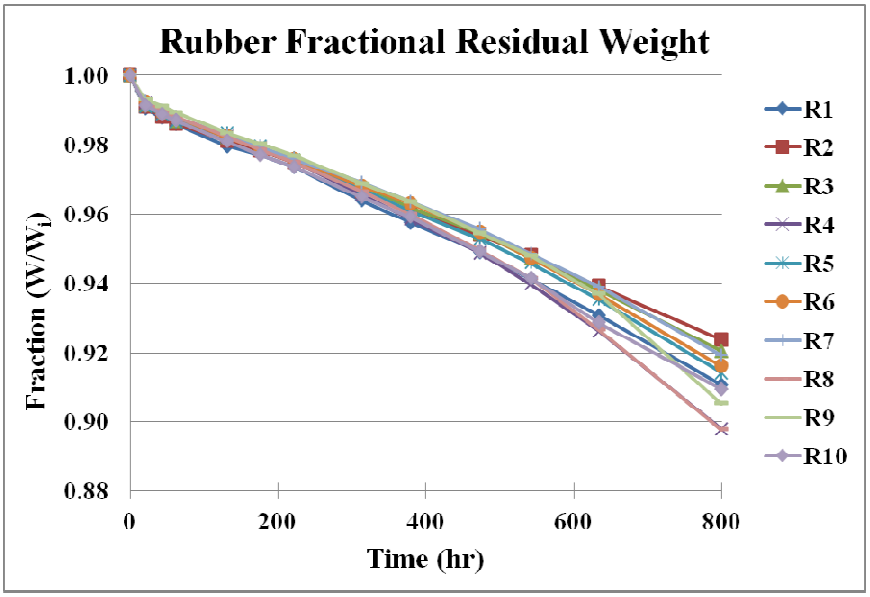

Figure 13: Fractional residual weight of the 10 rubber samples (W_R/W_{R-i})

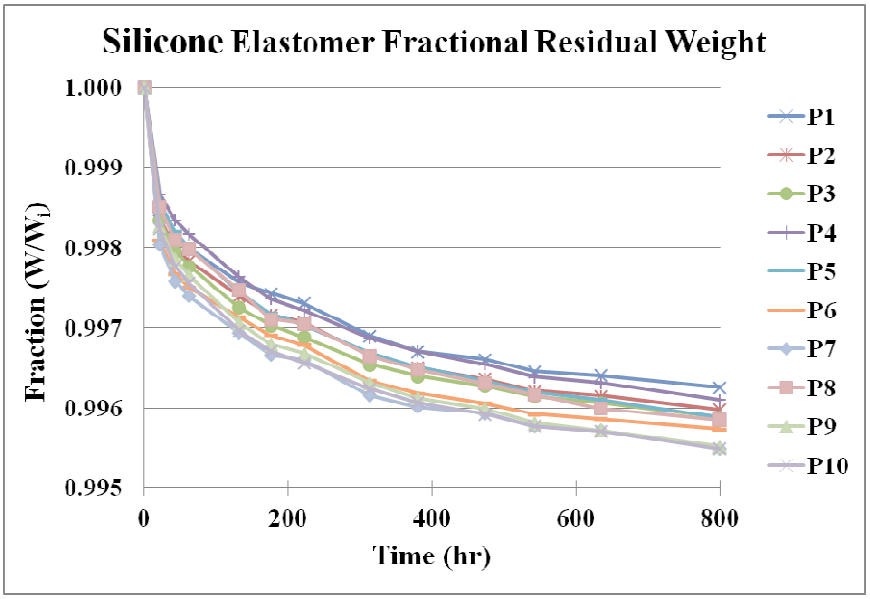

Figure 14: Fractional residual weight of the 10 silicone elastomer samples for both groups 1 and 2 (W_C/W_{C-i})

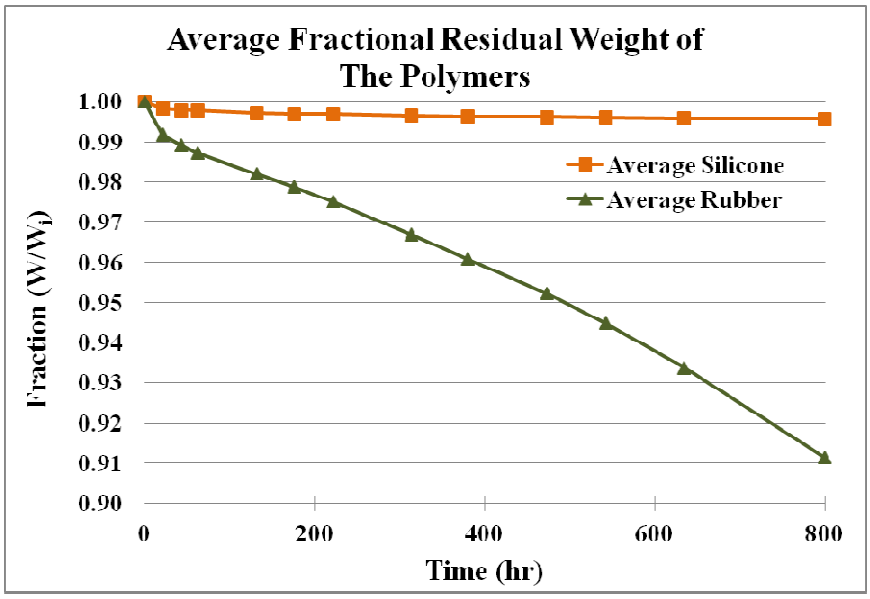

Figure 15: Average fractional residual weight of the rubber seal $(W_R/W_{R\text{-}i})^{avg}$ and the silicone elastomer $(W_C/W_{C\text{-}i})^{avg}$

It is important to note that these samples were prepared approximately 6 weeks prior to the start of the experiment. Therefore, both silicone elastomer and rubber seal absorbed moisture from the room environment during the period between specimen preparation and start of the experiment. Diffusivity of moisture in silicone elastomer at 155°C can be extracted from the Arrhenius model presented in Equation (15). The constants of the Arrhenius model were extracted based on moisture absorption experiment conducted in sources [38, 39].

$$D_{SE} = (5.48E-6) * \exp\left(\frac{4.390E-20}{k*T}\right) \quad \textbf{(15)}$$

D_{SE} = Diffusivity of moisture in silicone elastomer
k = Boltzmann constant

Source [40] indicates that time for a material to attain 99.9% of its maximum possible moisture content in a 1-D problem can be estimated by Equation (16).

$$t_m = \frac{0.67 * s^2}{D_x} \quad \textbf{(16)}$$

t_m = Time for polymer to attain 99.9% of its maximum possible moisture content
D_x = Diffusivity of moisture in polymer in the direction normal to the surface
s = Thickness of the polymer if moisture is exposed from both sides

Using Equation (16), a rough estimation of the time frame for the moisture to escape the silicone elastomer is determined to be 20 hours. By assuming the same diffusivity of moisture in rubber seal, the time frame for moisture to escape the rubber seal is determine to be 2 hours. In addition to the moisture, rubber seal samples also contained electrolyte which was absorbed from the capacitor (these rubber seal samples were removed from capacitors). Based on FEA modeling presented later in Chapter 3 of this paper, diffusivity of electrolyte inside rubber seal at 155^{o}C can be estimated to be 2.713E-11m^2/s. Again, using Equation (16) the time frame for electrolyte to escape the rubber seal can be estimated to be 200 hours.

Final weight measurement needed to estimate the weight of electrolyte inside the capacitors under test, was the weight history of all other components; aluminum can, anode and cathode foil, leads, and paper separator. These components will be referred to as capacitor

components for sake of simplicity in the text. In order to determine the weight of capacitor components five additional capacitors were disassembled, the rubber seals were removed and capacitor components including the electrolyte impregnated in the paper were measured. Then these components were dried out. Final 'dry' weight of these components was measured, which excluded the electrolyte. The resulting measured weight was considered to be due to all components of capacitor excluding the rubber seal and the electrolyte. The average value of this measurement was then subtracted from both unpotted and potted capacitors under test. The final weight of capacitor components excluding the rubber sealant and electrolyte are presented in Figure 16.

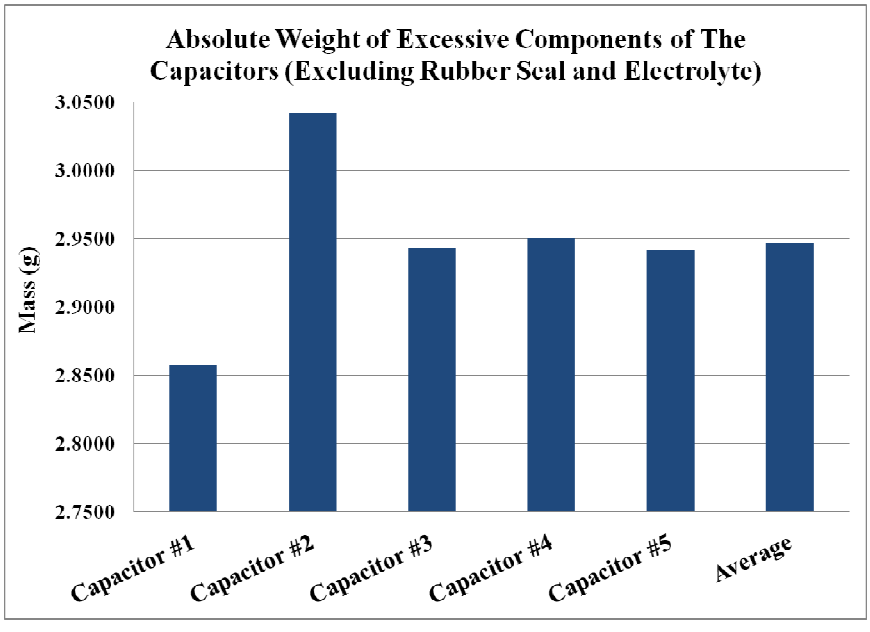

Figure 16: absolute weight measurement of excessive components (W_k^{avg})

Based on all the measurements conducted on the weights, the weight of the electrolyte can be determined approximately. The calculated absolute weight of the electrolyte inside the capacitors is presented in Figure 17 and Figure 18.

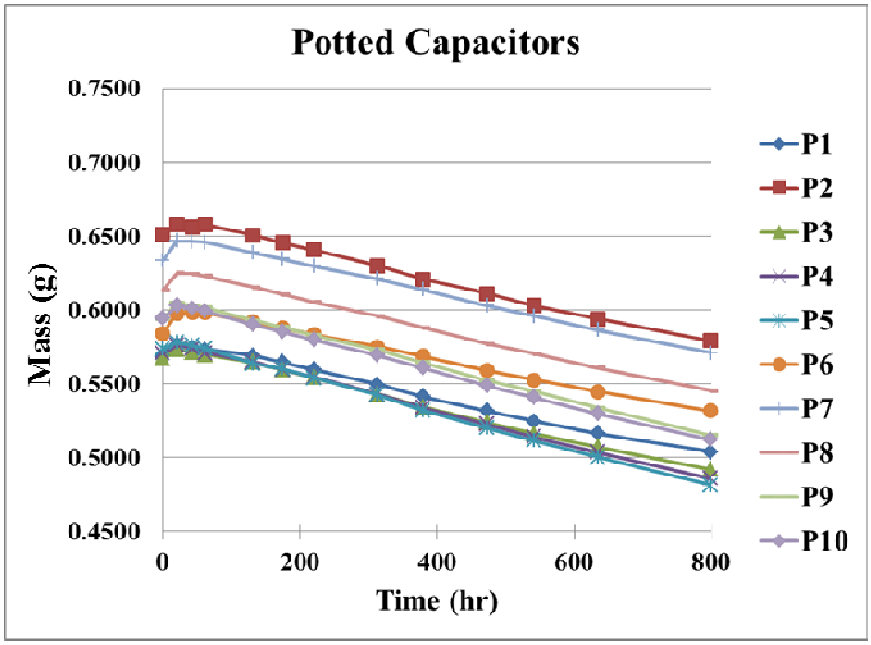

Figure 17: Calculated absolute residual weight of electrolyte inside the potted capacitors ($W_{E\ Potted}$)

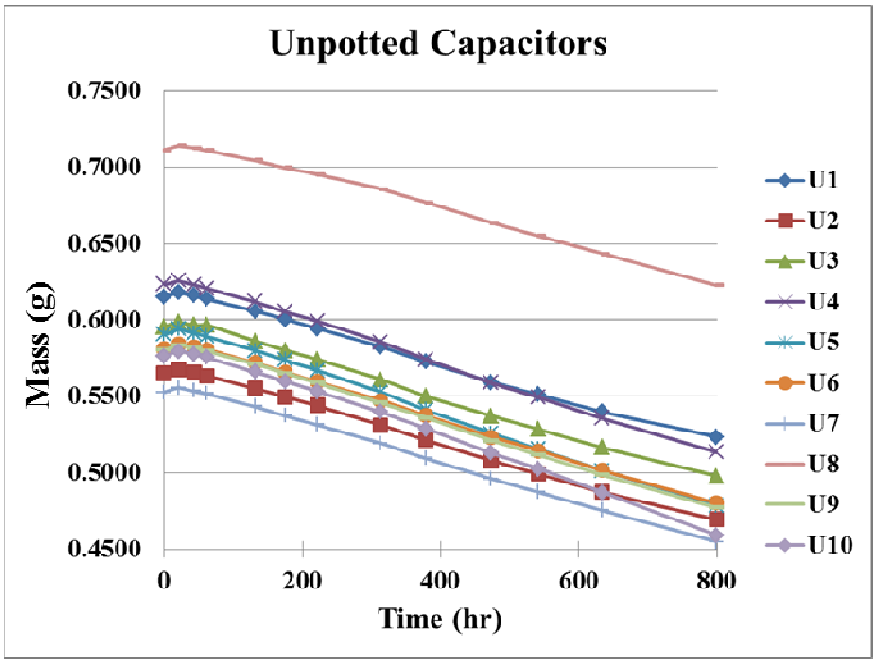

Figure 18: Calculated absolute residual weight of electrolyte inside the unpotted capacitors ($W_{E\ Unpotted}$)

One important conclusion from the calculated absolute weight of electrolyte from the unpotted capacitors is specimen U8 (unpotted 8) which contains more electrolyte than the rest of the capacitors. The fact that U8 contained more electrolyte is observed in the next two sections which are the capacitance and ESR. The absolute weight indicated that over time all tested capacitors lose weight, however, in the second reading the capacitors indicated an anomalous increase in electrolyte mass. When the fractional residual weight of polymers was observed, there was a sudden drop in the weights of both potting compound and rubber seal. The exact reason for this is unclear. However, one reason for this weight loss in the rubber seal could be that the initial residual electrolyte started to vaporized into the chamber. Another reason for this weight loss could have been loss of

the moisture which was gained from the room environment during the period between specimens preparation and the final test (approximately 6 weeks). Therefore, referencing all the readings to the initial reading for fractional residual calculation resulted in an initial increase in weight of the electrolyte inside the capacitors which does not physically make sense. Therefore, the fractional residual electrolyte was referenced with the second measurement in the reading. This allowed a relative comparison among the two populations. Figure 19 indicates the fractional residual weight of the electrolyte in both populations. Finally Figure 20 indicates the average plot of the two populations.

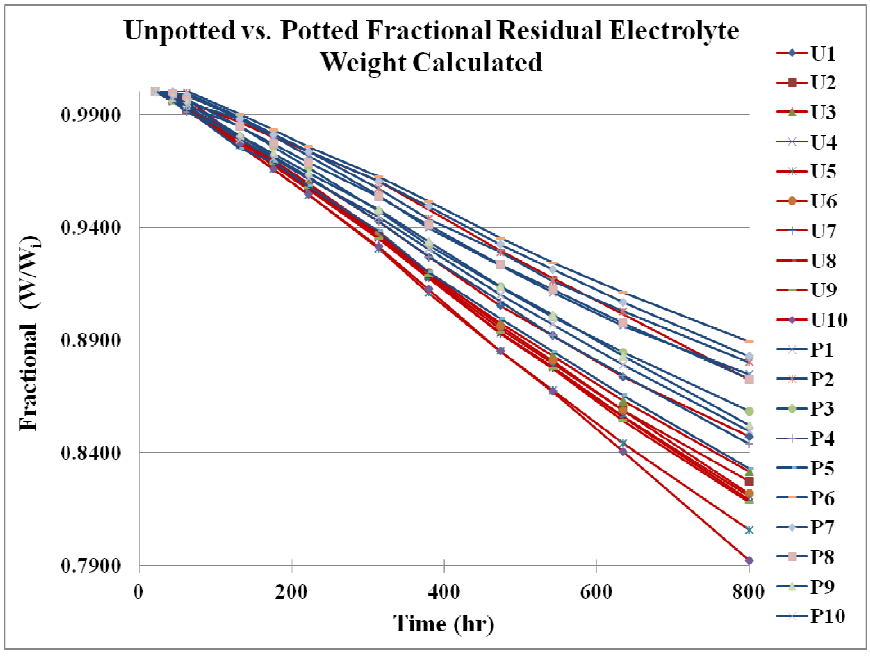

Figure 19: Calculated fractional residual weight of electrolyte inside the unpotted (red) vs. potted (blue) capacitors

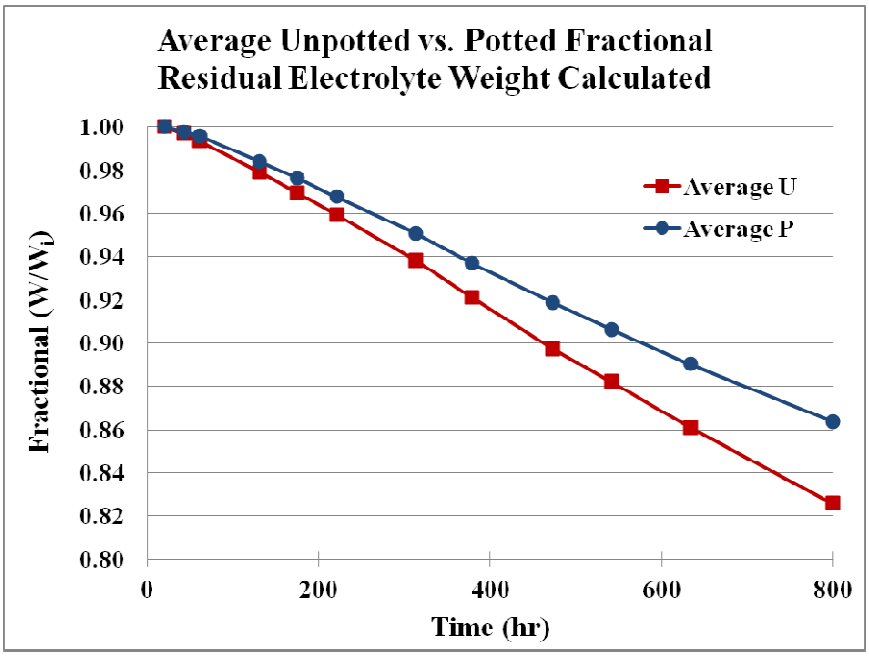

Figure 20: Calculated average fractional residual weight of electrolyte inside the unpotted (red) vs. potted (blue) capacitors

The results presented from the fractional residual weight of electrolyte indicate that the potted capacitors do in fact lose less weight than the unspotted capacitors. This indicates that the fractional amount of electrolyte leaving the system as a whole is less for the potted capacitors than for the unpotted capacitors, relative to the initial measurement. The limitations of these measurements are the following: (i) unique weight of rubber and capacitor components for each specimen is unknown, therefore, population averages are used; (ii) exact mass loss of each polymer is unknown, therefore, a side experiment was conducted and the mass loss of polymers was averaged; (iii) the mass of electrolyte leaving the system as a whole is measured, but the mass of electrolyte escaping the impregnated

separator paper is not measurable. Next, the electrical properties of the two populations will be compared.

2.3.2 ESR

According to many sources in the literature, as capacitors age at high temperatures, electrolyte vapors escape the capacitor and result in an increase in the ESR parameter of the capacitor [10] [6]. Figure 21, which is the absolute ESR value from this experiment for both potted and unpotted capacitors, illustrates this behavior as expected. It is important to note that since ESR is temperature dependent, these measurements were conducted at room temperature after the capacitors cooled down.

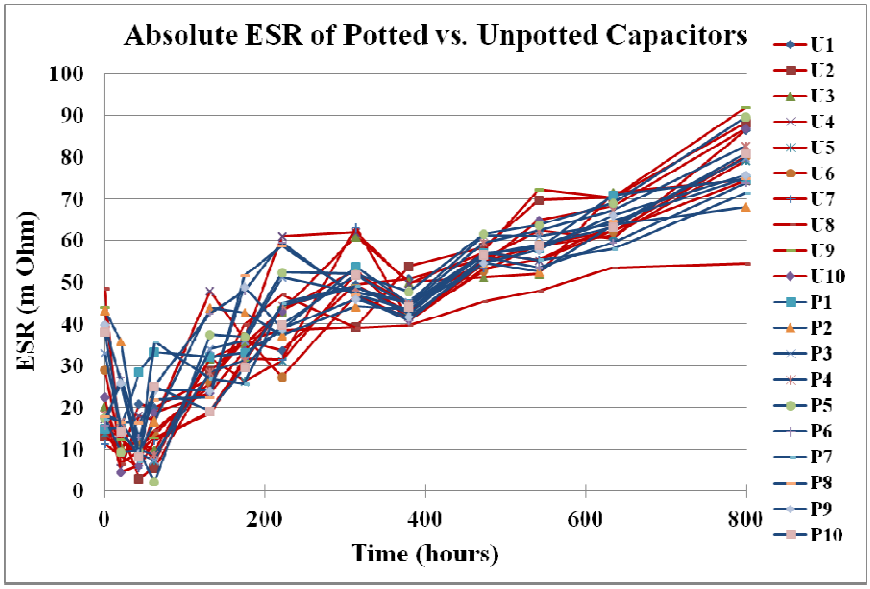

Figure 21: Absolute ESR value for the unpotted (red) vs. potted (blue) capacitors

As mentioned in the Section 2.2.2 ESR, the additional 6.5mm length of lead covered by the silicone elastomer in the potted capacitors results in slightly higher ESR measurement in that population. Therefore, the fractional value of ESR ($ESR_{current}/ESR_{initial}$) needs to be compared. However, from the absolute ESR values, it can be seen that the ESR value of all capacitors drops after 20 hours of 155°C exposure. One explanation of such an effect could be that it is not clear how long these capacitors have been stored at room environment before the start of the test. However, from the time these capacitors were purchased to the start of the test was approximately 5 months. This indicates that when the capacitors were subjected to high temperature the electrolyte inside could have dissolved and produced a more uniform electrolyte solvent which resulted in a decrease in ESR. In order to find a reference value for the ESR of each capacitor, it can be a safe assumption to take the first 3 reads up to 42 hours and average the ESR value of each capacitor and use that value as the reference to determine the fractional ESR change. Equation (17) presents the fractional change calculation of the ESR where subscripts are as follows $ESR_{\text{reading, specimen \#}}$:

$$ESR_{reference} = \frac{\left[ESR_{1,1} + ESR_{2,1} + ESR_{3,1}\right]}{3} \quad \textbf{(17)}$$

Based on this calculation Figure 22 illustrates the fractional ESR value for both unpotted and potted capacitors and Figure 23 presents their respective average.

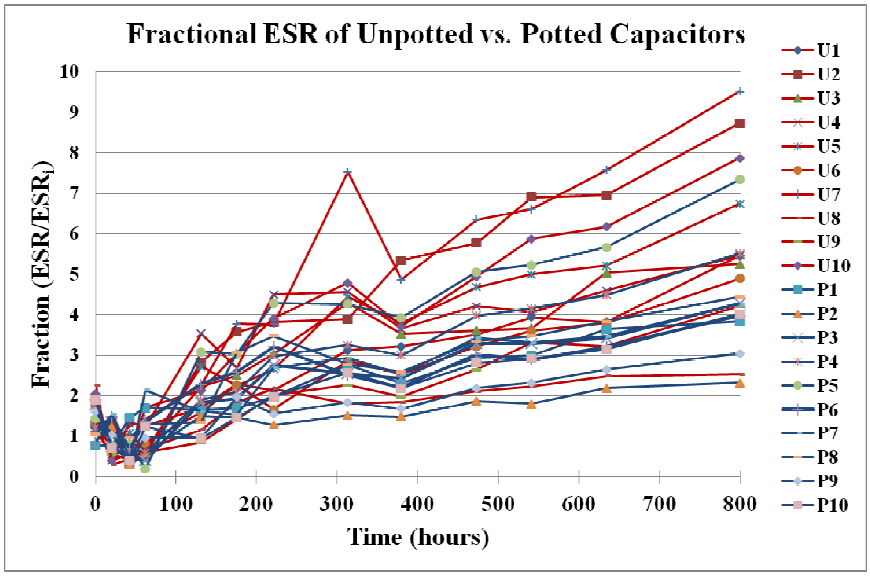

Figure 22: Fractional ESR value for the unpotted (red) vs. potted (blue) capacitors

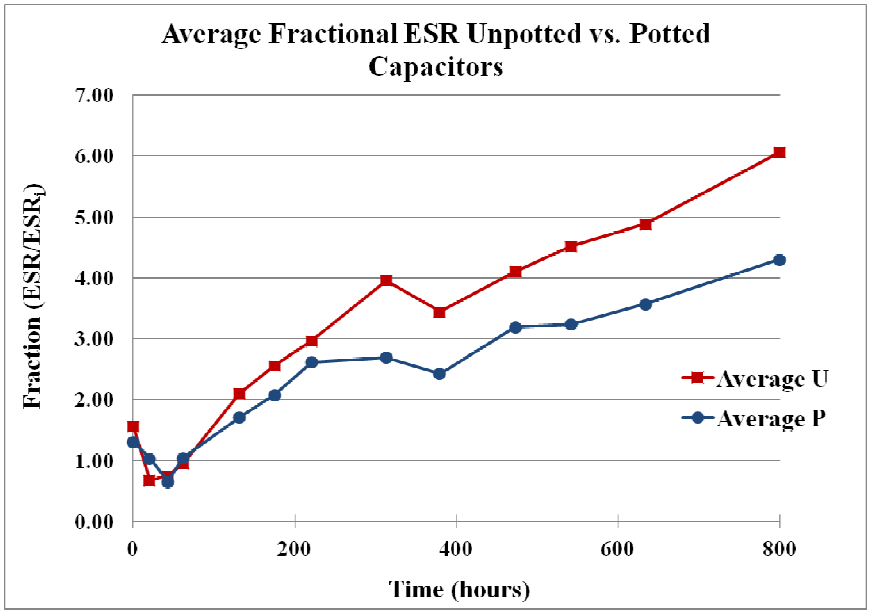

Figure 23: Average fractional ESR value for the unpotted (red) vs. potted (blue) capacitors

Figure 23 above indicates that the unpotted capacitors' fractional ESR increased more in comparison with the potted capacitors. Interestingly, some correlations exist between the fractional ESR values and the

fractional weight loss values. As shown in Figure 22, component P5 has the highest ESR degradation compared with the other potted capacitors and in Figure 19, component P5 had the highest rate of mass loss compared to the other potted capacitors. Although, U8 is an outlier in the experiment because it contained more electrolyte then the other samples Figure 18, it is still a good extreme case to observe. U8, which has shown the least amount of fractional residual electrolyte weight in Figure 19, also has the lowest fractional ESR among most of the capacitors, as seen in Figure 22. A One Way ANOVA test was conducted at each time between the unpotted and potted capacitors to determine if there is any statistically significant difference between the two means. As shown in Figure 24, two curves are plotted of the F-value from the ANOVA test. Considering 95% confidence, if F-value at each instant exceeds the F-critical, ANOVA test suggests that there is a significant difference between the two set of data. For this analysis two curves are plotted; (i) one includes the outlier U8, and (ii) one excludes the outlier U8. For both cases, it is clear that the mean fractional changes in ESR of the two capacitor populations are proven to be statistically different beyond 300 hours. As seen from graph showing the mean of fractional ESR of unpotted vs. potted, the potted capacitors depicted slower degradation rate. Therefore, the ESR results suggest that there is a correlation between electrolyte loss and increase in ESR. As seen from the fractional residual electrolyte weight loss,

the potted samples lose less weight and, therefore, have slower ESR degradation.

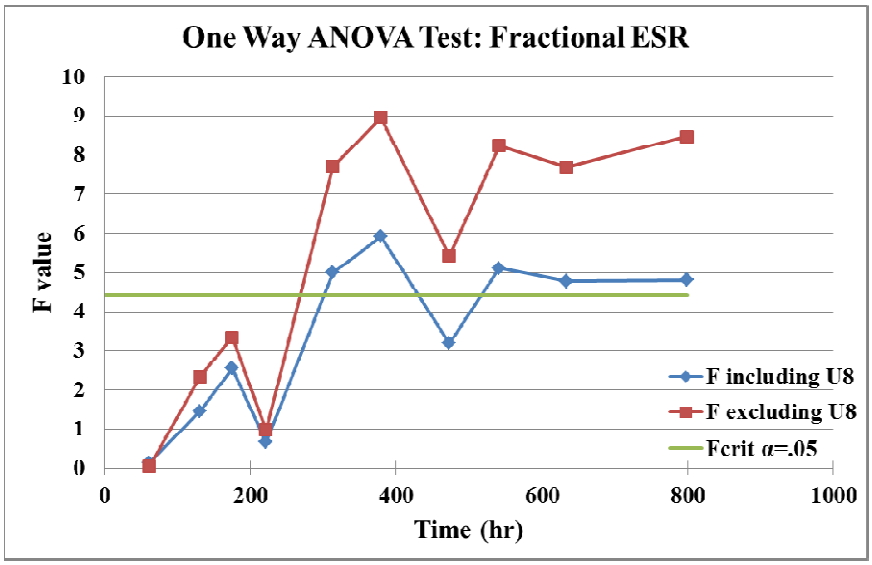

Figure 24: One way ANOVA test on fractional ESR of the potted vs. unpotted population (Once F-Value exceeds the $F_{critical}$-value it can be state that the mean of the two populations statistically vary with 95% confidence)

The results of the ESR suggest that the encapsulation process does play a significant role in decelerating the ESR degradation process.

2.3.3 Capacitance

The capacitance is expected to decrease as the electrolyte dries out. This effect was observed based on the raw experimental data from both populations, as shown in Figure 25. Red lines represent the unpotted capacitors and the blue lines represent the potted capacitors. As mentioned earlier in the paper, many sources suggest that the electrolyte vapor leakage results in a capacitance drop. Therefore, the results are in agreement with the expected behavior. Both populations

enter a steady state region immediately after 24 hours up-until 380 hours, which then decreases their degradation rate.

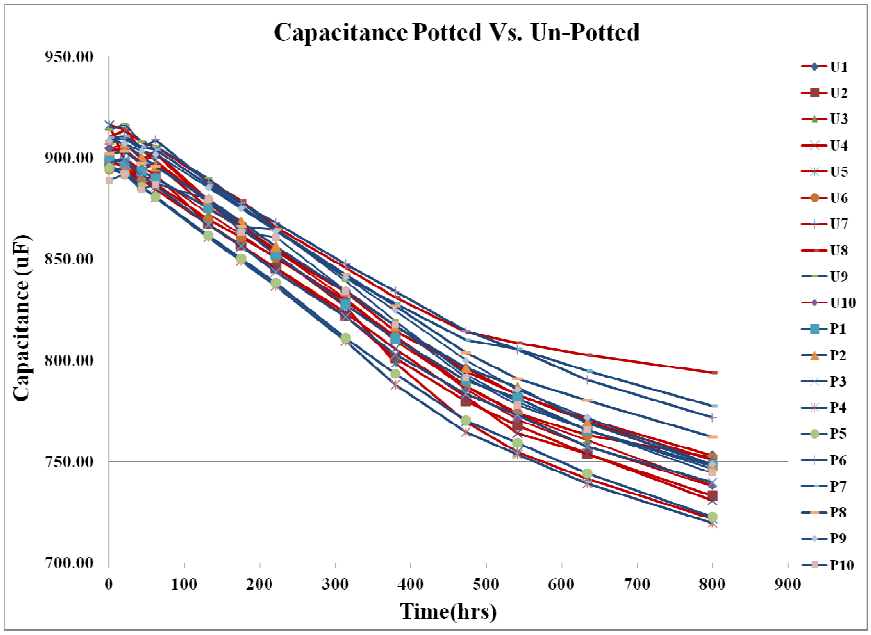

Figure 25: Absolute capacitance comparison unpotted (red) and potted (blue)

Due to the fact that the capacitors' initial starting capacitances vary, it is a better approach to compare the two populations by observing their fractional capacitance. The fractional capacitance ($C_{current}/C_{initial}$) plot is shown in Figure 26. Although there is very large variation in the fractional capacitance value beyond 470 hour, with careful observation a trend is observed in which the majority of the two populations are found to gradually drift apart. The majority of the potted capacitors indicate slightly slower capacitance degradation in comparison with the unpotted samples. However, again U8 indicated the least amount of capacitance degraded among all of the other capacitors. As

observed from the absolute weight of electrolytes (Figure 19) this specific capacitor contained much more electrolyte then all of the other capacitors. Therefore, this capacitor is considered to be an outlier in comparison with the other 19 capacitors in the test condition.

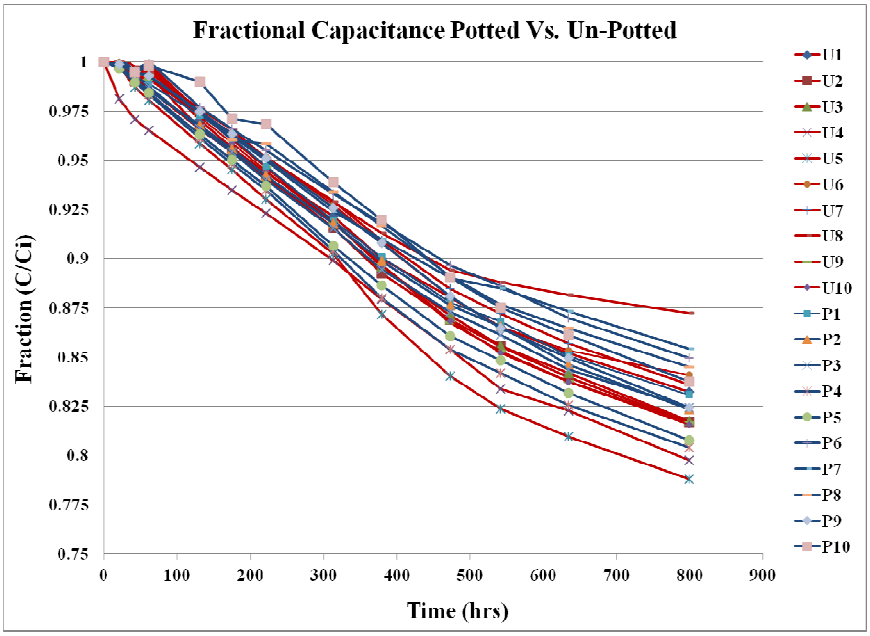

Figure 26: Fractional capacitance plot for unpotted vs. potted capacitors

Another visualization that helps outline the difference between the two sets of capacitors (potted vs. unpotted) is shown in Figure 27 and Figure 28. Two plots are presented that illustrate a normalized mean with 90% confidence bounds on both sides. Figure 27 includes the outlier (U8). Figure 28 is the same plot but excluding the outlier (U8). As seen in Figure 28 the unpotted 90% confidence bound narrows down from 41.48 µF to 12.93 µF by removing only that single outlier. Confidence bounds of unpotted capacitance reduce by approximately 70%. Figure 28 illustrates that the upper 90% bound of the unpotted

capacitor is approximately equals to the mean of the potted capacitors. Although there is a very slight different between the two population of capacitors, potted capacitors illustrate slightly less degradation in capacitance then the unpotted capacitors.

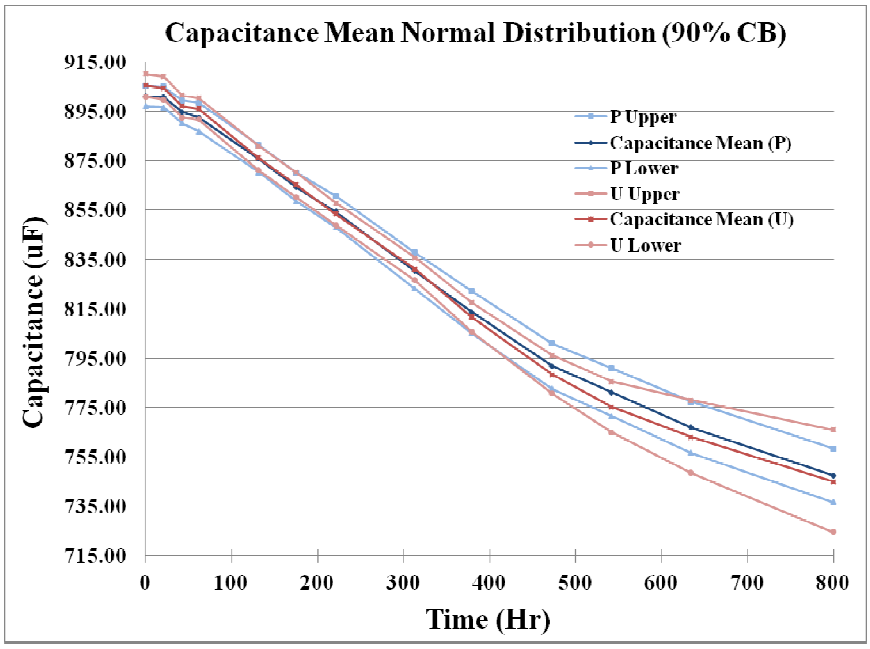

Figure 27: Normal distribution mean with 90% upper and lower boundary including outlier U8

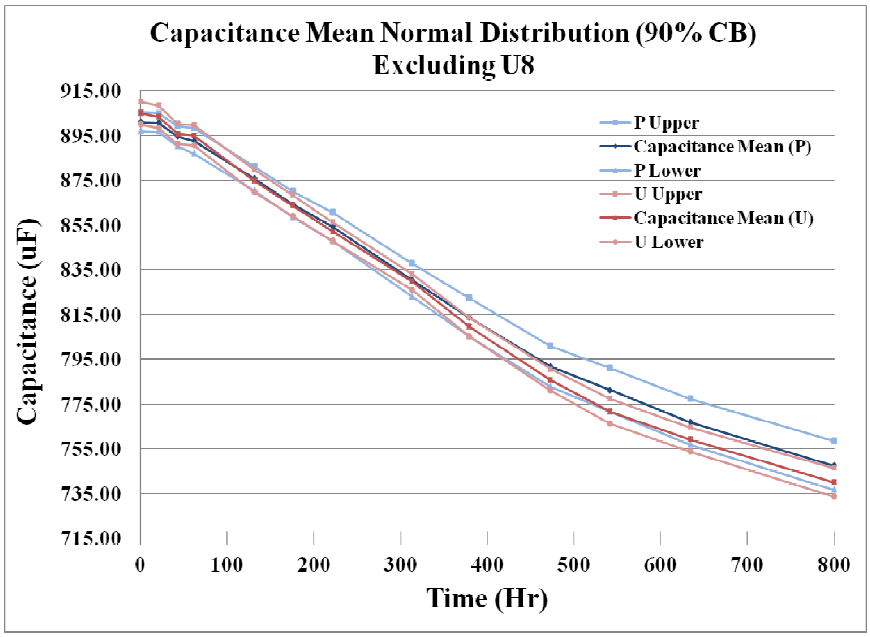

Figure 28: Normal distribution mean with 90% upper and lower boundary excluding the outlier U8

Furthermore, so far, all the visual inspections indicate a very small difference between the capacitance degradation of the two populations. In order to better quantify the difference among these populations, a single factor ANOVA test was conducted on the capacitance of both populations. At each measurement the mean of the two data were compared using the statistical approach of single factor ANOVA with 95% confidence. The single factor ANOVA test is conducted on the fractional capacitance due to the fact that test becomes more sensitive to the comparison between the two populations. As shown in the Figure 29 below, y-axis is the F-value of the ANOVA test which is used to either accept or reject the null hypothesis that the means are not significantly different.

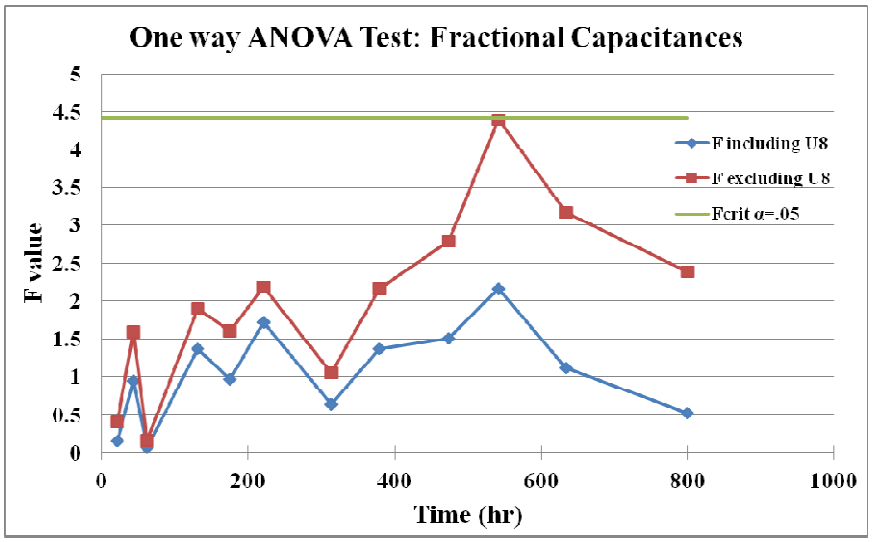

Figure 29: One way ANOVA test on fractional capacitance of the potted vs. unpotted population (Once F-Value exceeds the $F_{critical}$-value it can be state that the mean of the two populations statistically vary with 95% confidence)

The one way ANOVA test on the capacitance indicated a divergent trend which did not reach the minimum threshold to be considered statistically significant during the test preiod when excluding U8.

2.3.4 Encapsulated Capacitor Delamination Analysis

During the high temperature testing, visual inspections indicated that the silicone elastomer had delaminated from the lead for all the potted specimens. The delamination was observable only during the high temperature when the samples were uniformly at 155^{o}C. The reason for such observation is due to the mismatch in coefficient of thermal expansion (CTE). Comparing the CTE between aluminum (22.2 ppm/^{o}C) and silicone elastomer (200 ppm/^{o}C) and copper (17 ppm/^{o}C), with a simple ratio comparison it can be determined that the silicone elastomer will roughly expand 9 times more than the aluminum and 12

times more than copper. Therefore, an investigation was required to determine the depth of the delaminations. One common method that is used to visually observe cracks or delamination is dye penetration. In order to confirm that the dye penetration would be able to penetrate through the delamination a dummy sample was made and was exposed to 155^{o}C. After the specimen was exposed to 155^{o}C for one day and the delamination was visually confirmed, the specimen was submerged into the dye and was placed in a vacuum chamber for 30 min. This allowed the air to escape and dye to fill all and stained the delaminated areas. The result of the dummy sample is shown in Figure 30.

Figure 30: Dummy sample to observe dye penetration into the delaminations

After seeing the dye clearly visible on the dummy sample the same procedure was conducted on one of the actual test specimens (P5), which had the lowest fractional residual weight relative to all the potted specimens (Figure 19). Specimen P5 indicated that it had the highest mass loss relative to the other potted samples. Therefore, it

was the best case to observe for possible delamination. The result of the dye penetration test is shown in Figure 31.

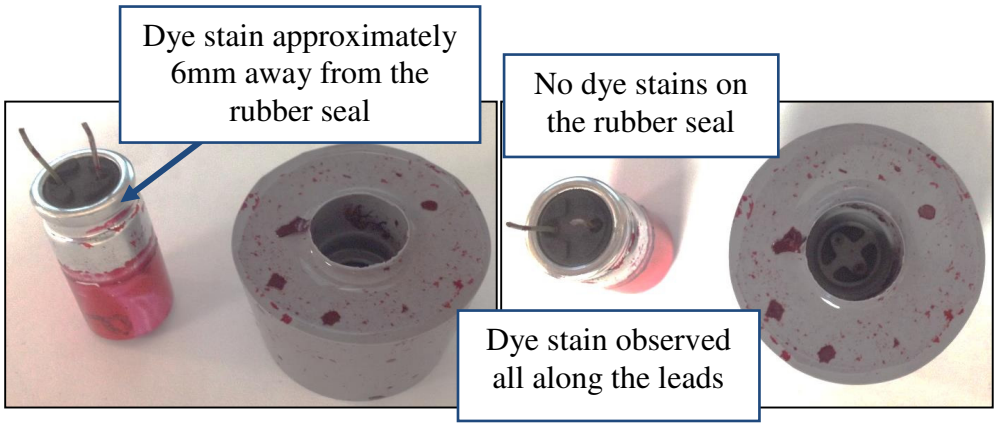

Figure 31: Actual potted specimen P5 taken from the experiment after 800 hours of test at 155^{o}C

Dye penetration results indicated that the silicone elastomer and rubber interface were perfectly sealed. However, stains of dye were visible all the way along the leads. This suggested that any electrolyte vapor that had diffused along the interface of the rubber seal and leads was able to freely escape. On the other hand, the silicone elastomer was a barrier to any electrolyte that leaked through the bulk of the rubber sealant. The delamination around the aluminum case reached the crimped region but was approximately 6mm away from the surface of the rubber seal. This information was very critical in the modeling section of the thesis. This delamination between the potting compound and the lead is implemented as a boundary condition in the potted capacitors, as discussed later in Section ***3.2.2** Boundary Condition*.

Chapter 3: Finite Element Analysis

This chapter will cover the use of finite element modeling of mass transport, to explore the effect of encapsulation on electrolyte vapor leakage in electrolytic capacitors.

3.1 Objective And Methodology

The objective of this FEA analysis is to gain insights into the electrolyte leakage process through the rubber seal and encapsulation (if any). To develop the model, the average residual fractional weight estimation from the experiment, is first used as guidance to roughly estimate reasonable material properties. Modeling mass transport in this problem is a challenging task due to the fact that the material properties of both of the polymers (encapsulation material and rubber seal) are required. Mass transport material characterization requires absorption or desorption test to extract both diffusivity and solubility. Since permeability is the product of diffusivity and solubility, only two of these three properties need to be characterized. Due to the assumptions and simplifications in electrolyte vapor leakage experiments, only the fractional residual electrolyte weight loss can be used to estimate reasonable parameters for this study.

3.1.1 Thermal-Moisture Analogy

It is important to note that this FEA analysis is purely an isothermal mass transport analysis since the experiment was conducted at one single temperature and there are no sources of heat generation in the test specimen. The thermal analysis code of a commercial FEA software is used to compute the moisture analogy. Therefore, the results are interpreted as mass transport and not heat transfer.. For a single material there are multiple solution methods such as direct methods based on absolute concentration or advanced analogies based on 'wetness' or on 'normalized concentration'. However, since the problem of interest contains multiple materials, the modeling approach based on 'wetness' cannot be used because it violates continuity conditions at interfaces [19]. The problem is also isothermal therefore the normalized concentration can be used, which is presented below:

$$\emptyset = \frac{C}{S} \tag{18}$$

where concentration (C) is normalized by solubility (S) and the result is ϕ which can also be interpreted as moisture partial pressure. It is important to note that partial pressure is just a pseudo variable for a solution which insures continuity between two materials and should not to be confused with partial vapor pressure. The normalized analogy assumes that the solubility is constant, however, in reality solubility is temperature dependent. Therefore, this analogy will work

only for an isothermal problem [19]. Since the problem of interest does not include ripple current which cause heat generation, there are no temperature gradients in the polymers and therefore the normalize analogy holds. Table 1 presents the conversion required for the thermal-moisture normalized analogy scheme.

Table 1: Thermal-moisture analogy scheme

	Heat transfer	**Normalized analogy**
Field Variable	Temperature, T	Normalized concentration, ϕ
Density	ρ	1
Conductivity	κ	DS
Specific heat	c_p	S

3.1.2 Approach

Conducting experiments such as absorption or desorption is challenging when it comes to electrolytes. Liquid electrolyte composition is proprietary and manufacturers do not disclose this information. However, due to the simple nature of the problem, an attempt can be made to estimate material properties, guided by the electrolyte weight loss experiment. The process used to estimate the material properties is shown in Figure 32. Details of this approach are explained in Section **3.4** Material Property Estimation.

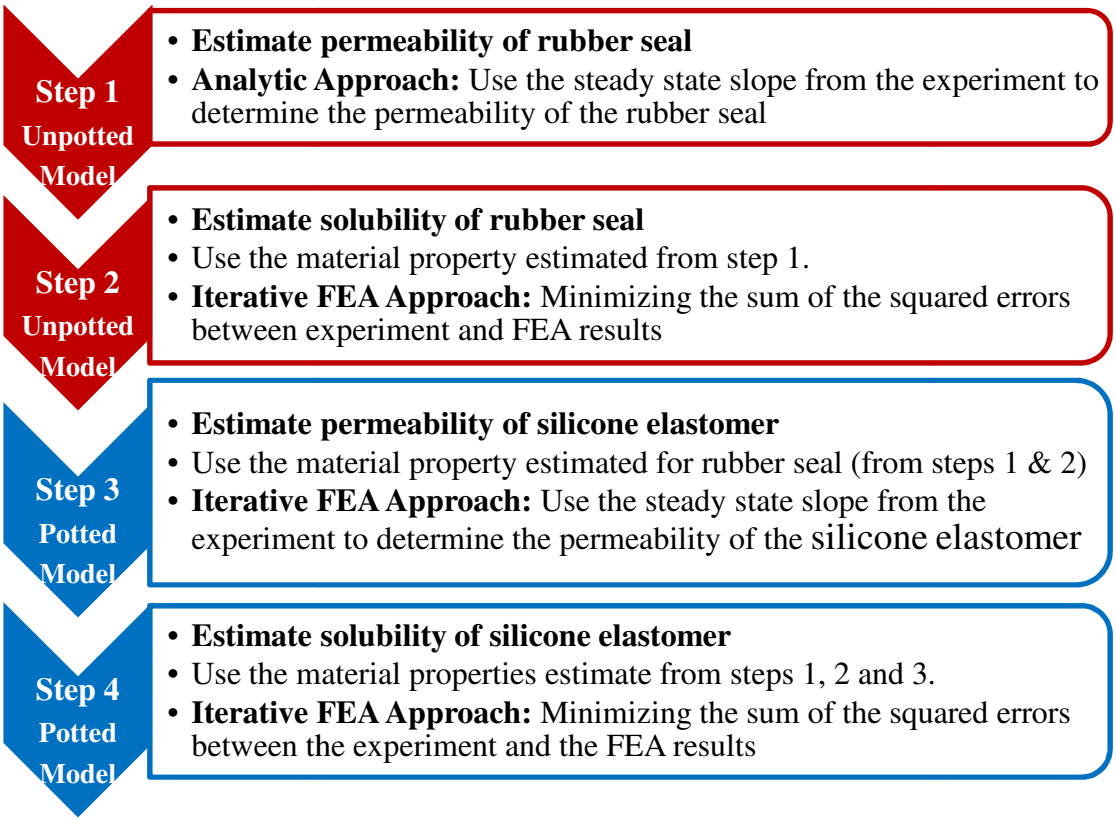

Figure 32: Step by step approach used to estimate the mass transport material properties of electrolyte through the polymers

The geometry of the tested electrolytic capacitor can be simplified to a single lead axisymmetric model. As a result, the mass transport effect can be modeled as a 1-D problem, as shown in Figure 33. Note the simplified model does not include the crimp of rubber seal.

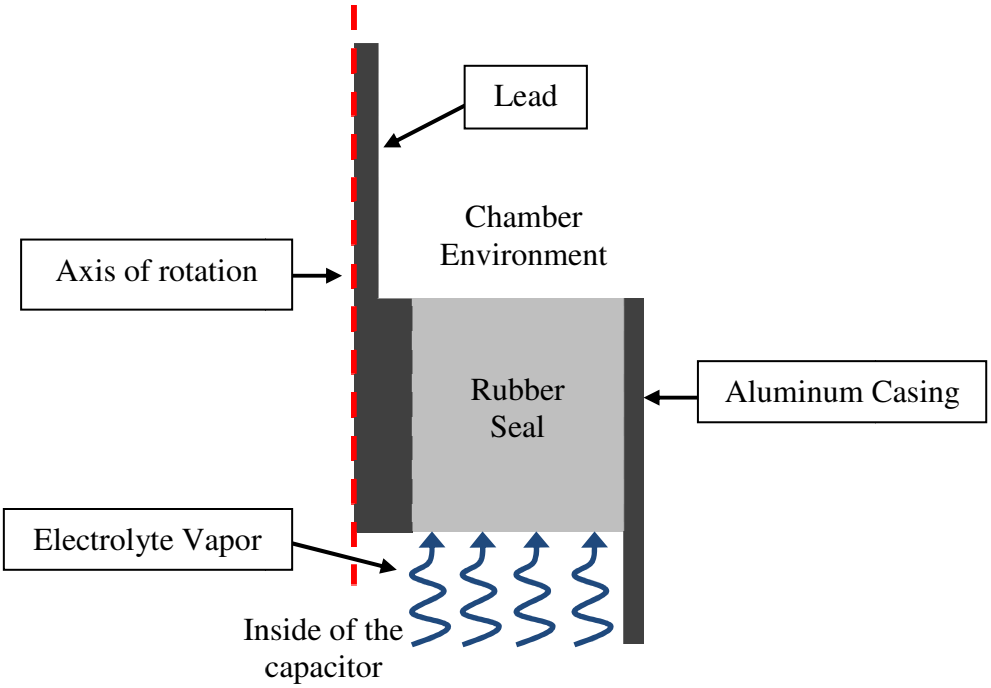

Figure 33: Simplified illustration of 1-D axisymmetric model of electrolyte vapor leakage (schematic not to scale)

Since the only parameter available from the experiment is the physical mass loss of electrolyte from the capacitor, the model must be calibrated using the mass flow out of the rubber seal into the chamber environment. As mentioned in Section *2.3.1 Weight Measurement*, five capacitors were disassembled and their electrolyte mass was measured. This was done by first measuring the electrolyte impregnated paper and then measuring the paper after it dried. Result of this experiment is shown in Figure 34.

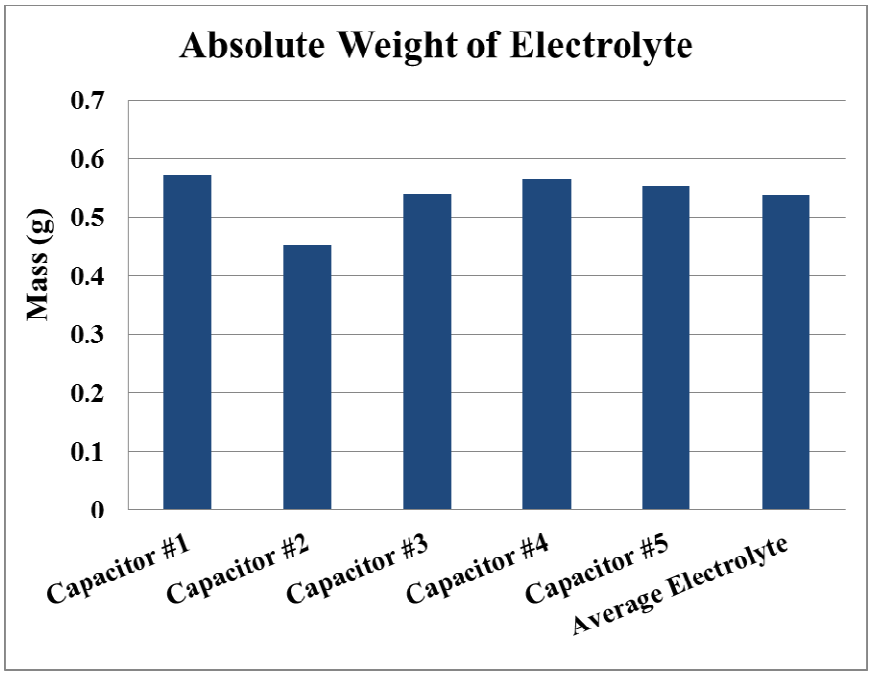

Figure 34: Average weight of electrolyte measured from 5 capacitors

The average weight of electrolyte measured (0.5368g) was assumed to be the initial weight of the capacitor in the FEA model. The initial electrolyte mass loss from the surface of the rubber seal into the chamber environment was assumed to be a loss starting from the average weight of electrolyte. As a result, the model prediction of fractional residual weight loss was plotted and calibrated to the experiment.

3.2 Model

This section will cover first the geometry of the model, then the boundary conditions which are applied, and finally, the mesh used for the model.

3.2.1 Geometry

For sake of simplicity, the capacitor geometry was modeled with a single-lead axisymmetric model. In order to represent the two leads with a single equivalent lead, the total area of the two leads were matched by the total area of the single lead in the model. Therefore a pseudo radius for the FEA single lead was calculated based on Equation (19).

$$r_{in} = \sqrt{\frac{2\,A_{sl}}{\pi}} = 1.41mm \tag{19}$$

r_{in} = radius of the single lead in the FEA model
A_{sl} = Area of single lead of the actual capacitor

Another feature of this model is that it captures the effect of interfacial leakage between the lead and rubber seal. In order to capture this effect a dummy material was introduced between the lead and the rubber seal, whose diffusion constants were tailored to represents the interfacial leakage. In order to determine the volume of the dummy interfacial region, another pseudo radius (r_{out}) was introduced. The sum of the circumference of the two leads in the capacitor was set equal to the outer circumference of the interfacial material, as shown in Equation (20).

$$r_{out} = \frac{C_{sl}}{\pi} = 2.00mm \quad \textbf{(20)}$$

r_{out} = outer radius of the interface (dummy) material
C_{sl} = circumference of single lead of the actual capacitor

As a result, the geometry of the simplified unpotted capacitor is shown in Figure 35. Rest of the dimensions were measured from the capacitors.

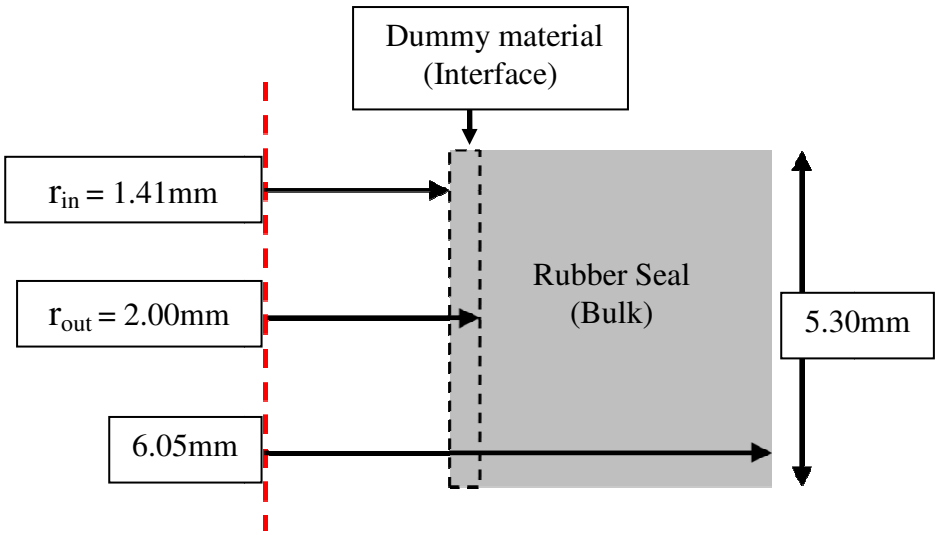

Figure 35: The rubber seal axisymmetric model with single lead and the interfacial material calculation (schematic not to scale)

Figure 36 presents the dimensions of the average potted capacitor. These dimensions were used to develop the finite element model the potted capacitors.

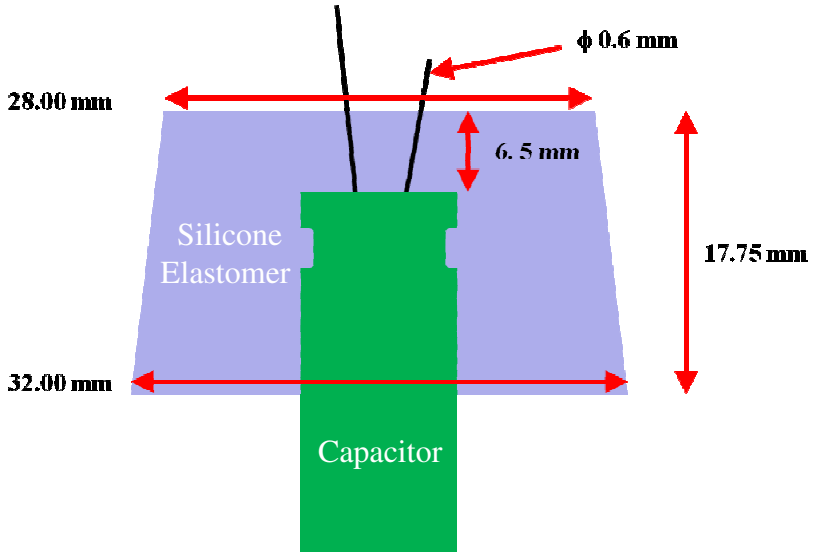

Figure 36: Dimensions of the potted capacitors (schematic not to scale)

Based on the dimensions measured, the simplified geometry for the potted capacitor is presented in Figure 37. For simplicity of the model all angles were assumed to be 90°. It is important to note that the diameter of the lead in the actual capacitor changed from 1mm to 0.6mm when extended out of the rubber seal.

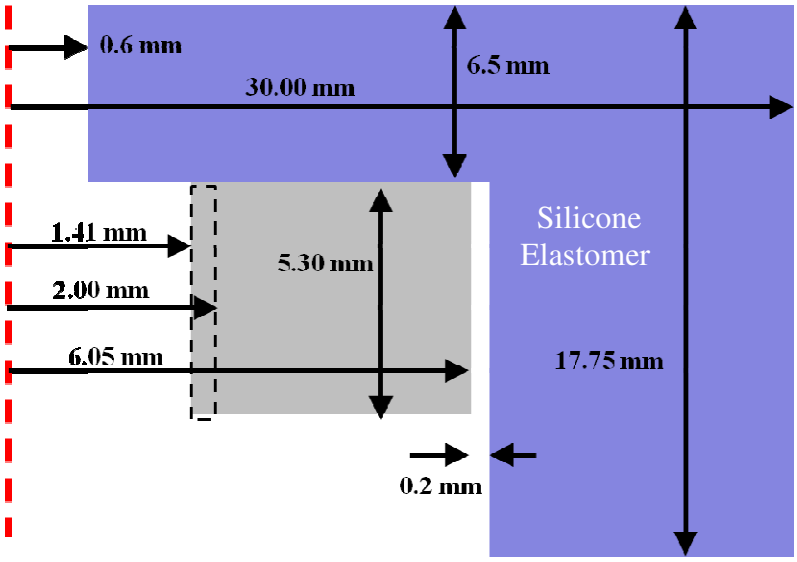

Figure 37: Dimensions of the potted capacitors for the modeling purpose (schematic not to scale)

3.2.2 Boundary Condition

The boundary condition for the normalized concentration thermal-moisture analogy scheme was the internal partial vapor pressure of the electrolyte. Although the electrolyte is not a simple compound, Fourier transform infrared (FTIR) analysis indicated that the main chemical composition of the electrolyte is gamma-Butyrolactone. The vapor pressure of gamma-Butyrolactone as a function of temperature is presented in Handbooks [20]. The vapor pressure of gamma-Butyrolactone at the test temperature (155^{o}C) can be estimated to be 24kPa according to the Handbook. As a result, the partial vapor pressure of electrolyte at the inner surface of the rubber seal, in contact with electrolyte, was set to 24kPa and at the opposite (outer) side was set to 0Pa. The radially outer and inner surfaces were assumed to be insulated. Figure 38 below shows all the boundary conditions applied to the unpotted capacitor. As shown in the figure, a dashed line separates the rubber interface from the rubber bulk.

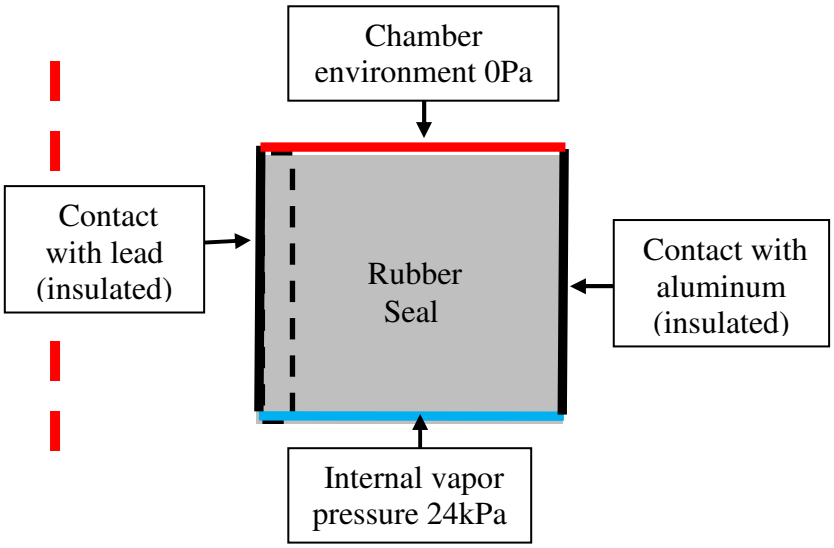

Figure 38: Boundary condition for the unpotted capacitors: insulated (black), internal vapor pressure (blue), and chamber environment (red) (schematic not to scale)

As discussed in Section *2.3.4 Encapsulated Capacitor Delamination Analysis*, encapsulated capacitors contained a delamination between the silicone elastomer and the capacitor leads. Therefore, the vapor pressure 0Pa boundary condition was extended into the delaminated surface region, as shown in Figure 39. As shown in the figure, any leakage through the interface of the rubber seal is free to escape because of the delamination between the potting compound and component lead. Silicone elastomer has only effect on electrolyte leaking through the bulk.

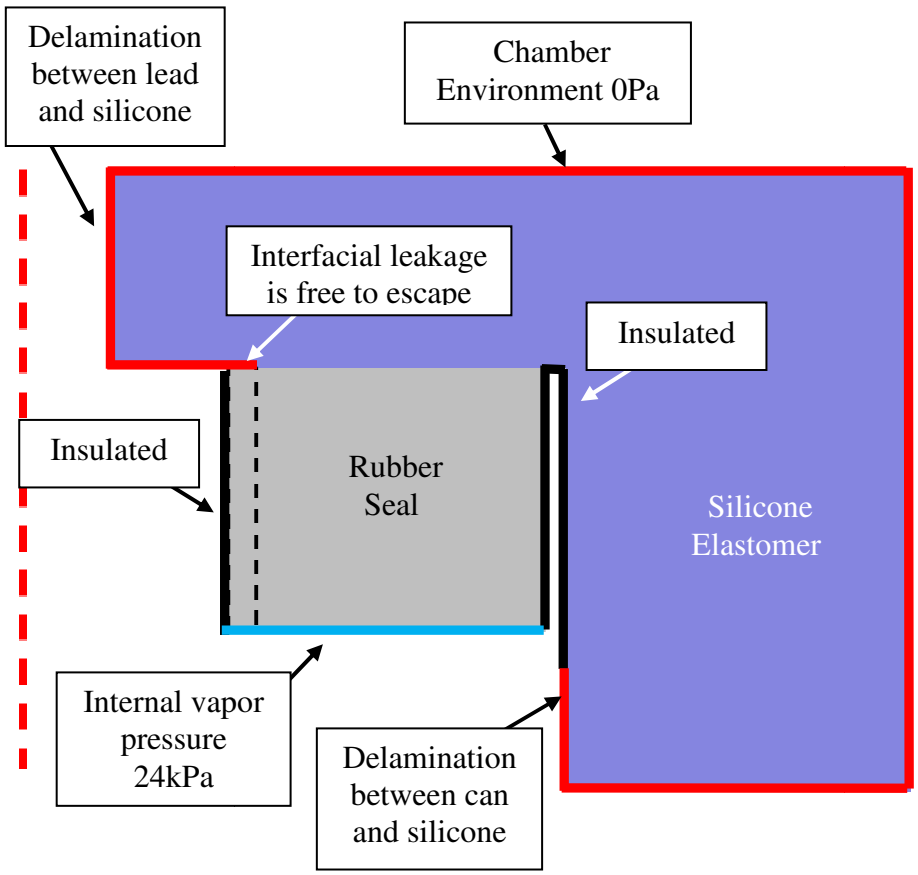

Figure 39: Boundary condition for the potted capacitors: insulated (black), internal vapor pressure (blue), and chamber environment (red) (schematic not to scale)

In reality there is a finite amount of electrolyte present in the capacitor. This indicates that the boundary condition on the inner side of the capacitor must change as a function of time. However, the assumption made was that initially some of the liquid electrolyte vaporized and filled the inner volume of the capacitor. Since it was assumed that the electrolyte leakage rate was lower than the electrolyte vaporization rate, the boundary condition was assumed to be constant 24kPa for the first 355 hours. This assumption was based off of the fractional residual weight presented from the experiment.

Finally, the initial normalized concentration of electrolyte within the polymeric seals was assumed to be 0Pa for both unpotted and potted models. In reality the rubber seal initially does contain some residual electrolyte at time t=0, since it is in direct contact with electrolyte. However, since the residual amount is not known, for ease of modeling, this initial concentration is ignored. The 0Pa normalized concentration is a more reasonable approximation when considering the silicone elastomer since the encapsulant is not in direct contact with the electrolyte. The encapsulation process was done approximately 1 month prior to the experiment and the samples were stored at room temperature.

A critical piece of information from the experiment which will guide the material characterization is the average fractional residual weight for both unpotted and potted capacitors. Figure 40 is a recap of the same plot presented in Section *2.3.1 Weight Measurement*.

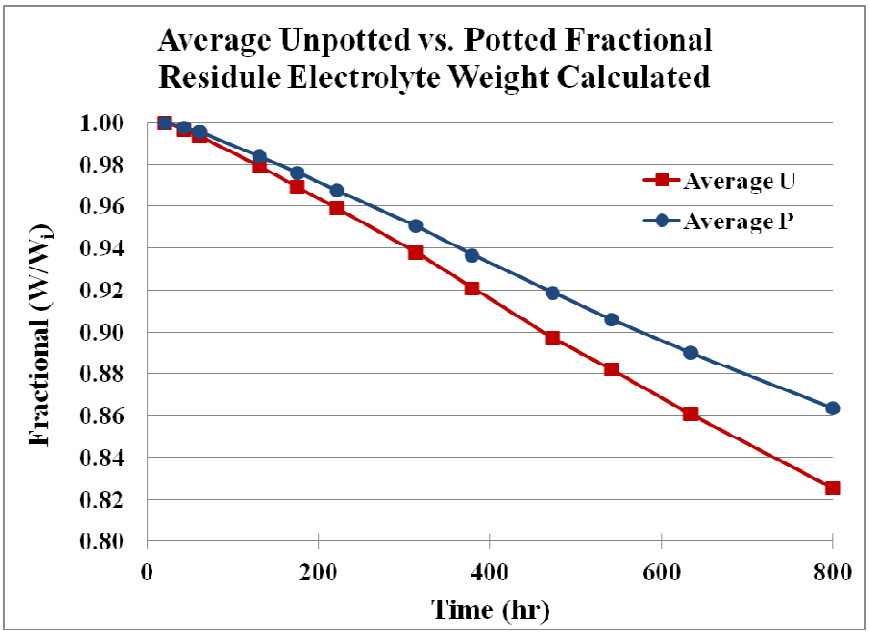

Figure 40: Calculated average fractional residual weight of electrolyte inside the unpotted (red) vs. potted (blue) capacitors from the experiment

One important factor about the residual electrolyte weight measurement was the steady state slope. The steady state behavior appeared to occur beyond 200 hours. In order to make closer observations, Figure 41 was constructed. Figure 41 is the time history slope of Figure 40.

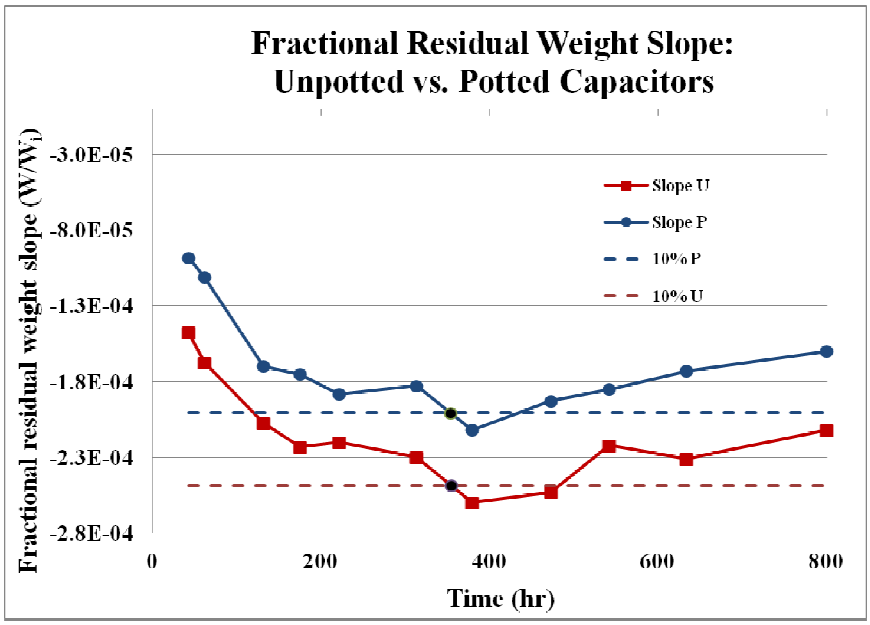

Figure 41: Slope of the average fractional residual weight of electrolyte inside the unpotted (red) vs. potted (blue) capacitors from the experiment

Figure 41 has a low resolution which is because of long intervals between each measurement. The slope ideally reaches its steepest value when the transport reaches the steady phase; however, due to the resolution of the data, the steady state portion is not easily identifiable. Therefore, 10% of the difference in slope from the initial reading (40th hour) and the absolute maximum slope (355th hour) were plotted from the absolute minimum which is the represented with a dashed line in Figure 41. The dashed value was assumed to be the steady state condition for each population, red dashed line is for unpotted capacitors (-2.485E-4/hr) and the blue dashed line is for the potted capacitor (-2.005E-4/hr). The time at which the low resolution curve crosses the 10% slope selection was approximated to 355 hours. Therefore, this model was developed based on the assumption that up

until 355 hour the electrolyte vapor was supplied from an 'infinite' source.

3.2.3 Mesh

The mesh used for the model consisted of quadratic elements, containing 8-node, serendipity, 2-D elements. The mesh structure and density for the rubber seal was consistent between the unpotted and the potted model. The unpotted model mesh is presented in Figure 42. As seen in the rubber seal, the density of mesh in the interface region was higher.

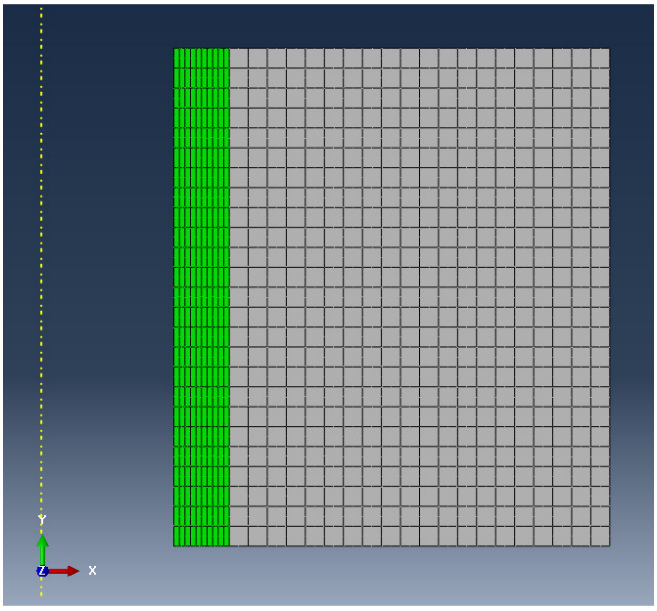

Figure 42: Mesh structure and density of the unpotted model, rubber seal interface (green), rubber seal bulk (grey)

The potted model mesh is presented in Figure 43. In order to match the nodes at the interface between the rubber bulk and the silicone

elastomer, matching meshes were defined for the silicone elastomer and for the rubber seal. The density of the mesh near the lead was higher because the mass flow per unit area of the interface was assumed to be higher than in the bulk.

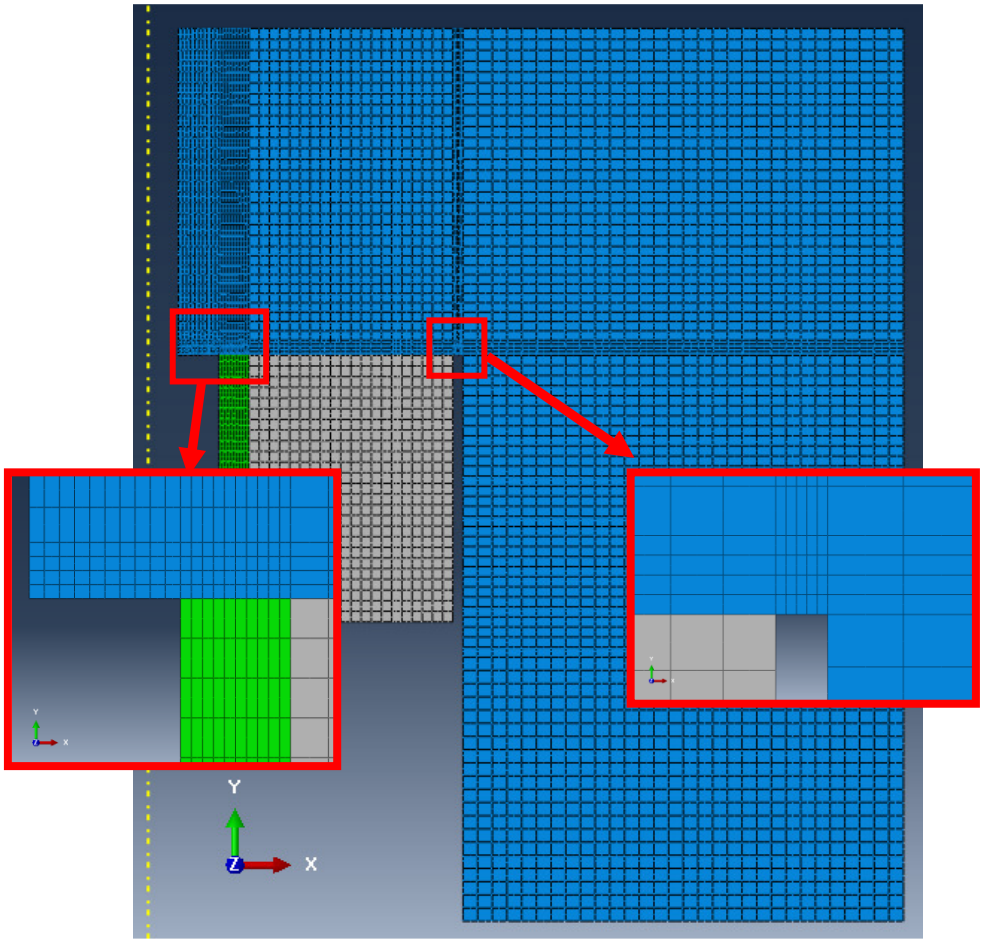

Figure 43: Mesh structure and density of the potted model, rubber seal interface (green), rubber seal bulk (grey), silicone elastomer (blue)

3.3 Output Request

Since the weight measurement of the experiment only detected electrolyte that escaped the rubber seal into the chamber environment, the FEA output request was to measure the mass flux leaving the rubber seal in the positive y direction, as shown in

Figure 44. Equations (21) and (22) indicate that the total mass loss from the unpotted FEA model was the sum of $M_{out\text{-}I}$ and $M_{out\text{-}B}$ as shown in Equation (23).

$$M_{out-I} = \sum_{1}^{j} integrate_{\ over\ time}\left(\vec{J} * A\right)_{elm\ j} \tag{21}$$

$$M_{out-B} = \sum_{1}^{l} integrate_{\ over\ time}\left(\vec{J} * A\right)_{elm\ l} \tag{22}$$

$$M_{out-U} = M_{out-I} + M_{out-B} \tag{23}$$

J_{elm} = *Centroid value of the mass flux per unit area of the element*
A_{elm} = *Area of the element (normal to the direction of* J_{elm}*)*
j = *number of rubber seal interfacial elements highlighted (red) in* Figure 44
l = *number of rubber seal bulk elements highlighted (orange) in* Figure 44

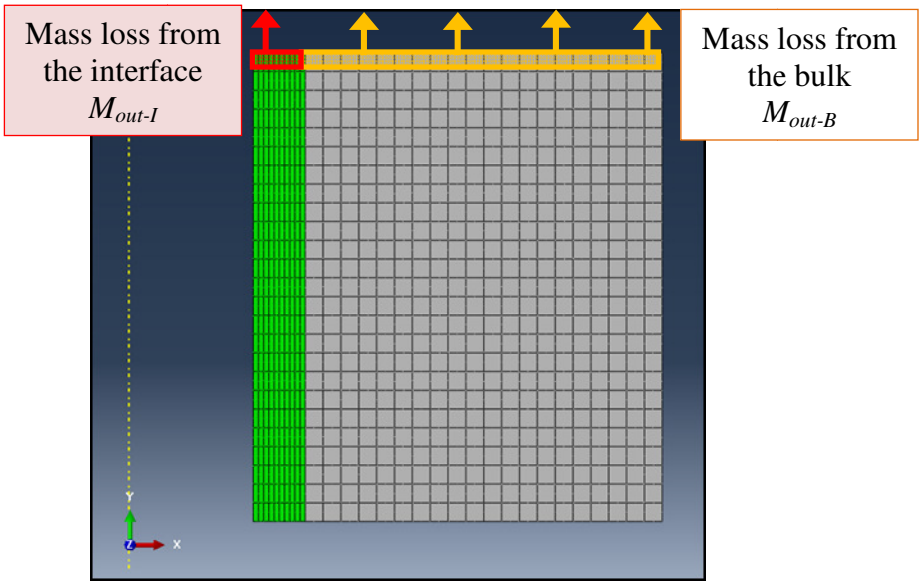

Figure 44: Total mass loss calculated from the highlighted elements in unpotted model

The output request of the potted model was slightly different because of the delamination. As shown in Figure 45, elements on the highlighted edge were used to output the mass flux. Equations (21)-(25) indicate the formula used to determine the mass flow of system.

$$M_{out-I} = \sum_{1}^{j} integrate_{\,over\ time}\left(\vec{J} * A\right)_{elm\ j} \tag{21}$$

$$M_{out-S} = \sum_{1}^{v} integrate_{\,over\ time}\left(\vec{J} * A\right)_{elm\ v} \tag{24}$$

$$M_{out-P} = M_{out-I} + M_{out-S} \tag{25}$$

J_{elm} = Centroid value of the mass flux per unit area of the element
A_{elm} = Area of the element (normal to the direction of J_{elm})
j = number of rubber seal interfacial elements highlighted (red) in
v = number of silicone elastomer elements highlighted (orange) in

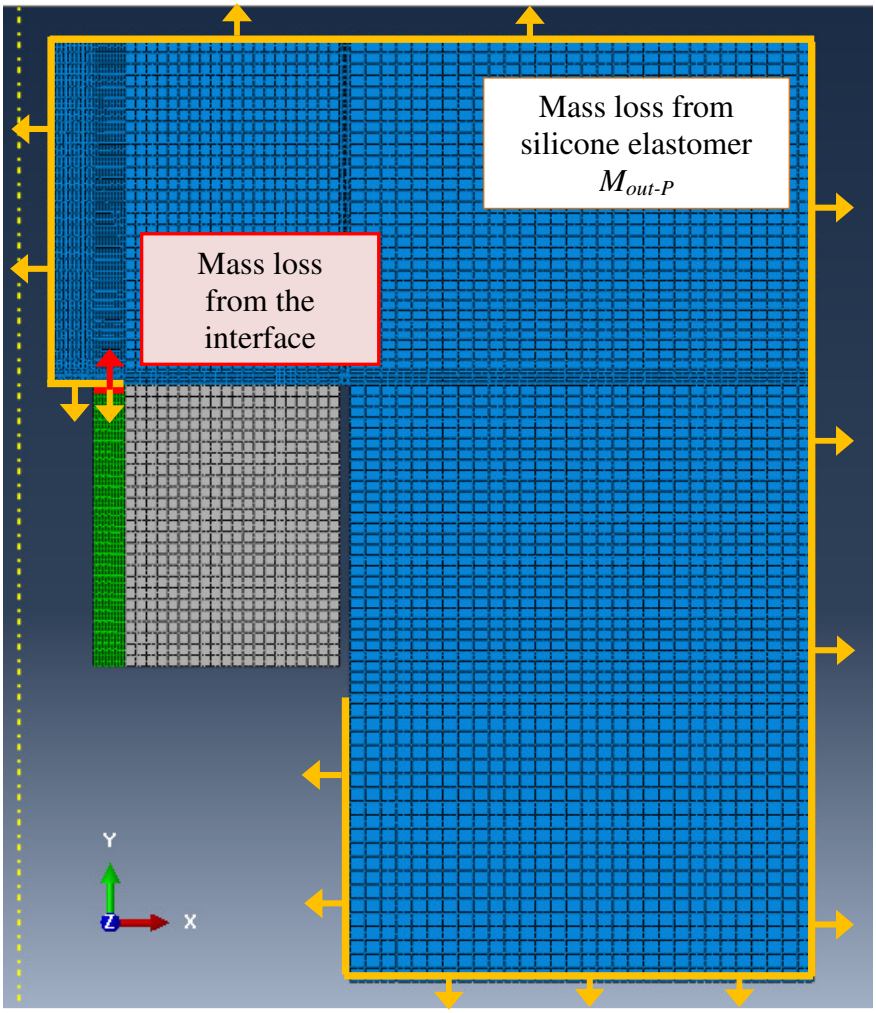

Figure 45: Total mass loss calculated from the highlighted elements in potted model

After the material properties were estimated based on the experimentally measured M_{out} of the system presented above, the elements M_{in} were examined for the (i) parametric study effect of encapsulation and (ii) transfer-function calculation for the unpotted case. Figure 46 illustrates the elements used to determine the mass loss for the parametric study of the potted capacitor. Figure 47 illustrates the elements used to calculate the mass flow from capacitor element. The transfer-function was then extracted based on the ratio of M_{in}/M_{out}.

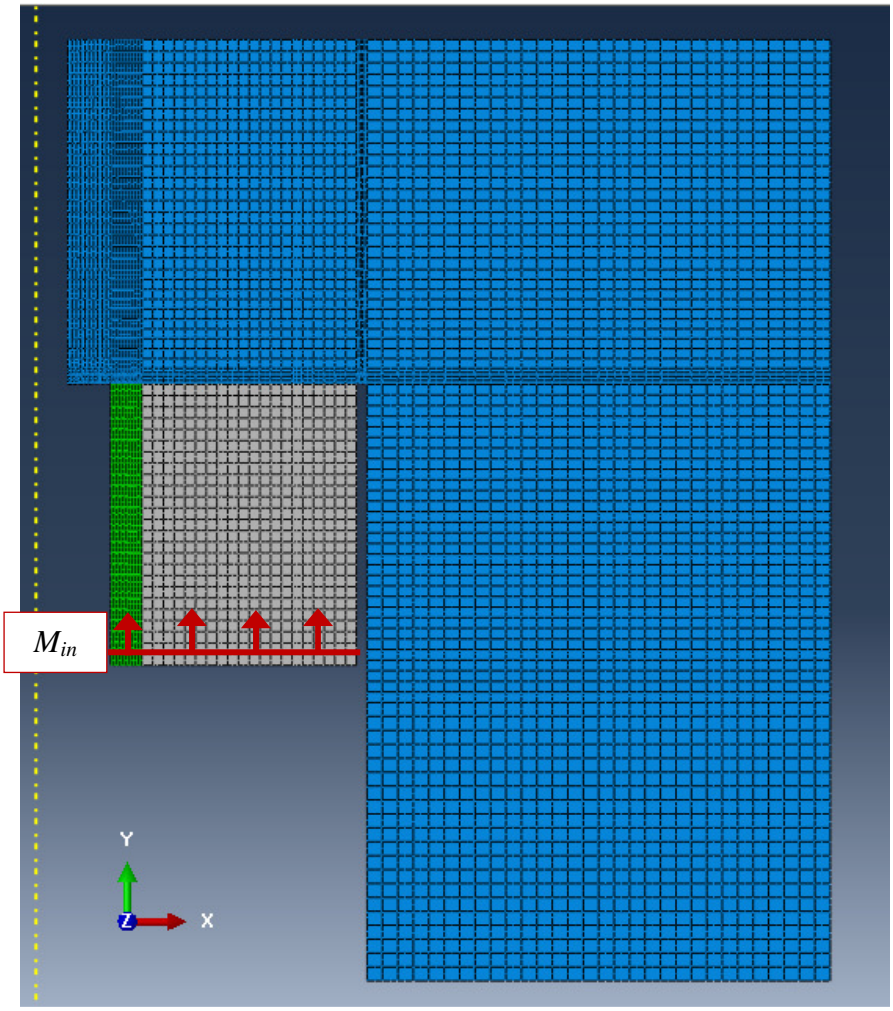

Figure 46: The output request used to conduct the parametric study for the effect of encapsulation on electrolyte leakage from the capacitor

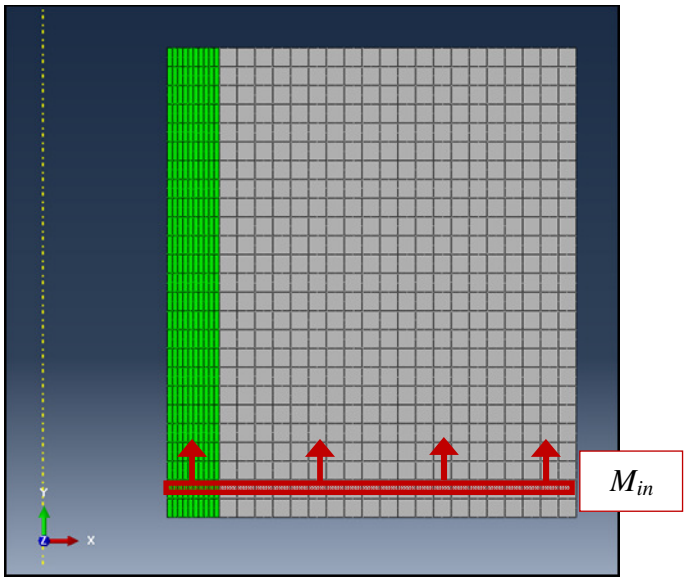

Figure 47: The output request used to determine the transfer-function between M_{in} and M_{out}

3.4 Material Property Estimation

As mentioned in the result Section *2.3.1 Weight Measurement* from the experiment, the FEA material properties were guided by the experiment. To recap, there were two key factors from the experiment which were used to estimate the material properties of the two polymers: (i) the average fractional residual electrolyte weight; (ii) the average weight of electrolyte measured from the 5 capacitors. The assumption was that in the FEA model both the unpotted and the potted capacitors started off with $M_e^{avg}=0.5368grams$ of electrolyte. The subsequent average fractional residual electrolyte weight curve is measured from the experiment for each specimen.

In this section, results are presented first. The over view approach to estimate the properties presented in Table 2 and have been presented in Figure 32 and the details are presented in the subsections of this section. Table 2 contains the summary of the material properties estimated for the rubber seal interface and bulk from the simplified model. The first column which is labeled as 'Cases' indicates the percent

of electrolyte loss from the interface of rubber seal and capacitor's lead (%I) vs. the percent of mass loss from the bulk of the rubber seal (%B). The cases presented were determined based on test and trail to find a unique case at which the silicone elastomer's solubility converged.

Table 2: Material property approximation of rubber seal interface and bulk for different cases guided by the experiment

Cases	P_I (s)	P_B (s)	S_I (s^2/m^2)	S_B (s^2/m^2)
35%I - 65%B	4.530E-13	5.192E-14	1.743E-02	1.856E-03
50%I - 50%B	**6.472E-13**	**3.994E-14**	**2.450E-02**	**1.450E-03**
57.5%I - 42.5B	7.443E-13	3.395E-14	2.738E-02	1.246E-03
65%I - 35%B	8.413E-13	2.796E-14	3.084E-02	1.042E-03
66.5%I - 33.5%B	8.607E-13	2.676E-14	3.171E-02	9.883E-04
75%I - 25%B	9.708E-13	1.997E-14	3.556E-02	7.511E-04
80%I - 20%B	1.035E-12	1.597E-14	3.798E-02	6.000E-04

Table 3: Calculated diffusivity based on the estimated permeability and solubility presented in Table 2

Cases	D_I (m^2/s)	D_B (m^2/s)
35%I - 65%B	2.599E-11	2.797E-11
50%I - 50%B	**2.642E-11**	**2.754E-11**
57.5%I - 42.5B	2.718E-11	2.724E-11
65%I - 35%B	2.728E-11	2.683E-11
66.5%I - 33.5%B	2.715E-11	2.707E-11
75%I - 25%B	2.730E-11	2.659E-11
80%I - 20%B	2.726E-11	2.662E-11

Table 4 presents the permeability values estimated for the silicone elastomer based on the simplified potted model.

Table 4: Material property approximation of silicone elastomer for different cases guided by the experiment

Cases	P_S (s)	S_S (s^2/m^2)
35%I - 65%B	2.154E-14	<< 1E-6
50%I - 50%B	**9.278E-15**	<< 1E-6
57.5%I - 42.5B	4.580E-15	<< 1E-6
65%I - 35%B	9.354E-16	<< 1E-6
66.5%I - 33.5%B	3.395E-16	<< 1E-6
75%I - 25%B	N/A	N/A
80%I - 20%B	N/A	N/A

One important observation from the material property estimation was that the 75%I and 80%I were unrealistic cases based on the model. This indicates that not enough material was diffusing through the rubber bulk to reach the steady state slope of the potted capacitor's electrolyte weight loss. Another observation was that the solubility for all of the cases was less than 1E-6 s^2/m^2 for the silicone elastomer. Model did not show any sensitivity for solubility less than 1E-6 s^2/m^2 (explained in more detail later in Section 3.6.2). Since the purpose of this model was to conduct a parametric study on the effect of encapsulation on the electrolytic capacitor the 50%I case was selected and the solubility value was selected to be in the same order of magnitude as that of the rubber seal bulk. Table 5 presents the material properties used for the parametric study based on the assumption that 50% mass escaped through the interface and 50% through the bulk of the rubber seal.

Table 5: Material property estimated mainly guided by the experiment based on the assumption 50%I-50%B

Material	P (s)	S (s^2/m^2)	D (m^2/s)
Rubber Interface	6.472E-13	2.450E-02	2.642E-11
Rubber Bulk	3.994E-14	1.450E-03	2.754E-11
Silicone Elastomer	9.278E-15	1.000E-03	9.278E-12

As shown in Figure 48 the experimental result is compared with the FEA result based on the material properties extracted for the unpotted case.

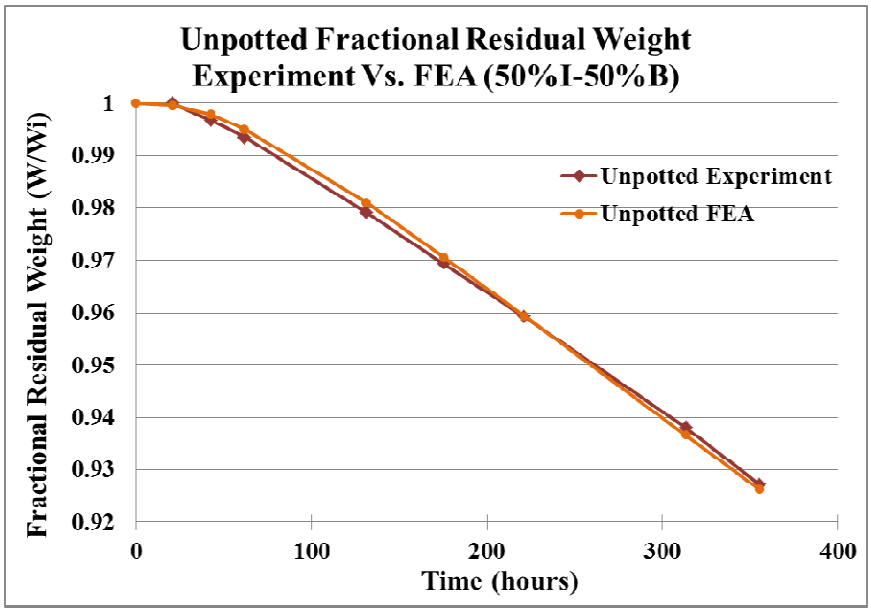

Figure 48: Unpotted experiment vs. FEA fractional residual electrolyte weight of the total unpotted capacitor (50%I-50%B)

Figure 49 presents the experimental result comparison with the FEA result for the potted capacitor. As mentioned earlier in this section, solubility of silicone elastomer was arbitrary selected in the same order of magnitude as the rubber seal bulk since we were unable to find a RMS fit to the test data. Therefore, the FEA results are slightly different from the experimental results.

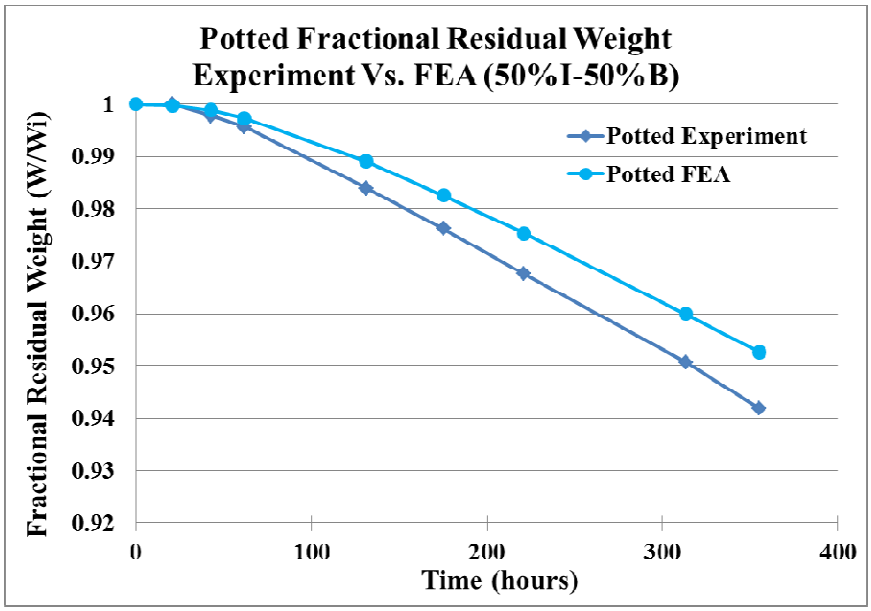

Figure 49: Potted experiment vs. FEA fractional residual electrolyte weight of the total encapsulated capacitor (50%I-50%B)

3.4.1 Rubber Seal's Permeability Estimation

As mentioned in Section ***3.2.1*** *Geometry*, an attempt is made to capture the effect of interfacial leakage between the rubber seal and the lead. Therefore, different amount of mass was assumed to leak through the interface and the bulk. However, the sum of the two mass losses had to equal to the average mass of the unpotted capacitors from the experiment in Equation (25) at steady state.

$$M_{out-I} + M_{out-B} = {M_e}^{avg}\left[1 - \left(\frac{M_u}{M_{u-i}}\right)^{avg}\right] \qquad \textbf{(26)}$$

$M_{out\text{-}I}$ = Mass loss from the interface (FEA)
$M_{out\text{-}B}$ = Mass loss from the bulk (FEA)
${M_e}^{avg}$ = Average mass of electrolyte measured from 5 capacitors (from experiment)
M_u = Instantaneous mass of electrolyte in the unpotted capacitor and its rubber seal (from experiment)
$M_{u\text{-}i}$ =initial mass of the electrolyte in the unpotted capacitor and its rubber seal (from experiment)

For this calculation first the approximate steady state slope of Figure 41 was used to determine the permeability of the interface and of the bulk of the rubber seal (% leak through interface vs % leak through the bulk). Considering the steady state condition, the concentration through the 1-D rubber mass transport analysis was linear. Therefore the permeability was extracted from Equations (27)-(32).

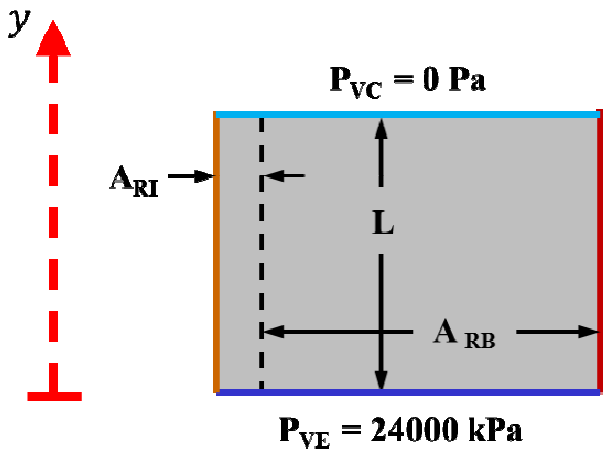

Figure 50: Unpotted rubber seal defining variable

A_{RI} = *Area of the interfacial material*
A_{RB} = *Area of the bulk of the rubber seal*
L = *Height of the rubber seal*
P_{VC} = *vapor pressure of the electrolyte in the chamber*
P_{VE} = *vapor pressure of the electrolyte inside the capacitor*

At steady state, mass transfer into the rubber must have equaled the mass transfer out of the rubber:

$$\dot{M}_{in} = \dot{M}_{out} \tag{27}$$

Therefore, the normalized concentration was linear inside the rubber seal both for interface and bulk:

$$\emptyset(y) = \left(-\frac{P_{VE}}{L}\right) y + P_{VE} \tag{28}$$

Then the gradient of the normalized concentration from the steady state was plugged into the mass flux equation:

$$J = \frac{\dot{M}}{A} = D\,S\frac{\partial\phi(y)}{\partial y} = D\,S\left(-\frac{P_{VE}}{L}\right) \quad \textbf{(29)}$$

$$J = \frac{\dot{M}}{A} = \frac{kM_e{}^{avg}}{A} \quad \textbf{(30)}$$

$\dot{M}$ = Rate of mass
A = Area of bulk or interface
k_u = Assumed steady state slope from the unpotted capacitors fractional residual electrolyte weight

The permeability of the rubber seal's bulk and interface was calculated by the following equations:

$$\frac{-(R_{RB})L\,k\,M_i}{P_v\,A} = D_{RB}S_{RB} = P_{RB} \quad \textbf{(31)}$$

$$\frac{-(R_{RI})L\,k\,M_i}{P_v\,A} = D_{RI}S_{RI} = P_{RI} \quad \textbf{(32)}$$

R_{RB} = Fraction of mass loss through the bulk
D_{RB} = Diffusivity of the bulk
S_{RB} = Solubility of the bulk
P_{RB} = Permeability of the bulk

R_{RI} = Fraction of mass loss through the interface
D_{RI} = Diffusivity of the interface
S_{RI} = Solubility of the interface
P_{RI} = Permeability of the interface

3.3.2 Rubber Seal's Solubility Estimation

Since permeability is the product of the solubility and diffusivity, only two of the three properties are independent and are needed to conduct the mass transport analysis. As explained in the previous section, the permeability of the bulk and interface were calculated based on the steady state condition. There are two approaches to estimate solubility: (i) first to either determine the diffusivity based on time to steady state, (ii) determine the solubility based on minimizing the sum of square error between the FEA output and experimental residual weight result. Since the resolution of the experiment result was low, it was a challenge to determine the time to steady state. Therefore, the solubility was approximated based on iterative approach to minimizing the sum of the errors squared between FEA output and experiment. The error between FEA and experiment was calculated using Equations (33) and (34). The sum of the error squared (Equations (35) and (36)) is then minimized to determine the solubility.

Experiment FEA

$$\hat{e}_B = R_{RB}\, {M_e}^{avg}\left[1-\left(\frac{M_u}{M_{u-i}}\right)^{avg}\right]-\sum_{1}^{l} integrate(\vec{J}*A)_{elm\,l} \quad \textbf{(33)}$$

$$\hat{e}_I = R_{RI}\, {M_e}^{avg}\left[1-\left(\frac{M_u}{M_{u-i}}\right)^{avg}\right]-\sum_{1}^{j} integrate\left(\vec{J}*A\right)_{elm\,j} \quad \textbf{(34)}$$

$$SSE_I = \sum {\hat{e}_I}^2 \quad \textbf{(35)}$$

$$SSE_B = \sum {\hat{e}_B}^2 \quad \textbf{(36)}$$

$\hat{e}_I$ = Error between FEA and experiment for interface
$\hat{e}_B$ = Error between FEA and experiment for bulk
J_{elm} = Centroid value of the mass flux per unit area of the element
A_{elm} = Area of the element (normal to the direction of J_{elm})
j = number of rubber seal interfacial elements in contact with the chamber environment boundary condition
l = number of rubber seal bulk elements in contact with the chamber environment boundary condition

As an example, the 35%I-65%B case curves of sum of the squared errors for interface and bulk are presented respectively in Figure 51 and Figure 52. For each curve a polynomial was fitted to the data. The derivative of the polynomial was set to zero to solve for the lowest solubility which resulted in lowest SSE.

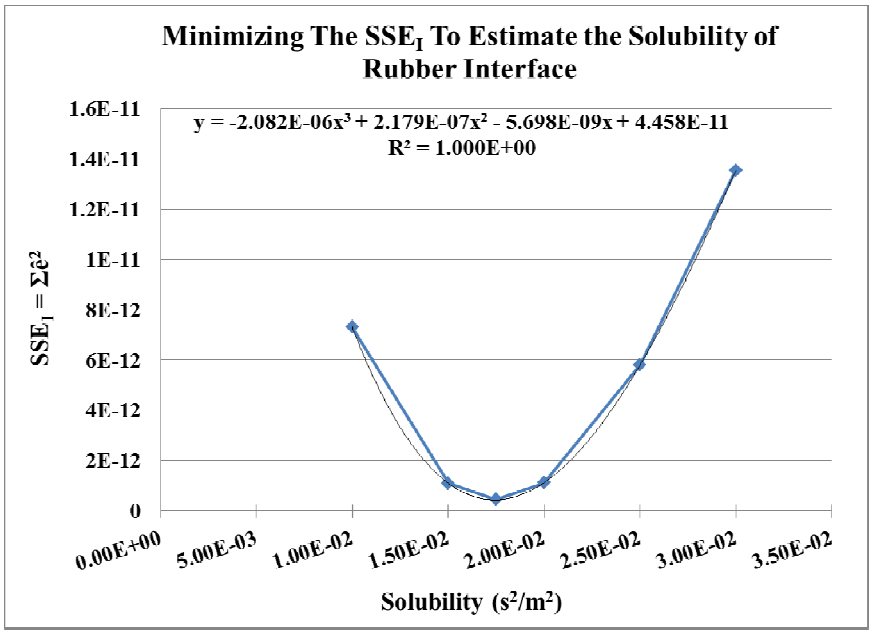

Figure 51: Minimizing the SSE$_I$ to estimate the solubility of the interface for the 35%I-65%B case

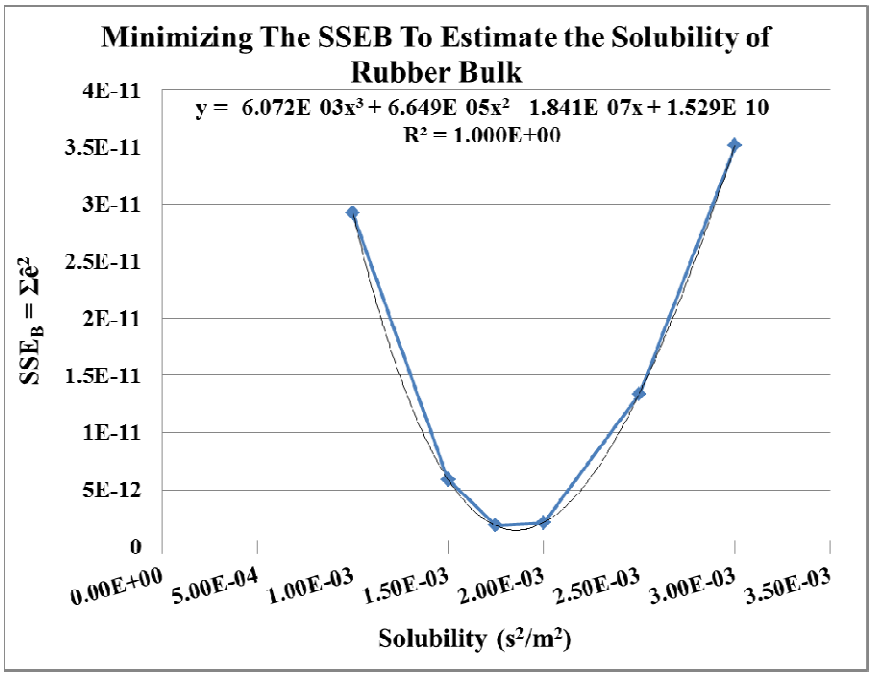

Figure 52: Minimizing the SSE$_B$ to estimate the solubility of the bulk for the 35%I-65%B case

3.4.3 Silicone Elastomer's Permeability Estimation

Similar to the unpotted case, the permeability of the potting compound was determined from the steady state. Under the assumption that any electrolyte vapor leakage through the interface would leak freely through the delamination, the total mass loss of electrolyte for the potted model is shown in Equation (37) at steady state:

$$M_{out-S} + M_{out-I} = {M_e}^{avg}\left[1 - \left(\frac{M_p}{M_{p-i}}\right)^{avg}\right] \quad \textbf{(37)}$$

$M_{out\text{-}S}$ = Mass loss from the potting compound (FEA)
$M_{out\text{-}I}$ = Mass loss from the interface of the rubber seal (FEA)
${M_e}^{avg}$ = Average mass of electrolyte measured from 5 capacitors (from experiment)
M_p = Instantaneous mass of electrolyte in the potted capacitor and its rubber seal and potting compound (from experiment)
$M_{p\text{-}i}$ =initial mass of the electrolyte in the potted capacitor and its rubber seal only (from experiment)

Due to the complex geometry and boundary condition of the potted model the analytical model could not be used. Therefore, an iterative approach was taken to approximate the permeability of the silicone elastomer. As an example, Figure 53 below indicates the iterative approximation of the permeability for the silicone elastomer. Same procedure was taken for all the other case.

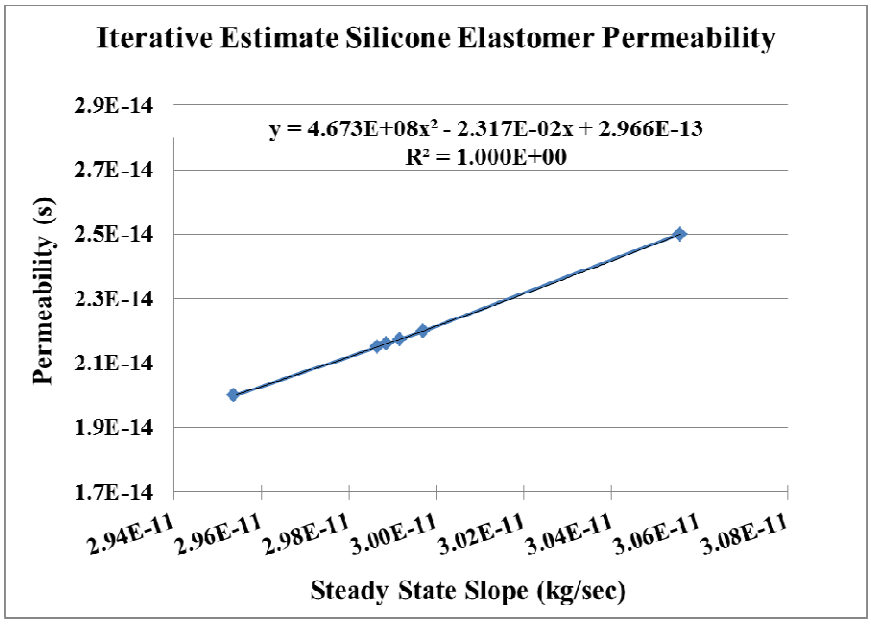

Figure 53: Iteratively the permeability of silicone elastomer for the 35%I-65%B

3.4.4 Silicone Elastomer's Solubility Estimation

Similar to the unpotted case the solubility was determined by the method of summing the squared errors between FEA and experiment. The experimental data used was the average fractional residual electrolyte weight of the potted capacitors. As mentioned previously the assumption is that the mass of electrolyte in the FEA model is M_e^{avg} which has been measured from 5 capacitors. The Equations (38) and (39) were used to determine the sum of the squared errors.

$$\hat{e}_P = {M_e}^{avg}\left[1 - \left(\frac{M_P}{M_{P-i}}\right)^{avg}\right] - \sum_{1}^{j} integrate\left(\vec{J} * A\right)_{elm\,v} \quad \textbf{(38)}$$

$$SSE_P = \sum {\hat{e}_P}^2 \quad \textbf{(39)}$$

$\hat{e}_P$ = Error between FEA and experiment for silicone elastomer
J_{elm} = Centroid value of the mass flux per unit area of the element (along the axis pointing towards the chamber environment)
A_{elm} = Area of the element (normal to J_{elm})
v = number of silicone elastomer elements in contact with the chamber environment boundary condition

As shown in Figure 54, the solution does not converge. As the solubility approaches zero the sum of the squared errors decreases without approaching a min. The model became very insensitive to solubility values below 1E-6 s^2/m^2. Therefore, the solubility of silicone elastomer did not converge.

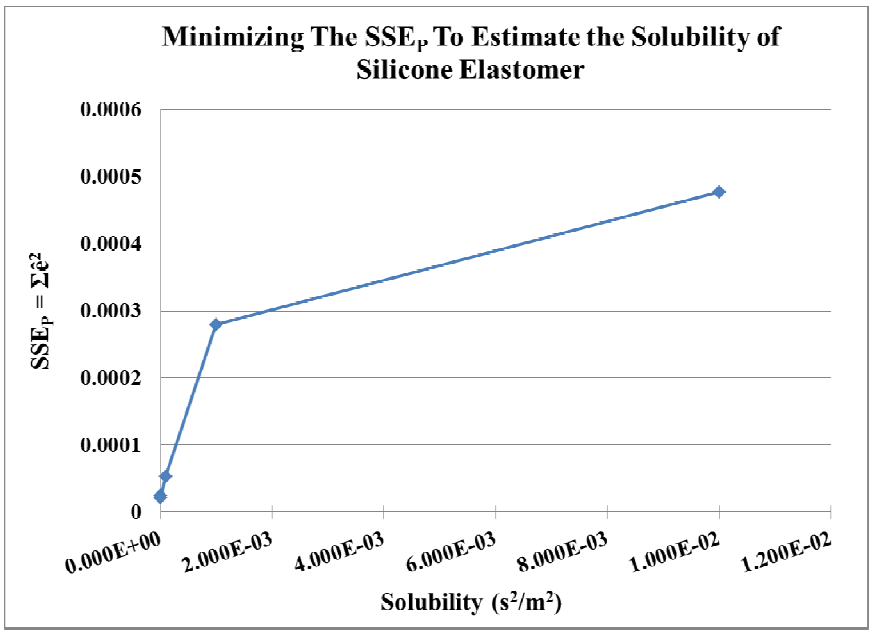

Figure 54: Minimizing the SSE_P to estimate the solubility of the silicone elastomer for the 50%I-50%B case

3.5 Modeling Assumptions

It is important to be aware of all of the assumptions made in the model. Therefore, following list recaps all of the assumptions made through this chapter:

1) Geometry
    a. Geometry was simplified to a single lead axisymmetric model.
    b. The unpotted capacitor model was treated as a 1-D mass transport analysis.
    c. Rubber seal mass transport material properties were estimated based on the assumption that half of the electrolyte leaked through the interface and the other half leaked through the bulk.
    d. The only interfacial leakage considered in the model was between the rubber seal and the capacitor lead. The interface between aluminum case and rubber seal was considered to be less of a concern since any leakage from that interface would have had the encapsulation as a barrier.
2) Steady State Assumptions
    a. The steady state slope was assumed in the following way: first the difference between the absolute initial slope and the absolute maximum slope was determine. Then 10% of the difference was calculated. Finally, the calculated value was subtracted from the absolute maximum slope.

b. Time to steady state was assumed to be the time at which the slope of experiment weight loss result crossed the steady state slope calculated in the assumption above (a).

3) Boundary conditions

a. The electrolyte inside the capacitor was assumed to be only gamma-Butyrolactone. Therefore, the capacitor's internal vapor pressure was determined based on gamma-Butyrolactone's vapor pressure at 155^{o}C.

b. The vapor pressure inside the capacitor was assumed to have rapidly saturated. Therefore, an instantaneous constant vapor pressure load was applied to the surface of the rubber seal exposed to electrolyte.

c. The vapor pressure outside of the capacitor was assumed to be 0 Pa.

d. In the potted capacitor model, the delaminated region between silicon elastomer and capacitor lead was considered to be 0 Pa boundary condition. This indicated that any leakage from the interface of rubber seal and capacitor lead would escape freely without any impact of silicone elastomer.

e. The initial residual electrolyte inside the rubber seal was assumed to negligible.

4) Weight of unpotted vs. potted

a. The initial electrolyte weight for both unpotted and potted capacitors was determined to be the electrolyte weight measured from the experiment (M_e^{avg}).

3.6 Parametric Study

Since the material properties estimated from the experiment contain many approximations, a parametric study was conducted on the effect of encapsulation. As mentioned in Section **3.4** Material Property Estimation the 50%I-50%B case was selected to conduct the parametric study. The parametric study conducted using this model was to observe the effect of encapsulation on the electrolyte from the capacitor.

3.6.1 Boundary Condition and Output

It is important to note that the experiment guided the material property estimation based on; (i) M_{out} which was the mass escaped the silicone elastomer, and (ii) full delamination between silicone elastomer and capacitor's lead as shown in Figure 55 below.

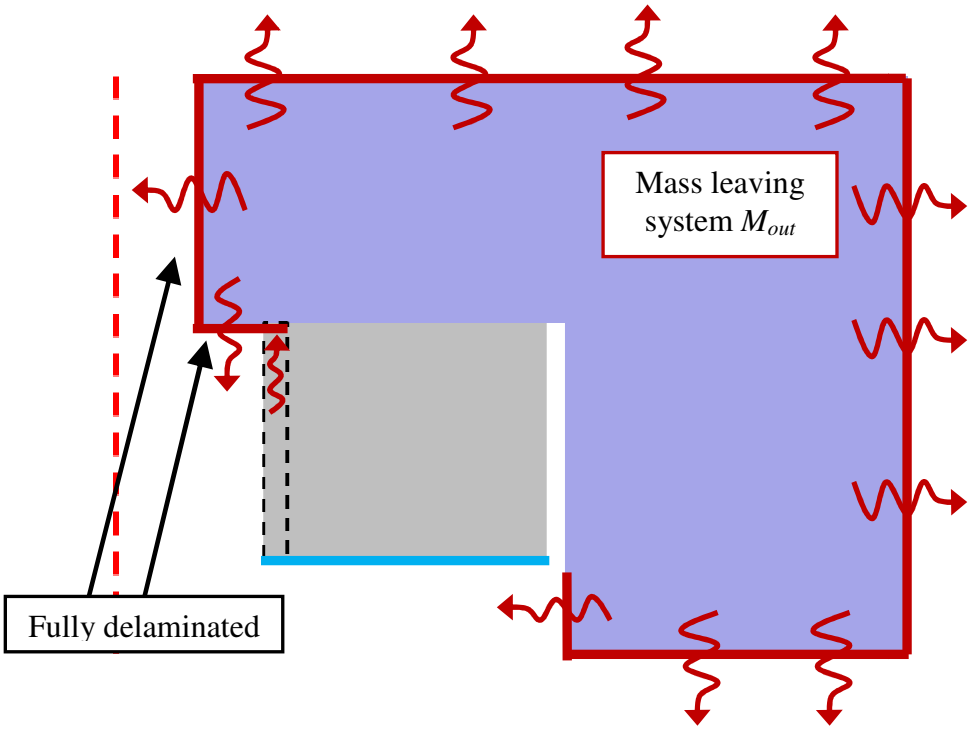

Figure 55: Model used to guide the material characterization estimation for 50%I-50%B

However, the parametric study focused on; (i) M_{in} which was the mass entering the rubber seal, and (ii) no delamination between the silicone elastomer and the lead. The reason for (i) was that only the mass inside the capacitor is effective in the electrical performance of the capacitor. The reason for (ii) was to examine the effect of encapsulation on an ideal encapsulated capacitor. Figure 56 illustrates the model used to conduct the parametric study.

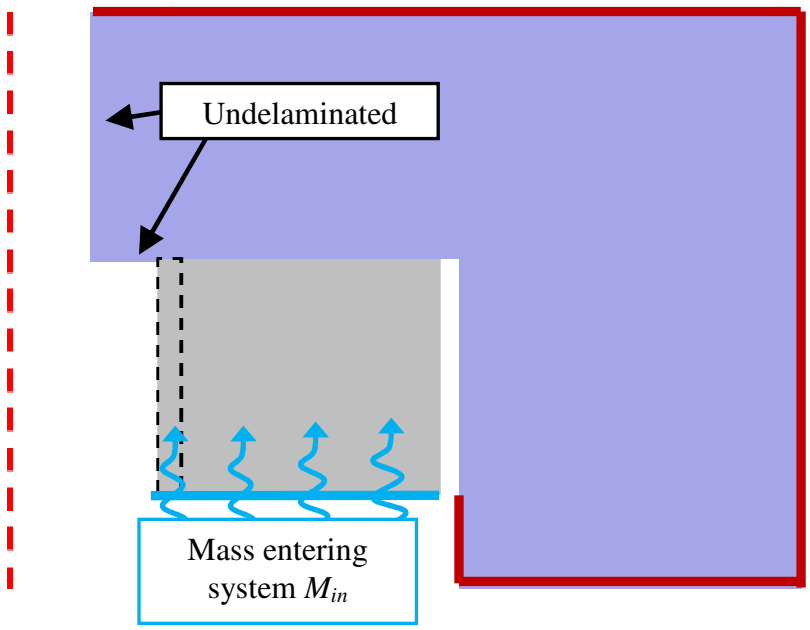

Figure 56: Model used to conduct the parametric study (effect of encapsulation on the electrolyte leakage from the capacitor)

3.6.2 Encapsulating Compound: Material Property Parametric Study

As discussed in Section 3.4 Material Property Estimation, the 50%I-50%B case was selected for the parametric study. For the two parametric studies, only the material properties of the silicone

elastomer will vary to observe the effect of the encapsulation on the electrolyte leakage from the capacitor. Fractional residual mass of the electrolyte inside the capacitor's element at 355 hours was compared for different combinations presented in Table 6. Equation (40) presents the equation used on the elements highlighted in Figure 46.

$$F_{rwe} = \frac{\left[{M_e}^{avg} - \sum integrate\left(\vec{J} * A\right)_{elm\,s}\right]}{{M_e}^{avg}} \quad \textbf{(40)}$$

Frwe = Fractional residual weight of electrolyte inside the capacitor
$J_{elm\ s}$ = Mass flux per unit area through elements 1 row of elements before the electrolyte vapor loading surface
$A_{elm\ s}$ = Area of the elements normal to mass flux vector

As mentioned in Section 3.4.4, solubility of the silicone elastomer did not converge. The results of the SSE indicated that solubility of electrolyte in silicone elastomer is a value close to zero. However, the permeability of the silicone elastomer was determined from the steady state condition. Therefore, for the first parametric study, solubility was reduced by orders of magnitude from 1E-3s^2/m^2 to 1E-6s^2/m^2 while maintaining constant permeability. Result of this study is presented in Figure 57.

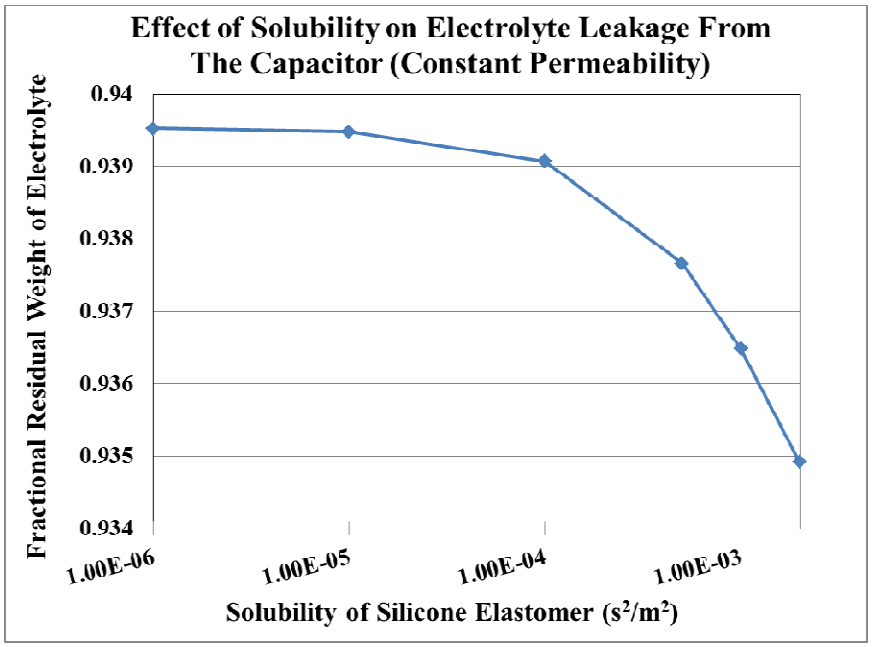

Figure 57: Parametric study on the effect of solubility of silicone elastomer on the electrolyte leakage from the capacitor (Constant permeability)

As illustrated in Figure 57, the FEA model indicates that the electrolyte leakage rate becomes insensitive to the solubility, for solubility values lower than 1E-4s^2/m^2.

The second parametric study focused on varying both solubility and diffusivity, as shown in Table 6. Nine different combinations of solubility and diffusivity were selected. To recap from Section 3.4, the solubility of silicone elastomer was selected to be 1E-3s^2/m^2 to be in the same order of magnitude as the solubility of the rubber seal bulk for this parametric study.

Table 6: Selected cases for the parametric study
Material property parametric study is only conducted on the silicone elastomer

		D_P (m^2/s)		
		x0.5	**Nominal**	**x2**
S_P (s^2/m^2)	**x0.5**	5E-4, 4.639E-12	5E-4, 9.278E-12	5E-4, 1.886E-11
	Nominal	1E-3, 4.639E-12	1E-3, 9.278E-12	1E-3, 1.886E-11
	x2	2E-3, 4.639E-12	2E-3, 9.278E-12	2E-3, 1.886E-11

The fractional residual weight of the electrolyte inside the capacitor was monitored at the 355th hour. Since permeability is the product of the solubility and diffusivity, an indirect parametric study was also conducted on solubility vs. permeability, and diffusivity vs. permeability. The next three tables present the fractional residual weight of electrolyte inside the capacitor at 355th hour for each of the nine cases. (solubility vs. diffusivity (Table 7), permeability vs. diffusivity (Table 8), and permeability vs. solubility (Table 9))

Table 7: Comparison of diffusivity vs. solubility fractional residual weight of electrolyte inside of the capacitor's element at 355th hour

Silicone elastomer		D_P (m^2/s)		
		x0.5	**Nominal**	**x2**
S_P (s^2/m^2)	**x0.5**	0.9416	0.9400	0.9377
	Nominal	0.9389	0.9365	0.9359
	x2	0.9349	0.9317	0.9278

Table 8: Comparison of permeability vs. diffusivity fractional residual weight of electrolyte inside of the capacitor's element at 355th hour

Silicone elastomer		D_P (m^2/s)		
		x0.5	**Nominal**	**x2**
P_P (s)	**x0.25**	0.9416		
	x0.5	0.9389	0.9400	
	Nominal	0.9349	0.9365	0.9377
	x2		0.9317	0.9359
	x4			0.9278

Table 9: Comparison of permeability vs. solubility fractional residual weight of electrolyte inside of the capacitor's element at 355th hour

Silicone elastomer		S_P (s^2/m^2)		
		x0.5	**Nominal**	**x2**
P_P (s)	**x0.25**	0.9416		
	x0.5	0.9400	0.9389	
	Nominal	0.9377	0.9365	0.9349
	x2		0.9359	0.9317
	x4			0.9278

In order to draw any conclusions from the FEA parametric study, the results presented in Table 7, Table 8, and Table 9 needs to be converted into percent difference $(F_{reference}-F_{cell})/F_{reference}$. This indicates that the percent different between each cell and the nominal (1D-1S-1P) cell was calculated. It is important to note that in these three tables, positive percent value is an indication that less electrolyte has escaped the capacitor's element. Alternatively, negative percent value indicates that more electrolyte has escaped from the capacitor's element.

Table 10: Calculated percent change of all cells in Table 7 to the nominal 1xS-1xD case in the center

Silicone elastomer		D_P (m^2/s)		
		x0.5	**Nominal**	**x2**
S_P (s^2/m^2)	**x0.5**	0.55%	0.37%	0.13%
	Nominal	0.26%	0.00%	-0.07%
	x2	-0.17%	-0.51%	-0.93%

As expected, Table 10 values indicates that as solubility and diffusivity of encapsulating compound increases, the amount of electrolyte escaping from the capacitor's element also increases. However, a more quantitative conclusion is that by doubling the solubility and diffusivity of the encapsulating compound, the electrolyte leakage increases by approximately 1%. Conversely, if the solubility and diffusivity are reduced by a factor of ½ the electrolyte leakage is reduced by 0.6%. Again, note that these comparisons are in reference with the nominal case.

Interestingly, results suggest that electrolyte leakage is more sensitive to the solubility of the encapsulation than the diffusivity. This indicates that an encapsulating compound with lower solubility is more effective in preserving the electrolyte inside the capacitor's element than an encapsulating compound with lower diffusivity. This is identifiable from the two corner cases Sx2-Dx0.5 and Sx0.5-Dx2. As seen in Table 10 cell Sx0.5-Dx2, solubility (reduced by a factor 0.5) dominated diffusivity (increased by a factor of 2) in preserving

electrolyte inside the capacitor's element in comparison with the nominal case. Whereas, in the alter case Sx2-Dx0.5, the capacitor's element leaked more electrolyte in reference with the nominal case. However, it is important to note that, since the permeability determines the steady state mass loss, both cases will result in the same mass loss rate.

Table 11: Calculated percent change of all cells in Table 8 to the nominal 1xP-1xD case in the center

Silicone elastomer		D_P (m^2/s)		
		x0.5	**Nominal**	**x2**
P_P (s)	**x0.25**	0.55%		
	x0.5	0.26%	0.37%	
	Nominal	-0.17%	0.00%	0.13%
	x2		-0.51%	-0.07%
	x4			-0.93%

As expected, Table 11 indicates that as permeability of the encapsulating compound increases the electrolyte leakage also increases. One counter intuitive behavior which is observed in Table 11 is that as diffusivity decrease while maintaining constant permeability, the electrolyte leakage increases. The reason for this effect was explained in the previous paragraph. As explained from Table 10's corner cases, electrolyte leakage from the capacitor's element is more sensitive to solubility of encapsulation rather than its diffusivity. Therefore, as the diffusivity decreases the solubility has to increase to compensate for the change in diffusivity to insure that the

product of the two remains the same (permeability). As a result, Figure 11 confirms that as diffusivity decrease, solubility increases to maintain constant permeability and as a result electrolyte leakage from the capacitor's element increases.

Table 12: Calculated percent change of all cells in Table 9 to the nominal 1xP-1xS case in the center

Silicone elastomer		S_P (s^2/m^2)		
		x0.5	**Nominal**	**x2**
P_P (s)	**x0.25**	0.55%		
	x0.5	0.37%	0.26%	
	Nominal	0.13%	0.00%	-0.17%
	x2		-0.07%	-0.51%
	x4			-0.93%

For completeness, Table 12 is also presented which presents the comparison of permeability vs. solubility of the silicone elastomer.

3.6.3 Encapsulating Compound: Parametric Study on Delamination

A parametric study was also conducted on the effect of electrolyte leakage from the capacitor's element based on different depth of delamination between the capacitor lead and encapsulating compound. Four different cases of delamination were selected for this study. These cases were expressed in terms of percentage of delamination. Percentage of delamination was determined based on the surface area of the delaminated region between the capacitor's lead and the encapsulating compound divided by the surface area of a fully delaminated case. Figure 58 presents the image of the four cases where

the red line indicates the exposed surface to the 0Pa vapor pressure boundary condition due to the delamination.

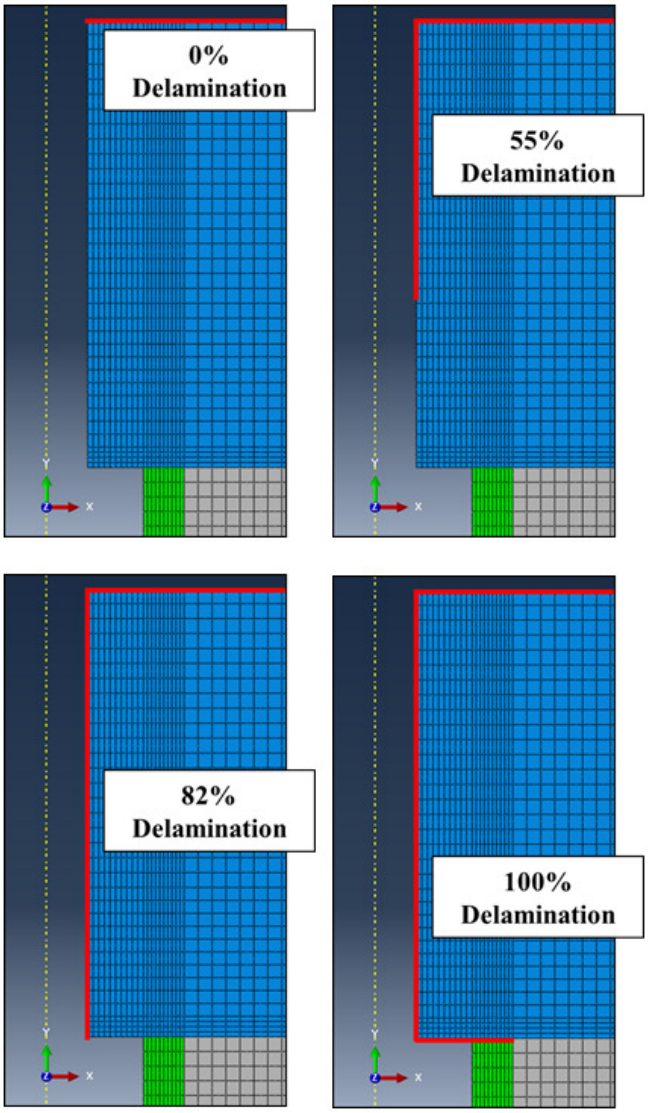

Figure 58: Four different delaminated cases for the parametric study

The material properties of the polymers were selected based on the 50%I-50%B assumption. The output parameter of interest was the fractional residual weight of electrolyte inside the capacitor at 355th

hour (M_{in}). Figure 59 illustrates the plot of fractional residual weight of electrolyte inside the capacitor against the percent of delamination.

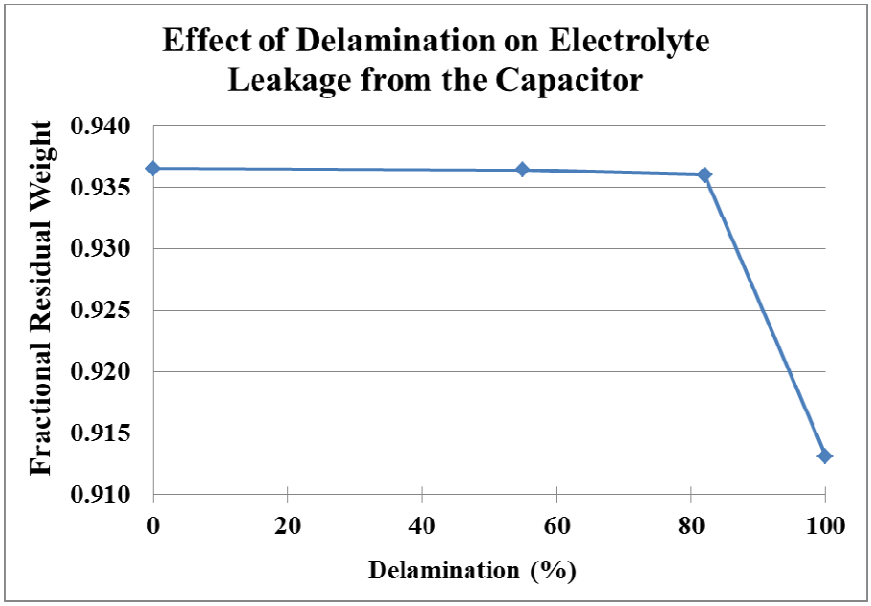

Figure 59: Effect of delamination on the fractional residual weight of electrolyte inside the capacitor at 355th hour (50%I-50%B)

As indicated in the results presented in Figure 59, electrolyte leakage from the capacitor significantly increased between 82-100% delamination. This parametric study confirmed the fact that the experiment results were highly affected by the full delamination between the encapsulating compound and capacitor lead.

3.6.4 Transfer-Function Extraction

The FEA model can also be used to extract a transfer-function between mass going into the rubber seal and mass leaving the polymer. The electrolyte going into the rubber seal is more valuable to know then the electrolyte leaving the polymers. This is because in the experiment

only the mass of electrolyte leaving the polymer was captured and any electrolyte which was absorbed by the polymers was shown in the measurements as residual electrolyte weight. However, the electrolyte absorbed by the polymer has no effect on the electrical parameter of the capacitor. Therefore, this transfer-function can be used to approximate the electrolyte loss from the capacitor. However, a more detailed FEA model and accurate material properties are needed to extract a reasonably accurate transfer-function.

As an example, the unpotted model with 50%I-50%B case was used to extract a transfer-function between electrolyte entering the rubber seal and electrolyte leaving the polymers. Equation (41) presents the transfer-function, M_{in} which is the mass entering the rubber sealant and M_{out} is the mass escaping from rubber seal into the chamber. Figure 60 presents the time history of the transfer-function extracted from FEA.

$$\left(\frac{M_{in}}{M_{out}}\right)_{FEA} = \left(\frac{M_{in}}{M_{out}}\right)_{Expe} \quad \textbf{(41)}$$

Variables defined in Figure 44 - Figure 47

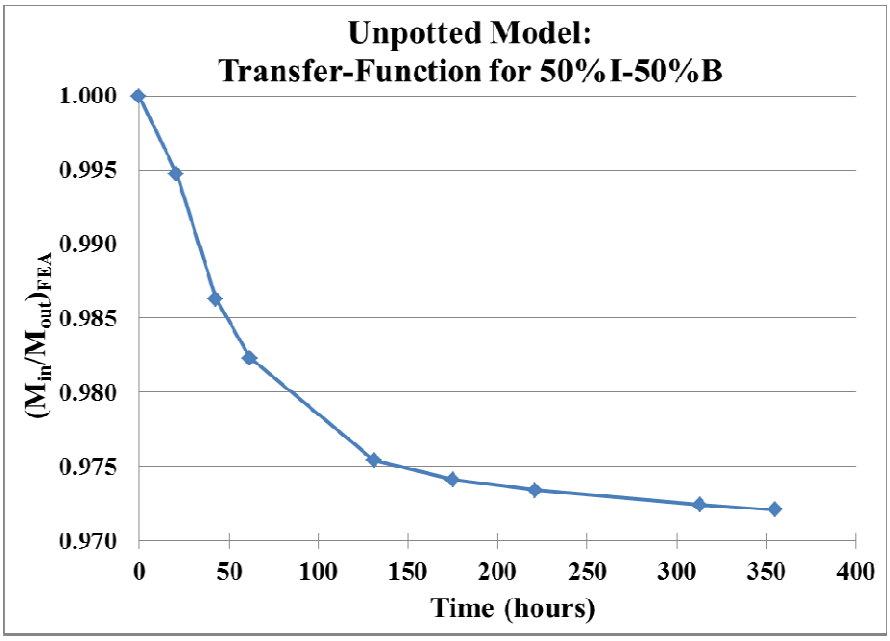

Figure 60: Transfer-function for the unpotted (50%I-50%B) extracted from the FEA analysis

In the experiment the electrolyte's M_{out} was captured. Therefore, the transfer-function was used to approximate the electrolyte which escaped the capacitor's element and diffused into the rubber seal. Figure 61 presents the approximate mass loss from the capacitor's element in the experiment.

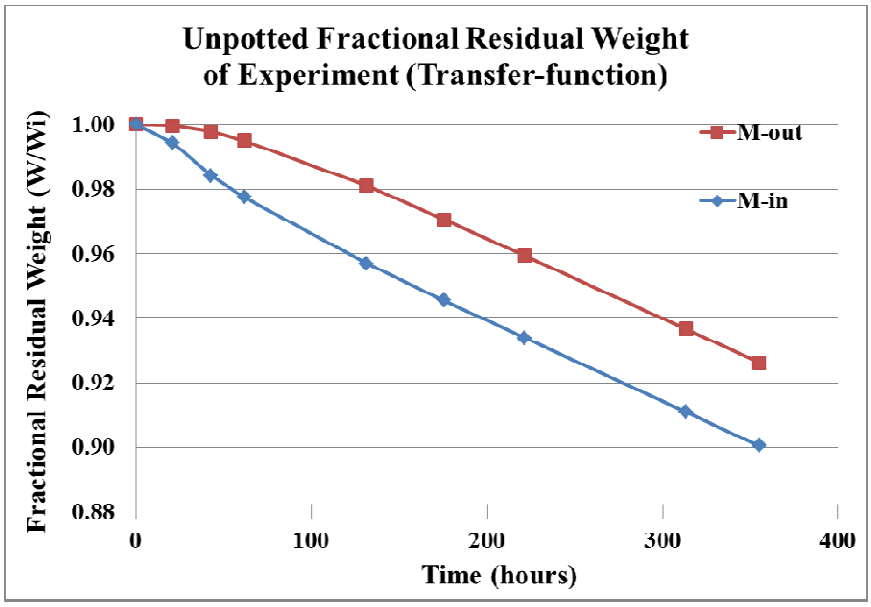

Figure 61: Used transfer-function extracted from FEA to approximate the effective electrolyte loss from the capacitor element

As shown in Figure 61, in the steady state region there is a 2% fractional residual weight difference between M_{in} and M_{out}. This indicates that approximately 2% of electrolyte vapor is diffused into the rubber seal. As a result this 2% electrolyte weight inside the rubber seal does not contribute in any ways to the capacitors electrical properties which is not captured in the experimental electrolyte weight measurements.

Chapter 4: Summary and Conclusion

This section contains an overview of work completed and reviews the conclusion made in each chapter.

4.1 Experiment

The overall objective of the experiment was to determine the effect of encapsulation on the electrolyte leakage from the electrolytic capacitor. A constant electrical (35VDC) and thermal (155^{o}C) loading was applied to the two populations of capacitors (unpotted vs. potted). Time history of three parameters was measured during the 800 hour test; (i) the physical weight of the capacitors, (ii) the equivalent series resistance (ESR), and (iii) the capacitance. Due to the high variability between one capacitor to another, the average fractional values of each parameter was compared between the two populations. Next three paragraphs will explain the observations made based on the average fractional value comparison between the two populations.

First, the absolute time history weight of the electrolyte was observed. Among the unpotted capacitor one outlier was detected which contained much more electrolyte than all the other capacitors. This unpotted capacitor was excluded from the ESR and capacitance comparison. In addition, the fractional electrolyte weight time history suggested that the unpotted capacitors resulted in higher electrolyte loss then the potted capacitors.

Second, the ESR measurements of the two populations were observed. The average fractional ESR time history indicated that the ESR degradation rate in the unpotted capacitors was higher than the potted capacitors. ANOVA test was performed on the

fractional ESR values of the two populations and the result confirmed with 95% confidence that the mean of the two populations are statistically different.

Finally, the capacitance of the two populations was observed. The average fractional capacitance time history indicated a very slight difference between the two populations with the potted capacitors degrading at a slightly slower rate. ANOVA test was performed on the average fractional capacitance value of the populations. The ANOVA test indicated that although the amount of difference had not yet reached the minimum threshold to be considered statistically significant in the strict sense of the definition, the two populations showed a divergent trend.

One of the encapsulated samples which depicted the highest mass loss during the test was examined for delaminations. Therefore, dye penetration task was performed on this sample. Dye stains on the capacitor revealed the fact that the silicone elastomer and capacitor leads were delaminated. Therefore, the encapsulation only conserved any electrolyte leaked from the bulk of the rubber seal and the interface of the aluminum case and rubber seal. This information was then used in the FEA modeling.

4.2 FEA Parametric Study

The average fractional weight of electrolyte calculated from the experiment was used to guide the material property estimated for the parametric study for the mass transport model. Capacitor was treated as an axisymmetric model. The unpotted model was assumed to be a 1-D problem with the inclusion of a dummy-material which represented the electrolyte leakage between the interface of rubber seal and the capacitor's lead. The experiment’s average electrolyte weight loss time history data was used to estimate the material property of the rubber seal bulk and the rubber seal

interface dummy-material. Material properties estimated for the rubber seal were then used to estimate the material property of the silicone elastomer based on the average fractional electrolyte weight loss time history of the experiment.

Three parametric studies were conducted on the effect of encapsulation on the electrolyte leakage from the element of the capacitor with the guided material properties. The output used to compare each set of properties was the electrolyte leakage from the capacitor's element at the 355th hour. In the first study, the permeability of silicone elastomer was held constant while the solubility was changed orders of magnitude. The results indicated that the electrolyte leakage from the capacitor became insensitive for solubility values lower than 1E-4s^2/m^2. In the second study, both the solubility and diffusivity were the changing parameters. The last parametric study conducted using the FEA model was to observe the effect of delamination on electrolyte leakage from the capacitor. The results from that study suggested that the electrolyte leakage from the capacitor was highly influenced as soon as the delamination reached the interface of rubber seal and capacitor lead.

The findings from the parametric study were the following; (i) the electrolyte leakage from the capacitor's element was more sensitive to the solubility (for values of solubility above 1E-4s^2/m^2) than the diffusivity of the encapsulating compound. (ii) the fact that the samples in the experiment were fully delaminated, prevented the encapsulating compound to play a significant role (iii) If a more detailed model is used, a transfer function can be extracted which relates the electrolyte loss from the polymers (capacitor and polymer) to electrolyte into the rubber seal. As an example the unpotted model was used to extract a transfer-function between electrolyte

leakage from the polymers to the electrolyte leakage into the rubber seal. Then the transfer-function was used on the experimental electrolyte leakage from the polymers to approximate the electrolyte leakage into the rubber seal. The electrolyte leaked into the rubber seal is a more accurate representation of the electrolyte loss of the capacitor since the electrolyte absorbed into the rubber seal has no effect on the capacitor's electrical performance.

Based on the limitations of this study, the experiment and FEA parametric analysis suggested that under constant DC voltage and high constant temperature, encapsulation can decrease the electrolyte leakage from the capacitor. As a result, the overall life expectancy of the capacitor can increase under the specific conditions.

4.3 Limitations of the Study

The limitations in this study are presented in a list below:

1. Limitation of experimental setup prevented the supply of ripple current to the tested capacitors, which would have represented a more realistic loading condition and accelerated the test even further. As a result, constant rated voltage was applied.
2. The initial weight of the electrolyte inside each capacitor could not be exactly determined. Therefore, the electrolyte loss history for each capacitor was approximated by estimating the difference between the total weight of each capacitor and the average weight of all of the remaining components other than the electrolyte. This procedure created significant uncertainty in the electrolyte loss estimates since this is a small quantity being estimated from the difference between two much larger uncertain quantities.

3. In the experiment, the sudden initial weight reduction of both silicone elastomer and rubber seal was not clearly understood, The reason was hypothesized to be possibly due to initial loss of moisture and/or electrolyte that could have been absorbed earlier in the polymers, but this explanation could not be verified or quantified. Therefore, the fractional electrolyte weight loss was referenced to the second reading rather than to the initial reading.
4. Unavoidable delamination between the encapsulant and the leads of the capacitor allowed free escape of any electrolyte that had leaked along the interface between the rubber seal and capacitor's lead. This spatial non-uniformity in the electrolyte flux increased the complexity of the test by reducing the influence of the encapsulant material properties on the electrolyte loss rate. Although this delamination was incorporated in the model, the resulting reduction in the role of the elastomer, prevented accurate estimation of the elastomer properties from the weight loss measurements.
5. The exact chemical composition of the electrolyte was not disclosed, however, FTIR studies indicated that one of the primary ingredients in the volatile portion was gamma-Butyrolactone. Therefore, in the FEA model, the electrolyte liquid was assumed to be gamma-Butyrolactone.
6. Material properties for the mass transport of electrolyte in the rubber seal and silicone elastomer were not known. Therefore, average fractional residual electrolyte weight loss measurement from the experiment on potted and unspotted samples was used to estimate the material properties.

7. The initial electrolyte concentration inside the rubber seal was not known. In the FEA analysis conducted, the initial concentrations of electrolyte and moisture were assumed to be negligible.

4.4 Contributions

- Provided the first comparative test data for the following parameters in encapsulated vs. unencapsulated aluminum electrolytic capacitors at constant thermal and electrical stress:
  - Weight change of the capacitors
  - Approximate weight change of electrolyte
  - Equivalent Series Resistance (ESR)
  - Capacitance
- Provided parametric insights into the radial nonuniformity of electrolyte transport through the rubber seal.
- Provided insights in to selected material properties, subject to assumptions and simplifications discussed earlier:
  - Permeability and solubility of electrolyte in rubber seal
  - Permeability of electrolyte in silicone elastomer
- Provided parametric insights into the effects of:
  - Mass transport properties of encapsulation on electrolyte leakage from capacitor
  - Fabrication defects such as delamination between the encapsulation and capacitor's leads

Acknowledgement:

This work reported here was sponsored by the members of the electronic Products and Systems Consortium at the Center for Advanced Life Cycle Engineering (CALCE) at the University of Maryland, College Park.

Appendices

Appendix I: Overstress Test

The aluminum electrolytic capacitor of interest is rated to operate at 105^{o}C and 35VDC for 7000 hours. Although, electrolytic capacitors are rated for a specific temperature, manufacturers de-rate the maximum temperature to insure that the capacitor will survive as specified in the spec sheet. Due to the lack of ripple current and for sake of time the temperature profile for the test was required to be high enough to accelerate the electrolyte leakage through the rubber sealant, but not too high to shift to a different failure mode such as melting of a component. Therefore, an over stress test was conducted to determine the maximum temperature limit for the capacitor to electrically perform within specifications.

i Temperature

Three capacitors were used for the overstress test. Capacitors were subjected to 105^{o}C with constant 35 VDC for 15min dwell period. Then capacitors were given 20min to cool down to room temperature and then parameters were monitored. The test temperature was then increased in increments of 10^{o}C until 155^{o}C. Beyond 155^{o}C the temperature increments were reduced to 5^{o}C and the experiment was continued to 185^{o}C.

ii Parameters Monitored

Parameters monitored in the experiment were capacitance and ESR. The purpose of this test was to determine the temperature at which the properties drifted beyond specified limits. This overstress limit provided the temperature for conducting the accelerated stress test where the intent was to accelerate the electrolyte leakage rate. All parameter measurements for both the overstress test and accelerated stress test were conducted at room temperature.

iii Results

The results of the overstress test are presented in Figure 62 and Figure 63. The overstress experiment results indicated that the capacitance suddenly drop beyond 165^{o}C which is a clear evidence that at this temperature capacitors experience catastrophic degradation. On the other hand, ESR does not show any unusual behavior for the given temperature range. Therefore, the temperature profile is selected to be 155^{o}C which is 10^{o}C lower than the temperature at which the capacitors demonstrated a dramatic change in their capacitance.

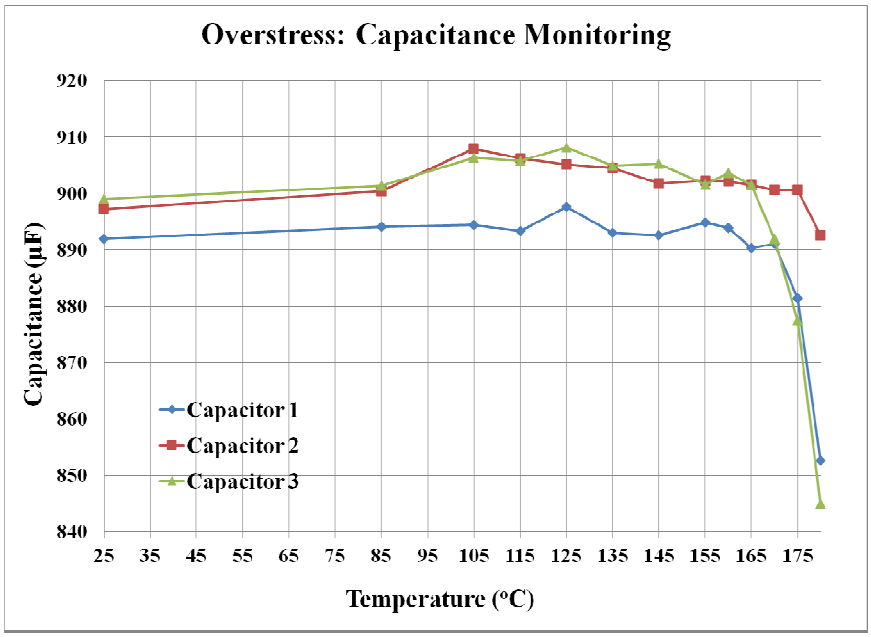

Figure 62: Capacitance cliff off at approximately 165°C

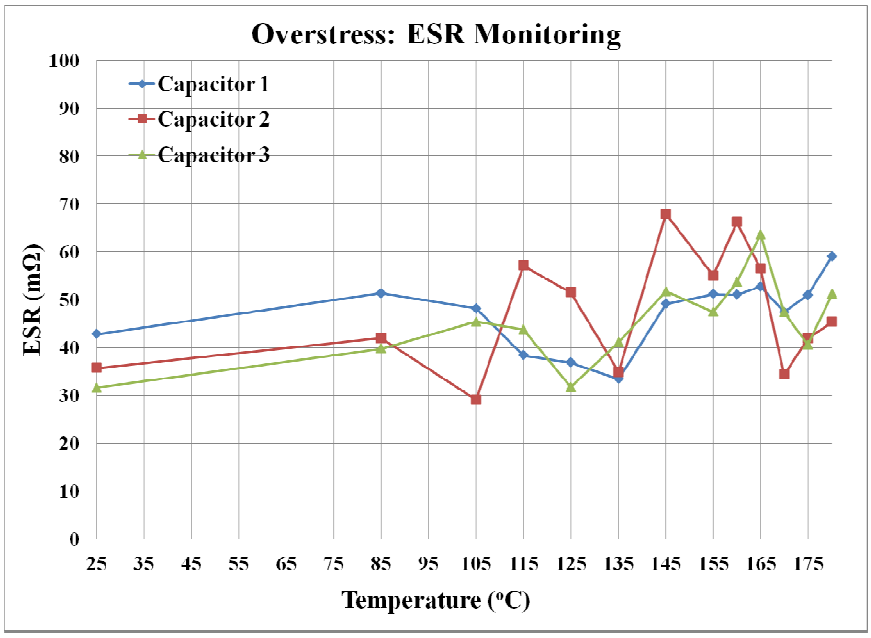

Figure 63: ESR does not look disturbed from the overstress experiment

Appendix II: Specimen Preparation

Specimen preparation process for the experiment was critical. The two main populations of interest for the experiment were unpotted capacitors (reference samples for comparison purposes) and potted capacitors. These two populations were placed in the temperature chamber at 155^{o}C constant profile. One of the critical parameters of interest which was monitored in the test was the weight of the capacitors. This parameter was critical due to the fact it physically represented the effect of the electrolyte which leaked out of the electrolytic capacitor. All excessive components were required to be excluded from the weight measurement in order to monitor the physical weight loss due to electrolyte leakage. All components other than electrolyte are assumed to be constant through the test expect for the rubber sealant and silicone elastomer polymers. These, polymers tend to lose mass as age at high temperature due to various reasons. Therefore, rubber sealant and the silicone elastomer specimens were also prepared to be weighted and subtracted from mass of the capacitors to extract the weight of the electrolyte leakage.

i Potted Capacitors

It is critical to prepare uniform specimens with a standard procedure to reduce specimen to specimen variability as much as possible. In order to prepare these specimens a mold was prepared in which silicone elastomer could easily de-bonded without damaging the capacitor or the silicone elastomer. Since the only leakage path for electrolyte is through the rubber sealant, the silicone elastomer is only required to seal the rubber end of the capacitor. This will also keep the safety

pressure release vent free in case of pressure build up inside the capacitor. Plastic cups were used as mold for the potting compound for three reasons: (1) silicone elastomer easily de-bonded from the cup. (2) The plastic cups are brittle and therefore, can break into small pieces which prevent the specimen from getting damaged in the process of removing the mold. (3) The plastic cups were easy to machine and drill two uniform holes with radius of 0.6mm approximately 9mm apart for the leads to pass through and extend out of the mold.

The most challenging portion of the process for encapsulating the potted capacitor specimen was the alignment of the capacitor accurately within the encapsulant without disturbing the potting compound and damaging the component in the removal process. As shown in Figure 64 mold-alignment fixture was designed and was created using a 3-D printer. This fixture was attached to the top of the cup to hold the capacitor's rubber end in the center of the cup and approximately 6.5mm away from the bottom of the cup.

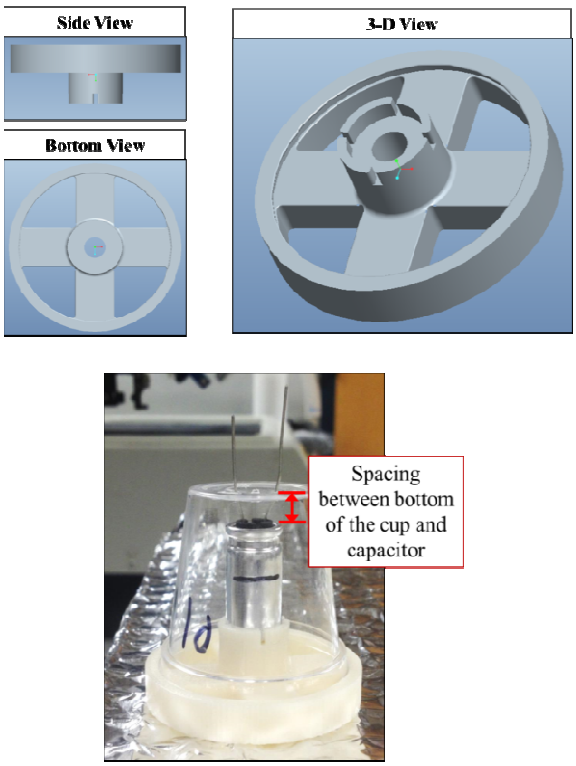

Figure 64: Capacitor suspending fixture, used to prepare potted capacitors

ii Weight loss of Silicone Elastomer

To produce consistent weight of silicone elastomer which encapsulates the capacitor is difficult, due to the fact in which some of the silicone elastomer liquid mixture poured on the wall of the mold and on top of the capacitor aligner. Therefore, each capacitor was measured and marked 10 mm from the rubber seal end towards the safety vent pressure release end. The 10mm mark was measured and silicone was poured to the measured length. However, there were some inconsistency in the amount poured, therefore, In order to accurately determine the weight loss of the electrolyte, the weight change of all other components had to be monitored and subtracted. This included the weight of the potting compound in the encapsulated population.

Since, polymers are known to lose mass at high temperatures, 10 silicone elastomer specimens were prepared and placed in the chamber to determine the mass loss of the polymer. This measurement allowed accurate accounting of the mass loss of the potting polymer which could be a source of error in the calculation of the mass loss of the electrolyte. Due to variability of the potting material, two different silicone elastomer specimens were prepared for the weight loss measurements: first specimen with approximately the same equivalent weight as the capacitor encapsulation, second specimen with approximately half the weight. The fractional mass loss is not expected to vary between the two silicone elastomer specimens.

iii Weight loss of Rubber sealant

Similar to silicone elastomer, the butyl rubber sealant is another polymer which is expected to lose weight as it ages at the elevated temperature. Therefore, 10 capacitors were disassembled and the rubber seals were removed for the test. The rubber seals were cleaned by the following procedure: (1) Rinsed with isopropyl alcohol and water, (2) then rinsed with ethanol, and (3) dried at room environment. The weight loss of the rubber seal was monitored the same manner as described above for the encapsulant material.

iv Capacitor Reform

All of the capacitors, 10 unpotted and 10 potted, were reformed initially before the experiment began because it was unclear how long these capacitors had been stored before the test. It was critical not to suddenly overload the capacitors and cause permanent damage. Therefore, all of the 20 parallel capacitors were subjected to a 10 minute cycle of charging/discharging with 5-minute dwells. The initial charging amplitude was 5VDC and the amplitude was increased in increments of 5VDC up until 35VDC, which is the rated voltage. Capacitors were then dwelled at 35VDC for 30min. Figure 65 indicates the reform process.

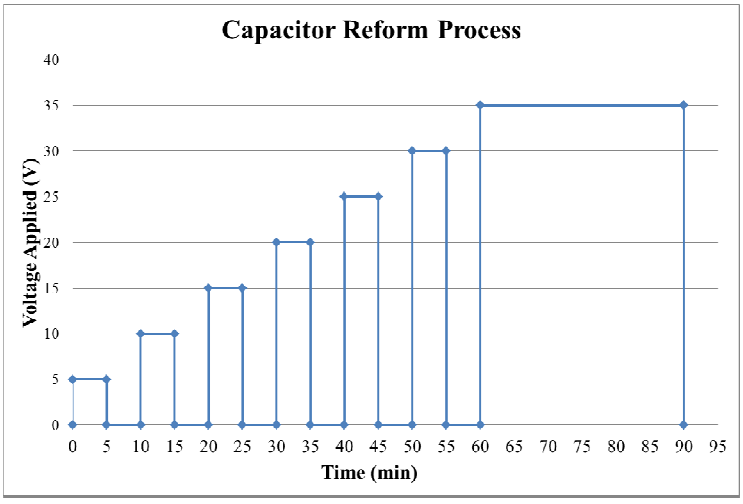

Figure 65: Reform process for all of the 20 capacitors later used for experiment

Appendix III: Circuit Design

To protect the power supply from getting damaged in case of a capacitor failure, a fuse was placed in series with each capacitor. This indicated that in a case where a capacitor failure caused a short in the electrical circuit the fuse would blow and prevent damage to the power supply. The current applied from the power supply was regulated to 20mA, therefore, the fuse current limit was determined by the resistor placed in parallel with the capacitors to discharge them safely. In order to discharge the capacitors at a reasonable time an 180Ω resistor was selected. This indicated that V/R=I give the maximum 35V, the maximum current traveling through the wires during the discharge of the capacitors will be 194mA. Considering the room for some error, the fuse rating was selected to be 250mA. The power of the resistor was determined using P=VI which indicated 6.8W, therefore, a 10W resistor was selected. A Single Pole Double Throw switch was selected to switch between charging and discharging the capacitors. The schematic of the setup is shown in Figure 66.

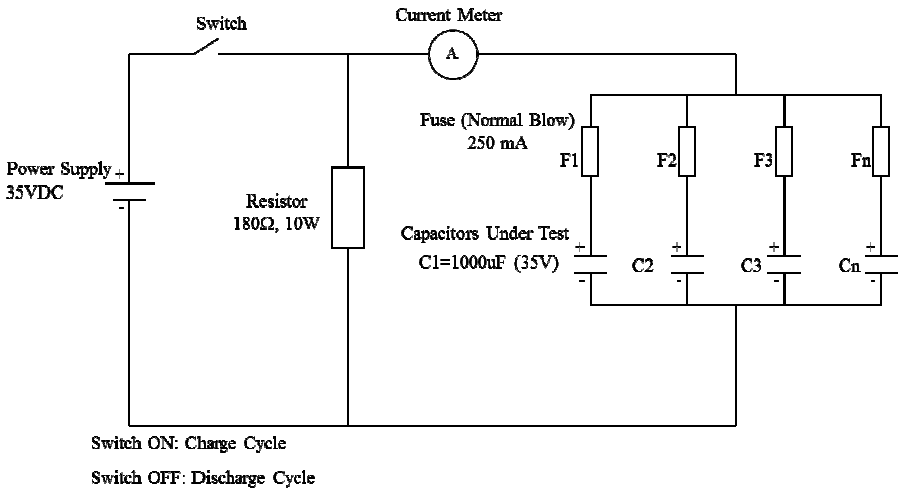

Figure 66: Electrical circuit design (by Swapnesh Patel)

Publications

1. E. Parsa, H. Huang, A. Dasgupta, “Multi-Physics simulation for combined temperature/humidity loading of potted electronics assemblies,” *Microelectronics Reliability*, 2014. In Press, Corrected Proof

2. E. Parsa, H. Huang, A. Dasgupta, “Multi-Physics simulations for combined temperature/humidity cycling of potted electronics assemblies,” in *IEEE*, Wroclaw Poland, 2013

3. Y. Sun, B. Han, E. Parsa, A. Dasgupta, “Measurement of effective chemical shrinkage and equilibrium modulus of silicone elastomer used in potted electronic system,” Submitted to the journal of *Materials Science*

References

[1] S. Koh, W. van Driel, C. Yuan and G. Zhang, "Degradation Mechanisms in LED Packages," in *Solid State Lighting Reliability Cinoibebts ti Systens*, New York, Springer Science Business Media, LLC, 2013, pp. 186-188.

[2] U. DoE, "Lifetime of White LEDs," 09 2009. [Online]. Available: http://apps1.eere.energy.gov/buildings/publications/pdfs/ssl/lifetime_white_leds.pdf. [Accessed 02 2014].

[3] B. Bose and D. Kastha, "Electrolytic capacitor elimination in power electronic system by high frequency active filter," in *Industry Applications Society Annual Meeting*, Dearborn, 1991.

[4] A. Lahyani, P. Venet, G. Grellet and P.-J. Viverge, "Failure prediction of electrolytic capacitors during operation of a switchmode power supply," *Power Electronics, IEEE Transactions on (Volume:13 , Issue: 6),* pp. 1199 - 1207, 1998.

[5] A. Shrivastava, S. Bangerth, M. Azarian, C. Morillo, M. Pecht, M. Levin, L. Steinhardt and A. Callini, "Detection of capacitor electrolyte residues with FTIR in failure analysis," *Journal of Materials Science: Materials in Electronics,* vol. 25, no. 2, pp. 635 - 645, 2014.

[6] M. L. Gasperi, "Life prediction model for aluminum electrolytic capacitors," in *Industry Applications Conference, 1996. Thirty-First IAS Annual Meeting, IAS '96., Conference Record of the 1996 IEEE (Volume:3)*, San Diego, 1996.

[7] C. Kulkarni, C. Jose, G. Biswas and K. Goebel, "Physics Based Electrolytic Capacitor Degradation Models for Prognostic Studies under Thermal Overstress," in *1st European Conference of the Prognostics and Health Management Society*, Dresden, Germany, 2012.

[8] CDM Cornell Dubilier, "Aluminum Electrolytic Capacitor Application Guide," [Online]. Available: http://www.cde.com/catalogs/AEappGUIDE.pdf. [Accessed 02 2014].

[9] S. W. Benson, "Experimental Characterization of Simple Kinetic Systems," in *The Foundations of Chemical Kinetics*, New York, Toranto, London, McGraw Hill Book Company Inc., 1960, p. 66.

[10] A. Dehbi, W. Wondrak, Y. Ousten and Y. Danto, "High Temperature Reliability Testing of Aluminum and Tantalum Electrolytic Capacitors," *Microelectronics Reliability,* pp. 835-840, 2002.

[11] H. Gualous, R. Gallay, G. Alcicek, B. Tala-Ighil, A. Oukaour, B. Boudart and P. Makany, "Supercapacitor Ageing at Constant Temperature and Constant Voltage and Thermal Shock," *Microelectronics Reliability,* pp. 1783 - 1788, 2010.

[12] R. Jánó and D. Pitică, "Accelerated Ageing Tests of Aluminum Electrolytic Capacitors For Evaluating Lifetime Prediction Models," in *Acta Technica Napocensis*, 2012.

[13] G. E. Rhoades and A. W. H. Smith, "Expected life of capacitors with nonsolid

electrolyte," in *34th Component Conf. Proc.*, 1984.

[14] J. A. Jones and J. A. Hayes, "The parametric drift behavior of aluminum electrolytic capacitos: An evaluation of four models," *1st European Capacitor and Resistor Technology Proc.,* pp. 171 - 179, 1987.

[15] Y. M. Chen, M. W. Chou and H. C. Wu, "Electrolytic capacitor failure prediction of LC filter for switching-mode power converters," in *Industry Applications Conference, 2005. Fourtieth IAS Annual Meeting. Conference Record of the 2005 (Volume:2)*, 2005.

[16] M. L. Gasperi, "A Method for Predicting the Expected Life of Bus Capacitors," in *Industry Applications Conference, 1997. Thirty-Second IAS Annual Meeting, IAS '97., Conference Record of the 1997 IEEE (Volume:2)*, New Orleans, 1997.

[17] M. L. Gasperi, "Life prediction modeling of bus capacitors in AC variable-frequency drives," *Industry Applications, IEEE Transactions on (Volume:41 , Issue: 6),* pp. 1430 - 1435, 2005.

[18] C. Kulkarni, G. Biswas, X. Koutsoukos, K. Goebel and J. Celaya, "Experimental studies of ageing in electrolytic capacitors," in *Annual Conference of the Prognostics and Health Management Society 2010*, Porltand, 2010.

[19] C. Kulkarni, G. Biswas, C. Jose and G. Kai, "Prognostics Techniques For Capacitor Degradation and Health Monitoring," in *The Maintenance & Reliability Conference, MARCON 2011*, Knoxville, 2011.

[20] S. Yoon, Z. Wang and B. Han, "On Moisture Diffusion Modeling Using Thermal-Moisture Analogy," *Jounral of Electronic Packaging,* vol. 129, no. 4, pp. 421 - 426, 2007.

[21] W. M. Haynes, CRC Handbook of Chemistry and Physics 94th Edition, Taylor and Francis Group, LLC, 2013.

[22] C. Gomez- Aleixandre, J. M. Albella and J. M. Martinez-Duart, "Pressure build-up in aluminum electrolytic capacitors under stressed voltage conditions," *Journal of Applied Electrochemistry 16,* pp. 109-115, 1986.

[23] C. Gomez-Aleixandre, J. M. Albella and J. M. Martinez-Duart, "Gas Evolution in Aluminum Electrolytic Capacitors," *The Electrochemical Society,* pp. 612 - 614, 1984.

[24] I. ic Illinois Capacitor, "Aluminum Electrolytic Capacitors Reliability," 2012. [Online]. Available: http://www.lintronicstech.com/index%20pdf/reliability_of_capacitors_general.pdf. [Accessed 2013].

[25] W. Greason and J. Critchley, "Shelf-Life Evaluation of Aluminum Electrolytic Capacitors," *Components, Hybrids, and Manufacturing Technology, IEEE Transactions on (Volume:9 , Issue: 3),* pp. 293 - 299, 1986.

[26] K. Harada, A. Katsuki and M. Fujiwara, "Use of ESR for deterioration diagnosis of electrolytic capacitor," *Power Electronics, IEEE Transactions on (Volume:8 , Issue: 4),* pp. 355 - 361, 1993.

[27] V. A. Sankaran, F. L. Rees and C. S. Avant, "Electrolytic capacitor life testing and prediction," in *Industry Applications Conference, 1997. Thirty-Second IAS Annual*

Meeting, IAS '97., Conference Record of the 1997 IEEE (Volume:2) , New Orleans, LA , 1997.

[28] C. Jose, G. Kulkarni, G. Biswas, S. Sankalita and G. Kai, "A Model-based Prognostics Methodology for Electrolytic Capacitors Based on Electrical Overstress Accelerated Aging," in *Annual Conference of the Prognostics and Health Management Society (PHM 2011)*, Montreal, Canada, 2011.

[29] Y. M. Chen, H. C. Wu, M. W. Chou and K. Y. Lee, "Online Failure Prediction of the Electrolytic Capacitor for LC Filter of Switching-Mode Power Converters," *Industrial Electronics, IEEE Transactions,* vol. 55, no. 1, pp. 400 - 406, 2008.

[30] C. Jang, B. Han, S. Yoon and S. Park, "Advanced Thermal-Moisture Analogy Scheme for Anisothermal Moisture Diffusion Problem," *Electronic Packaging,* vol. 130, no. 1, 2008.

[31] C. Jang, A. Goswami and B. Han, "Hermeticity Evaluation of Polymer-Sealed MEMS Packages by Gas Diffusion Analysis," *Microelectromechanical Systems,* vol. 18, no. 3, pp. 577 - 587, 2009.

[32] L. J. Hart and D. Scoggin, "Predicting Electrolytic Capacitor Lifetime," *Powertechniques Magazine,* pp. 24-29, 1987.

[33] R. S. SITETHIS Alwitt and R. G. Hills, "The Chemistry of Failure of Aluminum Electrolytic Capacitors," in *Physics of Failure in Electronics, 1964. Third Annual Symposium on the*, Chicago, 1964.

[34] J. A. Lauber, "Aluminum Electrolytic Capacitors Reliability, Expected Life, and Shelf Capability," *Sprague Tehcnical Paper,* pp. 83-89, 1985.

[35] M. A. Alam, M. Azarian, M. Osterman and M. Pecht, "Prognostics of Embedded Planar Capacitors Under Temperature and Voltage Aging," in *ASME 2010 Conference on Smart Materials, Adaptive Structures and Intelligent Systems*, Philadelphia, 2010.

[36] M. A. Alam, M. Azarian, M. Osterman and M. Pecht, "Accelerated Temperature and Voltage Stress Tests of Embedded Planar Capacitors With Epoxy–BaTiO3 Composite Dielectric," *Electronic Packaging,* vol. 134, no. 2, 2012.

[37] Xu, R., & Berduque, A. (2012). Rubber Sealing Materials for High Voltage and High Temperature . CARTS Int'l 2012. ecia.

[38] E. Parsa, H. Huang, A. Dasgupta, “Multi-Physics simulation for combined temperature/humidity loading of potted electronics assemblies,” Microelectronics Reliability, 2014. In Press, Corrected Proof.

[39] E. Parsa, H. Huang, A. Dasgupta, “Multi-Physics simulations for combined temperature/humidity cycling of potted electronics assemblies,” in IEEE, Wroclaw Poland, 2013.

[40] C. H. Shen, and G. S. Springer. "Moisture Absorption and Desorption of Composite Materials." Composite Materials, Vol. 10, 1976.